



HAL
open science

The high-resolution imaging science experiment (HiRISE) in the MRO extended science phases (2009–2023)

A.S. Mcewen, S. Byrne, C. Hansen, I.J. Daubar, S. Sutton, C.M. Dundas, N. Bardabelias, N. Baugh, J. Bergstrom, R. Beyer, et al.

► **To cite this version:**

A.S. Mcewen, S. Byrne, C. Hansen, I.J. Daubar, S. Sutton, et al.. The high-resolution imaging science experiment (HiRISE) in the MRO extended science phases (2009–2023). *Icarus*, 2023, pp.115795. 10.1016/j.icarus.2023.115795 . hal-04262337

HAL Id: hal-04262337

<https://hal.science/hal-04262337>

Submitted on 27 Oct 2023

HAL is a multi-disciplinary open access archive for the deposit and dissemination of scientific research documents, whether they are published or not. The documents may come from teaching and research institutions in France or abroad, or from public or private research centers.

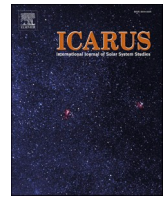
L'archive ouverte pluridisciplinaire **HAL**, est destinée au dépôt et à la diffusion de documents scientifiques de niveau recherche, publiés ou non, émanant des établissements d'enseignement et de recherche français ou étrangers, des laboratoires publics ou privés.



Distributed under a Creative Commons Attribution 4.0 International License

Contents lists available at [ScienceDirect](https://www.sciencedirect.com)

Icarus

journal homepage: www.elsevier.com/locate/icarus

The high-resolution imaging science experiment (HiRISE) in the MRO extended science phases (2009–2023)

A.S. McEwen^{a,*}, S. Byrne^a, C. Hansen^b, I.J. Daubar^c, S. Sutton^a, C.M. Dundas^d,
N. Bardabielias^a, N. Baugh^a, J. Bergstrom^e, R. Beyer^{f,k}, K.M. Block^a, V.J. Bray^a, J.C. Bridges^g,
M. Chojnacki^b, S.J. Conway^h, W.A. Delamereⁱ, T. Ebben^e, A. Espinosa^a, A. Fennema^a,
J. Grant^j, V.C. Gulick^{a,f,k}, K.E. Herkenhoff^d, R. Heyd^a, R. Leis^a, L. Ojha^l, S. Papendick^a,
C. Schaller^a, N. Thomas^m, L.L. Tornabeneⁿ, C. Weitz^b, S.A. Wilson^j

^a Lunar and Planetary Lab, University of Arizona, Tucson, AZ 85721, USA

^b Planetary Science Institute, Tucson, AZ, USA

^c Brown University, Department of Earth, Environmental, and Planetary Sciences, Providence, RI 02912, USA

^d U.S. Geological Survey, Astrogeology Science Center, 2255 N. Gemini Dr., Flagstaff, AZ 86001, USA

^e Retired from Ball Aerospace and Technology Corp., Boulder, CO 80301, USA

^f SETI Institute, Mountain View, CA 94043, USA

^g Space Park Leicester, School of Physics and Astronomy, University of Leicester, LE17RH, UK

^h Nantes Université, Université d'Angers, Le Mans Université, CNRS UMR 6112 Laboratoire de Planétologie et Géosciences, France

ⁱ Delamere Support Systems, Boulder, CO 80304, USA

^j CEPS, Smithsonian Institution, Washington, DC 20560, USA

^k NASA Ames Research Center, Moffett Field, CA 94035, USA

^l Department of Earth and Planetary Sciences, Rutgers University, Piscataway, NJ 08854, USA

^m University of Bern, Sidlerstrasse 5, CH-3012 Bern, CH, Switzerland

ⁿ Institute for Earth and Space Exploration, Western University, Dept. of Earth Sciences, 1151 Richmond Street, London, ON N6A 5B7, Canada

ARTICLE INFO

Keywords:

Mars, surface
Image processing
Instrumentation
Geological processes
Data reduction techniques

ABSTRACT

The Mars Reconnaissance Orbiter has been orbiting Mars since 2006 and has acquired >80,000 HiRISE images with sub-meter resolution, contributing to over 2000 peer-reviewed publications, and has provided the data needed to enable safe surface landings in key locations by several rovers or landers. This paper describes the changes to science planning, data processing, and analysis tools since the initial Primary Science Phase in 2006–2008. These changes affect the data used or requested by the community and how they should interpret the data. There have been a variety of complications to the dataset over the years, such as gaps in monitoring due to spacecraft and instrument issues and special events like the arrival of new landers or rovers on Mars or global dust storms. The HiRISE optics have performed well except for a period when temperature uniformity was perturbed, reducing the resolution of some images. The focal plane system now has 12 rather than 14 operational detectors. The first failure (2011) was a unit at the edge of the swath width, reducing image width by 10% rather than creating a gap. The recent (2023) failure was in the middle of the swath. An unusual problem with the analog-to-digital conversion of the signal (resulting in erroneous data) has worsened over time; mitigation steps so far have preserved full-resolution imaging over all functional detectors. Soon, full-resolution imaging will be narrowed to a subset of the detectors and there will be more 2×2 binned data. We describe lessons received for future very high-resolution orbital imaging. We continue to invite all interested people to suggest HiRISE targets on Mars via HiWish, and to explore the easy-to-use publicly available images.

* Corresponding author at: 1541 E. University Blvd., Tucson, AZ 85721, USA.

E-mail address: mcewen@pirl.lpl.arizona.edu (A.S. McEwen).

<https://doi.org/10.1016/j.icarus.2023.115795>

Received 20 December 2022; Received in revised form 4 September 2023; Accepted 7 September 2023

Available online 16 September 2023

0019-1035/© 2023 The US Geological Survey and The Authors. Published by Elsevier Inc. This is an open access article under the CC BY license (<http://creativecommons.org/licenses/by/4.0/>).

1. Introduction

1.1. Purpose and organization of this paper

This paper was written to provide information useful to the HiRISE data user community, updating the information in [McEwen et al. \(2010\)](#) about the Primary Science Phase (PSP) of Mars Reconnaissance Orbiter (MRO). There are 12 major sections:

1. Introduction
2. Science Publications and Team
3. Operations History
4. Summary of HiRISE Archived Dataset
5. Special Data Products and Analysis Tools
6. Imaging for Lander and Rover Missions
7. Science Planning and Uplink Tools and Techniques
8. Instrument Issues and Anomalies
9. Calibrations
10. Citizen Science and Machine Learning
11. Education and Public Outreach
12. The Future of Very High-Resolution Orbital Imaging of Mars

1.2. MRO and HiRISE overview

The Mars Reconnaissance Orbiter (MRO) was launched on August 12, 2005, carrying six scientific instruments ([Zurek and Smrekar, 2007](#)). In addition to the HiRISE camera ([McEwen et al., 2007](#)), MRO carries the Compact Reconnaissance Imaging Spectrometer for Mars (CRISM; [Murchie et al., 2007](#)), the Shallow Radar (SHARAD; [Seu et al., 2007](#)), the Context Camera (CTX; [Malin et al., 2007](#)), the Mars Color Imager (MARCI; [Malin et al., 2001](#)), and the Mars Climate Sounder (MCS; [McCleese et al., 2007](#)). The Primary Science Phase (PSP) covered slightly more than one Mars year, from November 2006 until December 2008, with MRO in its 255 × 320 km altitude mapping orbit. It was followed by the Extended Science Phase (ESP) for two Earth years, followed by Extended Missions (EM) 1–6. The first four EMs each lasted two years (a little more than one Mars Year (MY; [Piqueux et al., 2015a](#))), and EM5 was three years long. We find it useful to think in terms of MY rather than EM ([Table 1](#)). Results from the PSP were described by [McEwen et al. \(2010\)](#); this paper updates that information for mission extensions from 2008 through 2022 and describes future expectations. HiRISE image names from the PSP begin with “PSP”, while those from the ESP and all EMs begin with “ESP” (a small number of pre-PSP images in the transition phase (TRA), and aerobraking phase (AEB) also exist).

The HiRISE camera features a 0.5-m diameter primary mirror, 12-m effective focal length, and a focal-plane subsystem (FPS) that can acquire images containing up to 28 Gb (gigabits) of data in as little as 6 s ([McEwen et al., 2007](#)). However, the maximum image length has shrunk in the EMs due to thermal limits (Section 7.14). HiRISE images are acquired via 14 charge-coupled device (CCD) detectors, each with two

output channels, and with multiple choices for pixel binning and number of Time Delay and Integration (TDI) lines. The 10 CCDs that cover the full swath width (1.14° field of view, 6 km wide swath of Mars’ surface at a typical range of 300 km) are covered by broadband red filters (RED) and four extra CCDs in the middle are covered by blue-green (BG) and near-infrared (IR) filters to provide 3-color coverage in the center 20% of the image swath. With the failure of the electronics for RED9 in 2011, HiRISE has used the remaining nine RED CCDs covering a swath of 1.03°. RED4 failed in 2023 but the gap can be filled by the IR10 or BG12 image. [Fig. 1](#) shows the layout of CCDs in the HiRISE FPS. The very short orbital time separation between the BG, RED, and IR CCD image data is desirable to minimize parallax for good color registration, but has nevertheless enabled feature tracking and velocity measurements for rapid-moving avalanche clouds and dust devils ([Russell et al., 2008](#); [Choi and Dundas, 2011](#)).

MRO’s orbit altitude ranges from about 255 to 320 km above Mars (resulting in HiRISE nadir-pointed images at 0.255 to 0.32 m/pixel), and with a Local Mean Solar Time (LMST) ranging from 2:45 to 3:15 PM, although this shifted to somewhat later between 2020 and 21 to support entry, descent, and landing (EDL) for the Perseverance rover ([Farley et al., 2020](#)). Periapse is near the southernmost point of the orbit. MRO can routinely roll and point up to 30° to the left or right of the orbit groundtrack, allowing imaging of anywhere on Mars within one to two weeks and enabling stereo coverage. However, there are limits to off-nadir pointing (see Section 7.5), and there may be competition from other targets, so in practice, it may take months for repeat imaging of a location.

1.3. The People’s Camera

HiRISE has been called “The People’s Camera” because we aspire to make HiRISE as useful and accessible as possible to the science community and general public. This philosophy includes accepting public image suggestions (www.uahirise.org/hiwish) and releasing useful data products as quickly as possible. HiRISE is the only experiment within NASA’s Planetary Science Division that releases calibrated and map-projected products to the Planetary Data System (PDS) within just one to two months of data acquisition from the spacecraft. Data products associated with imaging of candidate landing sites and captioned image releases (prepared by science team members) may be released even sooner. There are 2249 captions as of June 2023 that are written for a public audience and explain the significance of the features in the image in layman’s terms. Furthermore, we have designed these data products for ease of use, including making tools available to analyze the data. The success of this approach is demonstrated by the existence of >1800 peer-reviewed science publications using HiRISE data, ~80% from lead authors who are not part of the HiRISE team, and by extensive use of HiRISE images by the general public. We describe these aspects of the experiment in greater detail below.

Table 1

Mars Years and MRO Science Phases. L_s stands for solar longitude, which describes the time of year, or season with $L_s = 0$ being the northern hemisphere’s spring equinox.

Mars Year (MY)	L_s range of HiRISE data	Earth Dates of MRO images (m/d/yr)	MRO Phase	MRO Orbits	# HiRISE Mars Images Returned
28	132–355	11/08/2006–11/29/2007	TRA, PSP	1330–6294	3790
29	2–328	12/13/2007–08/26/2009	PSP, ESP	6463–14,447	7882
30	25–360	12/16/2009–09/13/2011	ESP, EM1	15,894–24,051	8179
31	0–360	09/13/2011–07/31/2013	EM1, EM2	24,054–32,865	9800
32	0–351	07/31/2013–05/30/2015	EM2, EM3	32,870–41,445	9339
33	7–360	07/02/2015–05/05/2017	EM3, EM4	41,858–50,500	10,307
34	0–360	05/05/2017–03/23/2019	EM4, EM5	50,501–59,317	11,438
35	0–360	03/23/2019–02/07/2021	EM5	59,318–68,134	8420
36	0–360	02/07/2021–12/26/2022	EM5, EM6	68,135–76,952	8804
37	0–111	12/26/2022–8/28/2023	EM6	76,953–80,096	5404
			Total:		83,363

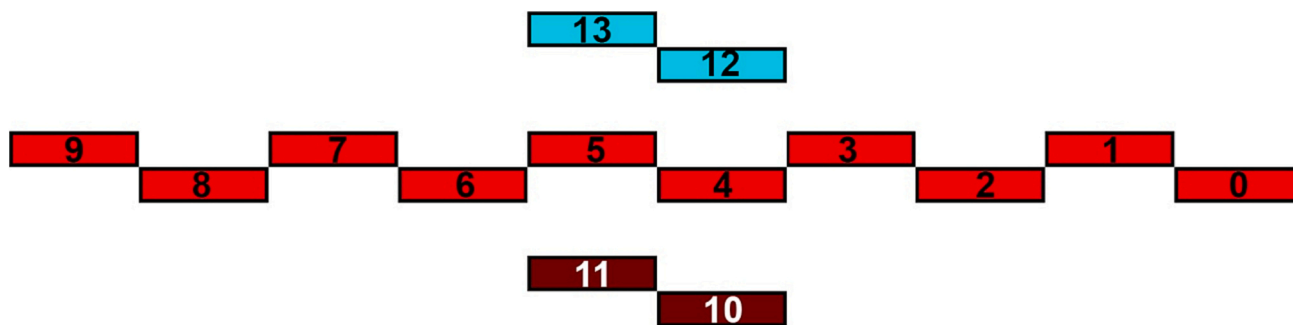


Fig. 1. HiRISE CCD layout in the FPA, with spacecraft motion up as shown here. Each CCD is 2048 pixels wide, and adjacent CCDs overlap by 48 pixels. Colors indicate spectral bandpasses (blue for BG (12,13), red for broadband RED (0–9), and brown for IR (10,11)). (For interpretation of the references to color in this figure legend, the reader is referred to the web version of this article.)

2. Science publications and team

2.1. Publications

HiRISE data have played a part in thousands of peer-reviewed papers since the beginning of operations in 2006. The MRO project maintains a database of team publications that has 294 peer-reviewed HiRISE papers in the 15-year period from 2007 to 2021 (Fig. 2; left). Assessing the number of publications enabled by HiRISE data from the wider community is more difficult as these papers have not been tracked systematically. As a proxy, a search of the NASA Astrophysics Data System (ADS) for peer-reviewed publications containing the words HiRISE and Mars yields 1817 results between 2006 and 2021 (Fig. 2; right), with over 2000 results as of June 2023. These results likely include some papers where HiRISE use is minimal, but also miss some publications that are not tracked by the ADS or do not have full text search available. Even with these uncertainties, the search result is useful to track the relative number of publications over time and provide a first-order estimate of the impact of the HiRISE experiment.

HiRISE team publications (Fig. 2; left) increased from the beginning of the mission and peaked in 2010 (likely due to special issues delaying some publications, so this peak is better understood as being split between 2009 and 2010). As extended mission funding decreased for the team and the MRO participating scientist program ended, team

publications decreased throughout the 2010s. Note that this count includes papers that team members carried out via other funding sources; the funding in the later extended missions was insufficient to support robust scientific investigations. A recent publications uptick lacks a simple explanation but is likely the result of other Mars mission publications using HiRISE data, the fruition of long-term monitoring campaigns, review papers, and HiRISE/CaSSIS collaborations. CaSSIS is the Colour and Stereo Surface Imaging System (Thomas et al., 2017) on ExoMars Trace Gas Orbiter (TGO). Total community papers (Fig. 2; right) show a similar increase from the beginning of the mission to a peak in 2010. Community paper production using HiRISE data was relatively constant from 2011 to 2015 and steadily increased since then. The number of papers in 2021 exceeded even the 2010 peak. This increase is likely due to the same reasons as the recent increase in team-led papers. Many of these papers are led by scientists funded by countries other than the United States.

2.2. Science highlights

Here we try to summarize the most significant results from HiRISE. Most of these results depend on other datasets in addition to HiRISE.

- HiRISE full-resolution stereo images enabled identification of small-scale hazards aiding successful landings by the Phoenix, MSL,

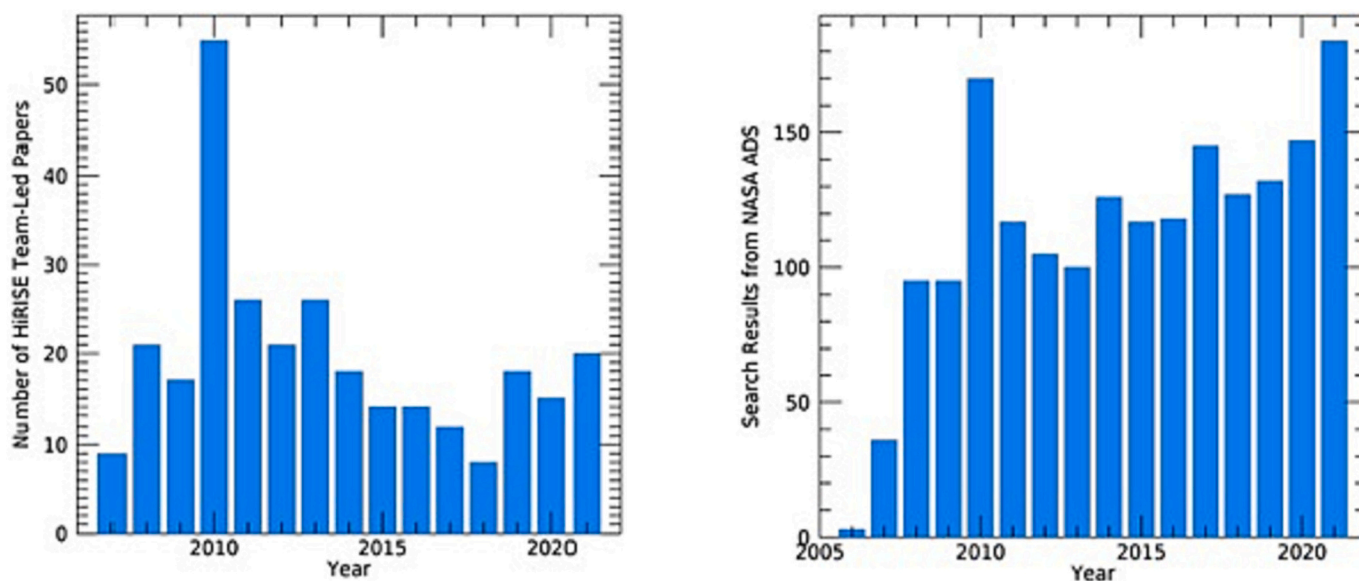


Fig. 2. (left) Number of peer-reviewed team-led papers over time through 2021 that are associated with HiRISE. Data are from the MRO publication database at: <https://mropd.psi.edu/>. (right) Number of search results on NASA's ADS at <https://ui.adsabs.harvard.edu/> for all peer-reviewed articles that contain the text Mars and HiRISE, including those led by team members and other scientists.

InSight, and Mars2020 missions (Golombek et al., 2012b, 2017, and others).

- Many current and candidate landing and traverse sites have been mapped in color and stereo, leading to regional geologic studies (Sun and Stack, 2020; Quantin-Nataf et al., 2021), enabling complementary surface results and traverse planning for rovers (see Section 6 and citations).
- New impact craters have constrained current impact rates and assisted the interpretation of seismic signals (Daubar et al., 2022; Posiolova et al., 2022).
- New craters also show that shallow water ice is present at lower latitudes than previously known, plus mid-latitude scarps have revealed thick bodies of massive ice (Dundas et al., 2021b, 2023).
- Mapping of shallow valleys, alluvial fans, channels, and deltas has shown that water flowed on Mars relatively recently, within the past 2 billion years (Grant and Wilson, 2019; Kite et al., 2019; Wilson et al., 2021).
- Mapping of sediments and ancient bedrock with stereo-derived topography combined with mineralogic information from MRO's CRISM has revealed that minerals containing water are widespread on early Mars (reviewed by Ehlmann and Edwards, 2014) and formed more recently than previously known, again within the past 2 billion years (e.g., Weitz et al., 2011, 2022).
- Pristine gullies on Mars have been shown to be forming at a high rate today from the action of carbon dioxide frost, rather than being remnants of a recent wetter climate (reviewed by Diniega et al., 2021 and Dundas et al., 2021a).
- Recurring Slope Lineae (McEwen et al., 2011) look like water seeps but are probably strange dry flows of dust and sand, showing that Mars today is very different than Earth (Dundas et al., 2017; McEwen et al., 2021).
- Sand dunes and other wind-driven bedforms are now known to be actively migrating across much of Mars (reviewed by Diniega et al., 2021). Another class of widespread bright ripple features is much less active, indicating that they were formed under different conditions than present-day Mars (Silvestro et al., 2020; Chojnacki et al., 2021).
- Some polar landforms like "spiders" or furrows are also actively forming on Mars today from seasonal processes involving carbon dioxide ice and gas (Hansen et al., 2011; Portyankina et al., 2017).
- HiRISE has revealed the remarkable diversity of volcanic landforms and processes on Mars, including mud volcanism (Okubo, 2016; Brož et al., 2022), flood lavas (Dundas et al., 2019b), and distinguishing aqueous from volcanic geomorphology (Hamilton et al., 2018; Sutton et al., 2022b).
- Sedimentary rocks have been studied in detail (McLennan et al., 2019), revealing periodicities in the layering that may relate to orbital cycles (Lewis and Aharonson, 2014).
- The north- and south-polar layered deposits and their outliers have periodic climate signals in the topography of their exposures stretching back millions of years (Becerra et al., 2016, 2019; Sori et al., 2022).
- Accumulation and erosion of the residual polar ice caps can be tied to the current climate and its variability from year to year (Byrne, 2008; Wilcoski and Hayne, 2020).
- The recognition of many glacial and periglacial landforms on Mars has only been possible using the detailed images of Mars (e.g., Butcher et al., 2020; Soare et al., 2014; Gallagher et al., 2011) and the story they tell us about Mars recent climate and hydrosphere has been instrumental in understanding the distribution of shallow ground ice that will underpin future human exploration (Morgan et al., 2021).

2.3. Science and operations teams and roles

The original HiRISE team had 12 Co-Investigators (Co-Is), which has

expanded over the years to 20 Co-Is. New Co-Is approved by the MRO project and NASA were chosen to add a range of expertise, institutions, and demographics. Each Co-I typically has both a relevant science specialty plus a skill essential to the successful outcome of a flight instrument investigation.

The high data volume represented by a single HiRISE image (typically gigapixel size) dictated from the outset that extensive spatial coverage would not be possible. Ideally, every site imaged by HiRISE should have a specific investigation or hypothesis in mind. A target database and catalog (HiCat) was built to be a repository of all the requests for HiRISE images. HiRISE images are broadly useful for Mars science, so HiRISE Co-Is and affiliates take responsibility for a particular science theme, becoming a Science Theme Lead (STL). The current list of STLs is given in Table 2. When someone requests a HiRISE image they must also designate an appropriate science theme, and the STL for that theme then assigns the target an initial priority. This is the time-independent part of the planning process. The STL is also responsible for interacting with peers in their theme area in the general Mars community to ensure that science targets are being identified and entered into the database.

HiRISE science planning is accomplished via a collaboration between a Co-I of the Pay Period (CIPP) science team member and a HiRISE Targeting Specialist (HiTS) uplink operations engineer. The HiRISE science team members serve as CIPP for typically 1–3 planning cycles per year. The CIPP role is open to all science team members and not limited to official Co-Is, thus giving early-career scientists the opportunity to gain experience in the planning and operations aspects of the mission. MRO commands are planned in 2-week cycles, starting ~4 weeks before the commands are sent to the spacecraft. At this point, the downlink capacity and orbit groundtracks are known to a high enough degree of accuracy to predict which targets will be observable. This time-dependent part of the planning process is tied to the uplink schedule with rigorous deadlines and requirements for command files to be sent to the Jet Propulsion Laboratory (JPL).

The HiTS creates a HiRISE Target List (HiTList) of seasonally appropriate targets viewable by the instrument considering roll limits, spacecraft exclusion zones, project input, scene requirements (like local illumination angle), and other factors, while the CIPP takes on the task of prioritizing these targets based on their initial priority from the STL, illumination, the state of the atmosphere, time criticality, frost coverage, etc. These factors change, thus the inclusion of CIPP scientific understanding into the decision-making process optimizes the science value of images acquired. Team members also propose a short list of important

Table 2
Science theme leads.

HiRISE Science Theme	Science Theme Lead
Climate Change	Margaret Landis, Patricio Becerra
Composition & Photometry	James Wray
Aeolian Processes	Matt Chojnacki
Fluvial Processes	Virginia Gulick
Future Exploration / Landing sites	John Grant, Alfred McEwen
Geologic Contacts / Stratigraphy	Dan Berman
Glacial/Periglacial Processes	Michael Mellon
Hydrothermal Processes	Virginia Gulick
Impact Processes	Ingrid Daubar
Landscape Evolution	John Grant
Mass Wasting Processes	Colin Dundas
Other	Shane Byrne
Polar Geology	Margaret Landis, Shane Byrne, Kenneth Herkenhoff
Rocks & Regolith	Mike Mellon
Seasonal Processes	Candice Hansen
Sedimentary / Layering processes	Cathy Weitz
Tectonic Processes	Chris Okubo
Volcanic Processes	Laszlo Kestay

Table 3

Ph.D. Dissertations where a HiRISE Team Member Played a Significant Role.

Name	Initial	Institution	Year	Dissertation Title
Atwood-Stone	C.	University of Arizona	2018	Planetary Granular Topography: Slope Angles and Crater Concentric Ridges
Banks	M.E.	University of Arizona	2009	Glacial processes and morphologies in the southern hemisphere of Mars
Bapst	J.	University of Washington	2018	Mars' Water Cycle Seen Through an Ice Lens
Becerra	P.	University of Arizona	2016	The poles of Mars, past and present: A high-resolution observational study of the martian polar regions and their connection to climate
Bramson	A.M.	University of Arizona	2018	Radar Analysis and Theoretical Modeling of the Presence and Preservation of Ice on Mars
Brooker	L.M.	Open University	2019	The History of Water at Lyot crater, Mars: Possible Surface Manifestations of Ancient Groundwater and/or Recent Climate Change
Butcher	F.E. G.	Open University	2019	Wet-Based Glaciation on Mars
Caudill	C.	University of Western Ontario	2020	Characterization of Impactite Clay Minerals with Implications for Mars Geologic Context and Mars Sample Return
Dapremont	A.M.	Georgia Inst of Technology	2021	Subsurface Sediment Mobilization on Mars: Insights Provided by Orbital Remote Sensing Datasets
Daubar	I.J.	University of Arizona	2014	New Dated Craters on Mars and the Moon: Studies of the Freshest Craters in the Solar System
Diniega	S.M.	University of Arizona	2010	Modeling Aeolian Dune and Dune Field Evolution
Dundas	C.M.	University of Arizona	2009	Investigations of the Martian Mid-Latitudes: Implications for Ground Ice
Eggers	G.L.	Georgia Inst of Technology	2021	Modeling and Observations of High-silica Magmatic Systems on Earth and Mars
Guimpier	A.	Nantes Université	2022	La géomorphologie des instabilités gravitaires sur Mars
Harrison	T.	University of Western Ontario	2016	Martian Gully Formation and Evolution: Studies From the Local to Global Scale
Kolb	K.	University of Arizona	2009	Investigating evidence of geologically recent liquid water on Mars
Landis	M.E.	University of Arizona	2018	Icy Craters on Mars and Ceres
McKeown	L.E.	Trinity College Dublin	2019	The Role of Contemporary CO ₂ Sublimation as a Geomorphic Agent on Mars
Ojha	L.	Georgia Inst of Technology	2016	Geophysical and remote sensing study of terrestrial planets
Wilson (Purdy)	S.A.	University of Virginia	2017	Fluvial landforms and the post-Noachian environment of Mars
Runyon	K.D.	Johns Hopkins University	2017	Agents of Planetary Geomorphic Change: Martian Aeolian Morphodynamics and the Emplacement of Crater Ejecta
Schaefer	E.I.	University of Arizona	2018	Quantifying geomorphic features: Relative albedos, skeletonization, and multifractality
Sutton	S.S.	University of Arizona	2022	Fissure-fed Volcanism on Mars and Earth
Viola	D.	University of Arizona	2017	Expanded Craters on Mars: Implications for Shallow, Mid-latitude Excess Ice
Wray	J.J.	Cornell University	2011	High-Resolution Studies of Aqueous Environments on Ancient Mars

suggestions each cycle that the CIPP evaluates and usually awards higher priority relative to other targets.

MRO mission management at JPL receives prioritized observation requests from several teams and determines MRO's activities through an automatic procedure, including enforcement of the MCS rules which limit the number and clustering of large rolls (>9°) that cause gaps in the

Table 4Major MRO¹ flight mission or Mars events.

Date (m/d/yr)	Mission or Mars Event
08/12/2005	Launch
03/10/2006	Orbit insertion
09/29/2006	Transition Phase imaging (1 week)
07/01/2007	Start of GDE of 2007
05/25/2008	Phoenix EDL
08/26/2009	Start extended spacecraft safe mode
12/16/2009	Resumed science operations
08/06/2012	Mars Science Laboratory (MSL) EDL
08/12/2013	MRO switches to inertial measurement unit (IMU)-2
10/02/2013	Comet ISON closest approach to Mars
10/19/2014	Comet Siding Spring closest approach to Mars
10/19/2016	Schiaparelli module crash
04/26/2017	First in-flight demo of All-Stellar mode
09/13/2017	Orbit Trim Maneuver (OTM)-49 pointed solar arrays off-point angle in sunlight, then entered eclipse, battery voltage dropped rapidly, all instruments powered off
06/02/2018	Start of GDE of 2018
11/26/2018	InSight EDL
06/10/2019	Completed battery reconditioning campaign
03/01/2020	Begin COVID-19 remote operations
02/18/2021	Mars 2020 Perseverance rover EDL
05/14/2021	Zhurong EDL
05/08/2022	CRISM no longer planning regular observations

¹ See Acronyms list at end of this paper.

MCS monitoring. Thus, only a minority of the prioritized HiTList is scheduled for observation. Once this subset is known, the CIPP may provide input for the image length and observation mode in accordance with data volume and other constraints. The HiTS has final responsibility for instrument settings, scheduling ride-along observations (adding HiRISE images to observations planned by CRISM or CTX), calibrations, and non-interactive observations, and creating a plan such that temperatures and spacecraft data storage use remain within an acceptable range. The HiTS turns the final sequence of observations into commands that are later radiated to the spacecraft. Parent suggestions for the planned observations are "retired" so they will not appear in later HiTLists.

The final responsibility of the CIPP is to look at the new images and decide whether any of their parent suggestions need to be un-retired (for example, if hazy atmospheric conditions lead to a poor image of the surface). The CIPP also writes several captions for images to be released on the public HiRISE site. Images are checked by student validators trained to evaluate image quality for rapid feedback to the CIPPs and HiTS. STLs routinely receive updates about images acquired in their science theme and check that each image satisfies the needs of its parent suggestion. Images with distinctive topography or layering may have their parent suggestion changed to stereo so that another image of the same target but at a different roll angle will be acquired.

2.4. Benefits to graduate students

Multiple generations of graduate students have matriculated and graduated while HiRISE has operated. The "People's Camera" model, encouragement of target suggestions from everyone, and HiRISE's rapid data release timeline significantly benefits graduate students, who typically work on several publishable projects within a few years.

Graduate students also benefit from the involvement of HiRISE team

Table 5
Major HiRISE flight events.

Date (m/d/yr)	HiRISE event
09/01/2005	First lunar images; IR10_1 bit-flip anomaly
12/01/2006	RED9_1 became very noisy due to bit flips
12/01/2006	Strategy of taking fewer but larger images to reduce number of thermal cycles
01/01/2007	RED0_1 and RED3_1 show minor bit-flips
02/03/2007	Reverse-clock warmup increased from 30 to 60 s
02/05/2007	Lowering FPE from 18 to 15 °C revealed bit-flips in RED1_1 and RED8_1
02/20/2007	Increase warmup to 71 s
04/01/2007	Began 200-s warmup, eliminated problems (temporarily) except IR10_1
05/18/2007	Engineering model aging test results show changes similar to those seen in-flight
09/01/2007	Passive heating of engineering model ADCs for 48 h at 85 °C, improved margin
12/20/2007	Passively-heated engineering model ADCs showed rapid decrease of margin when back in life test
05/13/2008	Higher-T EM life test showed improved margins, annealing in-flight seemed possible
07/01/2008	Stereo anaglyph pipeline production begins
07/01/2008	300-s warmup time, max possible without changing flight software
11/01/2008	300-s warmup insufficient, begin taking long nighttime warmup images
01/01/2009	8 of 14 CCDs show bit-flips in cold nighttime stim images
05/06/2009	HiRISE started monthly PDS releases
06/05/2009	MRO reinstated pausing solar array gimbals for high-stability observations (had been off since 1/2008) after demonstration that jitter was reduced.
07/01/2009	New product with color merged with full RED observation
07/01/2009	HiSEAS implemented using shadow tip algorithm
01/20/2010	HiWish launched
06/05/2010	SPORCs initiated
07/01/2010	Engineering model unit failed, no further life testing at Ball
07/21/2010	HiRISE safed because warmup images filled raw space on solid-state recorder (SSR)
10/01/2010	increased bit-flips when CRISM cryocooler off, cooling environment
12/20/2010	Inflight annealing test—no benefit apparent
06/01/2011	HiView implemented
06/13/2011	Lunar observations for calibration
08/01/2011	Majority of CCD channels show bit-flips when FPE at 18 °C for stim images
08/31/2011	RED9 electronics failed
10/24/2011	HiPrecision pipeline
10/24/2011	Implementation of CIPP-lite
01/23/2012	Raised FPE setpoint to 25 °C (heater almost always on), precludes cold stim images to monitor performance
04/10/2012	Fixed systematic crosstrack pointing error due to leap-second tracking
02/24/2013	Mars 3 candidate found in PSP_006154_1345
10/01/2013	Color orthoimages released to PDS
10/31/2013	“This is Mars” coffee table book published
06/29/2014	Beagle-2 located in ESP_037145_1915
01/12/2015	Corrected software error resulting in 1800-line downtrack targeting errors.
10/01/2015	Found bug is color registration; new color stretch parameters
06/01/2016	Revisit of procedures to swap sides of block-redundant electronics
11/20/2016	Lunar observations for calibration
11/21/2016	HiRISE safed—instrument electronics box over temperature limit due to use of multiple solar array motors for lunar observations
05/11/2017	“Mars: The Pristine Beauty of the Red Planet” coffee table book published
06/11/2017	HiRISE warmup images moved out of eclipse to reduce load on batteries
10/20/2017	HiRISE images in All-Stellar mode (also at apoapsis) often blurred
12/09/2017	HiKERS implemented
08/25/2018	Enabled optics heaters during imaging to eliminate blur
11/13/2018	HiRISE decision to adapt stand down during some cycles to work on simplifying operations
10/01/2019	HiRISE decision to stop raising FPE-T, target max 50 °C (AFT at 65 °C)
12/03/2019	Begin ADC setting test campaigns
08/02/2020	Change RED1–3 to ADC 74_74
03/01/2021	Change Bin1-2A mode so RED3 is binned
08/03/2021	Updated HiRISE LUTs for range of possible new ADC settings
01/30/2022	New procedures developed; rapid testing of many ADC settings
07/03/2022	New ADC settings implemented for RED0–3, 7–8
07/14/2023	HiRISE safing due to RED4 electronics failure

members on their committees and as PhD advisors. Twenty-five such students (Table 3) are known to have graduated over the course of the MRO mission from 2009 to present day. Many of these students attended HiRISE team meetings and remain active on the project. Some of these graduates have gone on to advise their own students who are also now involved with HiRISE. Many other graduate students have utilized HiRISE data in their research, but without direct team involvement.

3. Operations history

Although an orbiter in a nearly circular orbit and with a consistent local mean solar time (LMST) may sound ideal for stable operations, there have been many complications due to gaps in observing, roll

restrictions, dust storms (including the Global Dust Events, GDEs), special events (like supporting entry, descent, and landing (EDL) activities of other Mars missions), spacecraft or instrument anomalies, and other orbit or hardware changes. MRO or Mars events relevant to HiRISE are summarized in Table 4; HiRISE events are summarized in Table 5. Many of these events are explained in subsequent sections of this paper.

There have been multiple extended periods (at least 2 weeks) with no HiRISE observations (Table 6). Solar conjunctions (roughly every other year) pauses imaging for 4 to 5 weeks. There was an extended spacecraft “safe” (or contingency) mode in 2009, plus a 2-week cycle in 2020 with no imaging during a spacecraft non-volatile memory rewrite. On top of these interruptions, in 2019–2020 HiRISE needed to “stand down” and not participate in some cycles to free up resources to develop

Table 6

Periods when HiRISE did not image for 2 weeks or longer.

DATE	CYCLE	ORBIT	L_S	EVENT
2008-Nov-22–2008-Dec-19	54–55	10,902–11,260	162° - 177°	Solar conjunction
2009-Oct-10–2009-Dec-04	77–80	15,034–15,752	352° - 19°	S/c safe mode
2011-Jan-15–2011-Feb-11	110–111	20,964–21,322	218° - 235°	Solar conjunction
2013-Apr-06–2013-May-03	168–169	31,384–31,743	296° - 312°	Solar conjunction
2015-May-30–2015-Jun-26	224–225	41,446–41,805	350° - 004°	Solar conjunction
2017-Jul-15–2017-Aug-08	280	51,418–51,738	34° - 45°	Solar conjunction
2019-Mar-02–2019-Mar-15	322	59,054–59,232	349° - 356°	Stand down cycle
2019-Apr-27–2019-May-10	326	59,773–59,952	17° - 23°	Stand down cycle
2019-Jun-22–2019-Jul-05	330	60,492–60,670	42° - 49°	Stand down cycle
2019-Aug-17–2019-Aug-30	334	61,210–61,569	67° - 79°	Stand down cycle
2019-Aug-31–2019-Sep-13	335	61,390–61,569	73° - 79°	Solar conjunction
2020-Jan-04–2020-Jan-17	344	63,007–63,186	130° - 137°	Stand down cycle
2020-Feb-15,2020-Feb-28	347	63,546–63,725	151° - 158°	Non-volatile memory rewrite
2020-Jul-18–2020-Jul-31	358	65,522–65,700	241° - 250°	Stand down cycle
2020-Sep-12–2020-Sept-25	362	66,241–66,420	276° - 285°	Stand down cycle
2021-Sep-25–2021-Oct-22	389–390	71,094–71,453	104° - 117°	Solar conjunction
2022-Mar-12–2022-Mar-25	401	73,250–73,429	189° - 197°	Stand down cycle
2022-Jun-18–2022-Jul-01	408	74,508–74,687	249° - 258°	Stand down cycle

streamlined operations and to continue HiRISE with reduced funding. In 2022, there were additional stand down cycles due to lack of available personnel.

4. Summary of HiRISE archived datasets

4.1. Image products

The HiRISE data archive is a NASA Planetary Data System (PDS) version 3 (PDS-3) archive that can be directly accessed at <http://hires-pds.lpl.arizona.edu/PDS/>. The data archive can be broken down into two classes of products: standard products and various extra products (Table 7). The standard products consist of the raw data or Experimental Data Record (EDR) products, calibrated and map-projected Reduced Data Record (RDR) products, and Digital Terrain Models (DTMs), which include sets of orthorectified images derived from each DTM. The standard products can also be accessed at doi:[10.17189/1520303](https://doi.org/10.17189/1520303) for RDRs, doi:[10.17189/1520179](https://doi.org/10.17189/1520179) for EDRs, and doi:[10.17189/1520227](https://doi.org/10.17189/1520227) for DTMs. The extra products are derived from the standard products, and various cosmetic corrections, color stretching, size reductions, and lossy compression may have been applied that may make these products unsuitable for quantitative scientific analysis (McEwen et al., 2010). The NOMAP products consist of CCD mosaics in the raw geometry, without any pixel resampling, thus preserving the full resolution. As of August 2023, the archive contains >2.2 million standard products with a total data volume of 116 terabytes, and 6.3 million extra products with a total data volume of 126 terabytes. Browse images are available with and without annotations that include a scale bar and elevation range (for DTMs).

4.2. Imaging modes

Because HiRISE can be commanded with up to 14 CCDs, each with its own binning and TDI setting, there are many possible imaging configurations. Standard imaging modes were established to simplify the application of these configurations (McEwen et al., 2007). In the years that HiRISE has been operating, some standard imaging modes have been applied much more frequently than others. Modes with red CCDs in 4×4 binning are often saturated over illuminated terrain and are currently exclusively used for very low light scenes. Binning modes 8×8 and 16×16 are not useful for imaging Mars, and we have chosen to not use 3×3 binning to simplify the data processing. Modes that enable only a subset of the 14 CCDs have also gone largely unused in favor of full swath width modes, with a handful of exceptions. Narrow images with only the center two or four RED CCDs, and all four BG and IR CCDs have utility over potential landing sites, where full monochrome

coverage exists but additional color coverage is desired, and over small targets during periods with low downlink rates. Several additional modes restricted to only those CCDs less affected by bit-flips due to ADC issues (Section 8.9) at low temperatures were defined in 2017. Additionally, changing susceptibility to bit-flip degradation in certain CCDs has resulted in occasional updates to some mode definitions; for example, Bin 1-2A historically specified RED3 as unbinned, but is now 2×2 binned to mitigate bit-flips.

Table 8 lists the HiRISE standard imaging modes and their definitions as currently in use (see McEwen et al., 2007, for other defined modes). Of these, the most frequently used are Bin 2A, Bin 1A, and Bin 1-2A. Bin 2A, with all CCDs binned 2×2 , strikes a good balance between coverage extent, resolution, and high (>100:1) Signal-to-Noise Ratio (SNR) for most martian terrains under most lighting and frost conditions. Bin 1A, with un-binned red CCDs and 2×2 binning for the color CCDs provides the highest resolution (BG and IR CCDs require 2×2 binning for high SNR). Bin 1-2A, with RED3 (until recently) and REDs 4–6 at full resolution and all remaining CCDs binned 2×2 , has proven useful to cover small features or samples of patterned terrain at full resolution, with additional binned coverage for local context. The mode can also serve as a compromise when operational or lighting constraints make full resolution over the full swath width unfeasible. Another new mode is called the “no-warmup” mode, consisting of a subset of CCDs that return good data when the FPE is relatively cold (below the minimum temperature for full images). That subset includes REDs 4–6, BG12–13, IR11, and IR10 channel 0 (we also acquire channel 1 with some erroneous data). We now also include REDs 7–8 with recently improved ADC settings (Section 8.9), although they may be removed in the future depending on ADC bit-flip degradation rates.

In response to the failure of RED4 in 2023, perhaps due to cycling to high temperatures, we expect to reduce bin-1 imaging in RED0–3 to enable operation at lower temperatures. This leads to a new mode that uses bin-1 for RED5–8 and bin-2 for RED0–3.

Almost all HiRISE images of Mars are acquired with 2 types of data compression, and a third type of compression is used on the ground. First, the input 14-bit data are converted to 8 bits via non-linear look-up tables (LUTs), then the lossless Fast and Efficient Image Compression System (FELICS; Howard and Vitter, 1993) is applied in the spacecraft solid-state recorder. Returning uncompressed data is also possible but takes ~5 times more data volume per image. For data products on the ground we use JPEG2000 format (Taubman and Marcellin, 2012), typically just slightly lossy, for rapid browse and zoom over the images (Section 5.2).

Table 7

HiRISE archive product listing organized by type (Standard or Extra), the current PDS-3 storage format and the planned storage format after conversion into PDS-4.

Product	Type	PDS-3 Format	PDS-4 Format
Experimental Data Records (EDR)	Standard	PDS-RAW (IMG) + attached PDS-3 label	PDS-RAW (IMG) + detached PDS-4 label
EDR browse and thumbnail products	Extra	JPEG	JPEG + PDS-4 label
Reduced Data Records (RDR) (Map- Projected Products)	Standard	Non-lossy compressed JPEG2000 image with detached PDS-3 label	Uncompressed PDS-RAW or geotiff product + detached PDS-4 label
RDR browse and thumbnail products	Extra	JPEG	JPEG + PDS-4 label
RDR “Quicklook” products	Extra	Lossy compressed JPEG2000	Lossy compressed JPEG2000 + PDS-4 label
Merged products (IRB and simulated RGB)	Extra	Lossy compressed JPEG2000	Lossy compressed JPEG2000 + PDS-4 label
RED, BG, IR, IRB, RGB NOMAP products	Extra	Lossy compressed JPEG2000	Lossy compressed JPEG2000 + PDS-4 label.
Stereo Anaglyphs	Extra	Lossy compressed JPEG2000, JPEG	JPEG2000, JPEG + PDS-4 label
Digital Terrain Model (DTM)	Standard	PDS-RAW (IMG) + attached PDS-3 label	PDS-RAW + detached PDS-4 label
DTM-derived Orthorectified images	Standard	Compressed JPEG2000 image + detached PDS-3 label	Uncompressed PDS-RAW or geotiff + PDS-4 label
DTM browse and thumbnail images	Extra	JPEG	JPEG + PDS-4 label
DTM Figure of Merit (FOM) map	Extra	JPEG2000	JPEG2000 + PDS 4 label
DTM Slope Maps (coming soon)	Extra	PNG	PNG + PDS 4 label

Table 8

Common HiRISE Imaging Modes.

Name	Description	RED 4–6*†	Other REDs†	NIR†	BG†	Size‡
Bin 1A	Highest res at >100:1 SNR; stereo	Bin 1 TDI 128	Bin 1 TDI 128	Bin 2 TDI 128	Bin 2 TDI 128	0.66
Bin 1	Bin 1 full FOV RED, 4 × 4 color	Bin 1 TDI 128	Bin 1 TDI 128	Bin 4 TDI 64	Bin 4 TDI 64	0.61
Bin 1-2A	Bin1 RED4–6; others bin 2	Bin 1 TDI 128	Bin 2 TDI 64	Bin 2 TDI 128	Bin 2 TDI 128	0.37
Bin 1–2	Bin1 RED4–6; others binned	Bin 1 TDI 128	Bin 2 TDI 64	Bin 4 TDI 64	Bin 4 TDI 64	0.32
Bin 2A	Bin 2 everything	Bin 2 TDI 64	Bin 2 TDI 64	Bin 2 TDI 128	Bin 2 TDI 128	0.22
Bin 2	Bin 2 full FOV RED, 4 × 4 color	Bin 2 TDI 64	Bin 2 TDI 64	Bin 4 TDI 64	Bin 4 TDI 64	0.17
Bin 4	Bin 4 everything	Bin 4 TDI 32	Bin 4 TDI 32	Bin 4 TDI 64	Bin 4 TDI 64	0.06
Bin 1A No Warmup	Bin 1 RED4–8, 2 × 2 color	Bin 1 TDI 128	–	Bin 2 TDI 128	Bin 2 TDI 128	0.40
Bin 2A No Warmup	Bin 2 RED4–8, color	Bin 2 TDI 64	–	Bin 2 TDI 64	Bin 2 TDI 128	0.15
Bin 1 No Warmup	Bin 1 RED4–8, 4 × 4 color	Bin 1 TDI 128	–	Bin 4 TDI 64	Bin 4 TDI 64	0.10

* Includes RED3 for Center Bin 1A, REDs7–8 for No Warmup modes.

† TDI varies with lighting conditions.

‡ Gb/10 K bin-1 lines (compressed), varies with scene and atmospheric conditions.

4.3. Coverage over Mars

HiRISE coverage of Mars is highly non-uniform; Fig. 3 shows how many HiRISE images are within 100 km of each point of the surface; some locations have hundreds of images. About 0.85% of Mars has no HiRISE coverage within 100 km, while the most-frequently imaged 1% of the planet’s surface has at least 120 images within that distance. MRO’s polar orbit ensures the scientifically interesting polar regions are well covered. Some non-polar locations stand out as programmatically important (e.g., potential or actual landing sites such as Meridiani Planum, Jezero crater, or Gale crater) and/or scientifically important (e.g., Valles Marineris). Broad areas that are heavily imaged often have regions to their north and south with poor coverage due to limits on how closely HiRISE images can be spaced along MRO’s south-to-north dayside orbit; isolated hot spots (Fig. 3) result from monitoring sites where many images are concentrated. Many such sites occur in the southern highlands between 30°–60°S as a result of monitoring gullies and RSL.

HiRISE coverage of Mars has increased in a quasi-linear fashion (Fig. 4) throughout the mission, with occasional hiatuses (Table 6). Fluctuations in the data return rate (with a period of approximately 26 months) are driven by the changing Earth-Mars distance. The most recent fluctuations are muted in amplitude as HiRISE is increasingly limited by thermal constraints rather than downlink during high data rate periods.

Stereo coverage has also increased quasi-linearly with additional slow periods corresponding to seasons with spacecraft roll restrictions. As of 19 June 2023, 7578 complete planned stereo pairs have been acquired. There are also unplanned stereo pairs, typically with poorer convergence angles or illumination angle matches.

4.4. How Mars affects the images

Mars and its atmosphere have numerous effects on images, both predictable and unpredictable. The most obvious of these is surface reflectivity which affects the signal received by HiRISE, thus driving the choice of the number of TDI lines and binning to receive adequate signal (McEwen et al., 2007).

Although MRO is in a Sun-synchronous orbit that results in a nearly fixed local imaging time (Zurek and Smrekar, 2007), the lighting at that local time varies with latitude and season. The incidence angle describes the angle between a vector to the Sun and the local vertical. Small incidence angles emphasize color and albedo variations, while topographic effects dominate the appearance of images at larger incidence angles. Shadows grow at larger incidence; their abundance depends on local topography, but they are usually not severe at incidence angles <65°, thus serving as a typical criterion for stereo targeting. SNR is also lower at large incidence angles. Sub-solar azimuth (the direction to the Sun) also varies with the season. The details of the lighting variation are latitude dependent. For the typical 3 PM MRO local time, equatorial sites

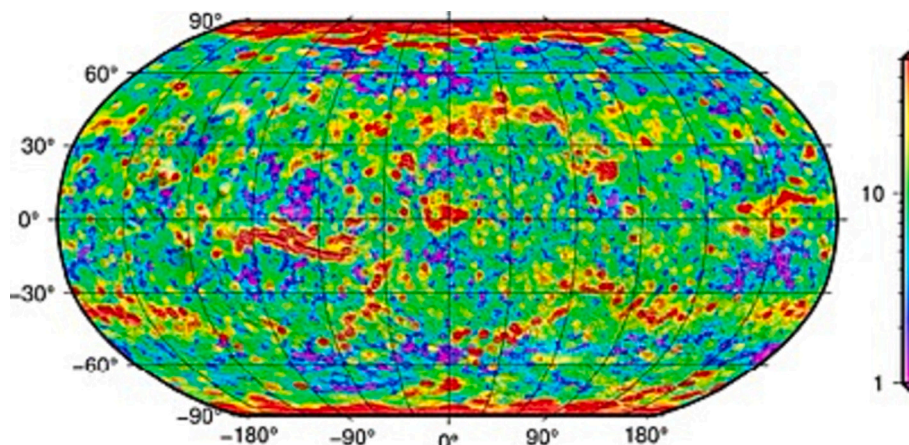


Fig. 3. Global view of the number (on a log scale) of HiRISE observations (up to orbit 74,507) within 100 km. The color scale saturates at 50.

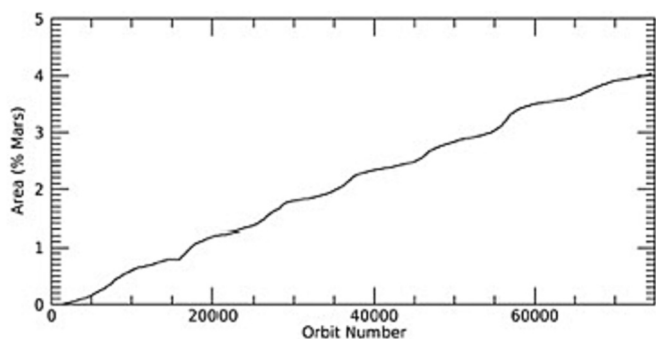


Fig. 4. Area of all HiRISE images through time (units of % of Mars surface covered). Many targets are imaged multiple times for stereo or change-detection investigations so the unique area of Mars with HiRISE coverage is lower than the area of the images.

have their smallest incidence angles near the equinoxes, but even at solstices, the surface is well-illuminated. The mid-latitudes are never in complete darkness but have severe shadows around the winter solstice, so imaging non-seasonal targets is concentrated in spring and summer. The poles are in darkness for half the year, but incidence angles approach 60° at the summer solstice.

Atmospheric dust also influences imaging and image quality. The globally averaged optical depth of dust in the atmosphere is typically $\sim 2\times$ higher in southern spring and summer (e.g., Smith, 2008), thereby reducing image quality. These seasons also include most dust storms (often between L_s 240–320°), including the GDEs of MY28 and MY34. Those two GDEs resulted in severely degraded images and led to restricted target selection (favoring the south pole and high-elevation sites) for many weeks. Regional dust events sporadically degrade image quality as well. For example, the Hellas basin is often obscured by dust or condensate haze except for imaging windows that are usually best between L_s 0–50° and 140–180°.

Another atmospheric effect is the formation of condensate clouds as well as diffuse hazes. The most significant cloud effect is the northern polar hood, which occurs through most of northern autumn and winter, starting near the pole but eventually extending into the mid-latitudes (Calvin et al., 2015). Images near the north pole commonly have degraded quality starting near $L_s = 160^\circ$, and the effects reach 35–40°N in northern winter.

Another significant influence that Mars has on imaging is the occurrence of seasonal frost mainly composed of CO_2 (Wood and Paige, 1992). Frost is of interest for some science objectives but a hindrance for others. This frost covering is a dynamic agent of surface change but

obscures the underlying materials and challenges the stereo matching algorithms. Seasonal frost has both a latitude and slope dependence. On level ground, it is present throughout fall and winter near the poles while appearing only briefly near the winter solstice at its lowest latitudes, around $\pm 50^\circ$ (Piqueux et al., 2015b). Local frost on pole-facing steep slopes extends to proportionately lower latitudes (Dundas et al., 2019a).

4.5. Statistics of each science theme

HiRISE suggestions are divided into 17 science themes and an additional “Other” category for planning purposes. Over time, some themes have proved less prevalent, and their use has evolved. For instance, the “Hydrothermal Processes” theme has had few suggestions; the “Climate Change” theme now concentrates on north polar avalanches and south polar residual cap changes (although neither necessarily indicates that any climate change is occurring); and the “Other” theme is now restricted to observations acquired with no prior suggestion, such as ride-along observations with other instruments.

Each suggestion is assigned one primary science theme (and an optional secondary theme), and the observation that retires the suggestion inherits that categorization. STLs (Table 2) prioritize these suggestions and verify the data acquired satisfies the needs of the suggestion. Table 9 summarizes the number of observations that stemmed from suggestions in each science theme and the number of remaining suggestions in each priority category.

4.6. Remaining observation suggestions

As of August 2022, 22,603 suggestions prioritized by STLs are still active (not yet retired). The spatial distribution of active HiRISE suggestions is extremely non-uniform (Fig. 5), as is the spatial distribution of acquired images. Poleward of about 60° , active suggestions are sparse as MRO’s polar orbit provides many opportunities to image these areas. Extensive dust-covered areas (such as Tharsis) provide fewer high value targets at HiRISE scales and so have fewer suggestions. Also, suggestions that are entered in “unpopular” regions tend to be quickly planned and retired. Popular target areas (e.g., Valles Marineris, Syrtis Major) have many remaining high-priority suggestions as opportunities to image there are limited and are further reduced by competition with other MRO instruments. MRO orbits in the vicinity of recent landing sites have been heavily used for programmatic candidate landing site characterization and data relay (Section 7.16) and so many other suggestions in these areas remain to be acquired, particularly because such areas are often of high scientific interest. Over time the suggestion map has become increasingly non-uniform because the few high-priority targets in unpopular regions are soon acquired. We encourage new targets in

these unpopular regions.

4.7. Data biases

HiRISE observations have a variety of spatial and temporal biases. Seventeen years since the start of full operations, HiRISE images cover a cumulative area of $\sim 4.5\%$ of the martian surface; however, unique coverage (excluding repeats for stereo and monitoring) is $<3\%$. That coverage is not random and is subject to both targeting preferences and operational constraints.

Because HiRISE is a targeted imager, coverage is inherently concentrated on sites thought to be of interest. Thus, images preferentially cover features such as fresh craters or outcrops of layered deposits, compared with featureless areas. This selection strategy is necessary to best use the limited HiRISE coverage; as a result, the images are not random samples. Another result of this strategy is that sub-polar latitudes ($\sim 60\text{--}80^\circ$ in each hemisphere) and other regions have a relatively low density of images.

Various operational considerations also influence the HiRISE data set. Because MRO is in a polar orbit, the poles can be imaged most easily and are of high scientific interest, which is why they have the most coverage per unit area. MRO data-relay procedures for landed spacecraft result in restricted imaging on orbits that pass near landers and rovers (Section 7.16). A similar effect arises when any given target competes with nearby suggestions that cannot fit in the same field of view, and with observations along the same orbit track. These constraints mean that frequent monitoring of one site limits the ability to image nearby sites. Additionally, targets along the same orbit tracks as Valles Marineris, candidate landing sites, or other regions with many high-priority target suggestions are harder to acquire and may be underrepresented.

A final consideration is that some regions have limited intervals when high-quality images can be acquired, such as seasonal shifts of coverage and resolution due to frost, lighting considerations, and the polar hood (Section 4.4). The most pronounced effect is in the low-elevation Hellas basin due to the combination of atmospheric haze in summer and darkness in winter.

4.8. Surface change detection

Observations to characterize surface changes (also called monitoring) include both designated seasonal series and occasional (often yearly) repeat images testing for longer-term changes. These were a relatively small part of HiRISE operations in the early mission, focused

on seasonal defrosting processes. They have increased over time, driven particularly by the discovery of bedform migration (e.g., ripples, megaripples, dunes) (Silvestro et al., 2010, 2020; Bridges et al., 2011) and multiple types of slope activity (Diniega et al., 2010; Dundas et al., 2010; McEwen et al., 2011) and the opportunities afforded by multiple extended missions for change detection. During the PSP, 6.2% of acquired observations were in the Seasonal Processes science theme, 3.4% in Aeolian Processes, and 2.0% in Mass Wasting. In contrast, during MY35, 10.5% of acquired observations were in Seasonal Processes, 7.4% in Aeolian Processes, and 17.0% in Mass Wasting. While not every observation in those themes is a monitoring suggestion, a large majority are, indicating the growth in change detection imaging. This temporal coverage has resulted in some of the most significant HiRISE science results but, as a consequence, reduced non-monitoring observations of new, unique locations. More non-monitoring image suggestions are needed to help restore balance to future observations.

4.9. Coordination with other instrument experiments

Coordinated observations—the simultaneous observations of a common target by multiple instruments—are acquired at locations where the synergy between HiRISE, CRISM, CTX, and CaSSIS can address significant scientific questions. HiRISE/CRISM/CTX coordinated observations have enabled detailed geological and compositional characterization of many targets on Mars. For example, coordinated HiRISE observations have allowed researchers to correlate CRISM-based mineral detection with morphological features, stratigraphic relationships, and spatial distributions (e.g., Murchie et al., 2009; Wray et al., 2011; Weitz et al., 2022). HiRISE color ratios complement CRISM-based spectral characterization of geological units (Delamere et al., 2010). Coordinated CRISM and HiRISE observations have allowed a detailed characterization of the seasonal evolution of the composition of the seasonal ice on the polar caps (Pommerol et al., 2011). Limited spectral and morphological characterization of dynamic, seasonal features on Mars, such as recurring slope lineae and topographic slumps, have been possible with coordinated HiRISE-CRISM observations and MARCI daily global images (Ojha et al., 2017). SHARAD observations are also important for joint analyses (e.g., Morgan et al., 2021) but are typically acquired at night, so they are not simultaneous with optical datasets. MCS operates both day and night, and MCS plus HiRISE data have been used to understand seasonal processes and the evolution of polar volatiles (e.g., Wilcoski and Hayne, 2020).

In addition to the compositional and morphological characterization,

Table 9

Science Theme Statistics extracted in August 2022.

Science Theme	Number of Observations	Remaining Prioritized Suggestions with this priority				
		10	9	8	7	6
Climate Change	1743	29	108	142	53	51
Composition & Photometry	3615	21	105	149	119	39
Aeolian Processes	4311	184	431	542	591	92
Fluvial Processes	5327	32	510	612	181	3010
Future Exploration / Landing sites	2425	27	81	143	63	57
Geologic Contacts / Stratigraphy	5424	64	225	1052	996	52
Glacial/Periglacial Processes	6031	26	71	218	182	227
Hydrothermal Processes	384	4	55	33	12	4
Impact Processes	8720	36	159	698	517	179
Landscape Evolution	4809	10	53	354	860	790
Mass Wasting Processes	7978	513	1496	2176	585	79
Other	2478	0	2	7	6	24
Polar Geology	4225	17	128	129	31	29
Rocks & Regolith	1501	0	5	34	31	25
Seasonal Processes	6930	162	235	309	112	74
Sedimentary / Layering processes	3124	40	169	264	100	22
Tectonic Processes	3087	29	142	264	58	132
Volcanic Processes	3752	8	92	360	225	35
Total	75,864	1202	4067	7486	4722	4921
Percent		6	18	33	21	22

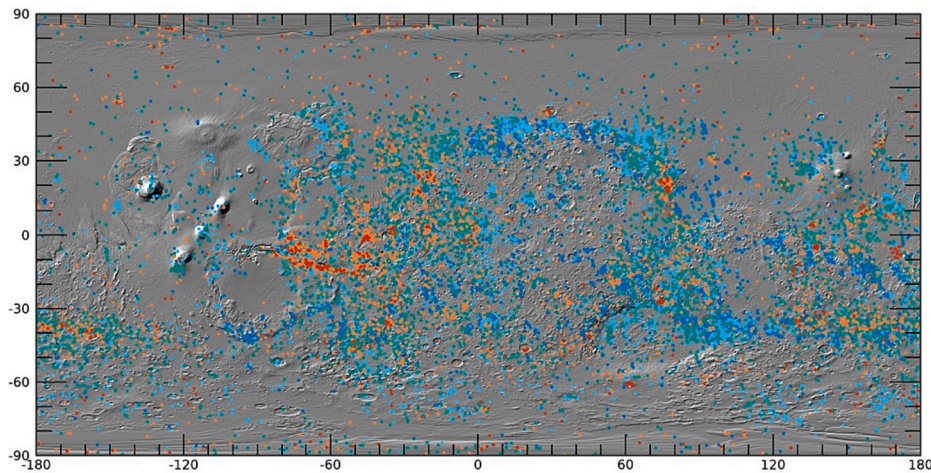


Fig. 5. Global view of current active HiRISE suggestions. Colors are Science Theme Lead priority 10 (red), 9 (orange), 8 (teal), 7 (cyan), and 6 (blue). (For interpretation of the references to color in this figure legend, the reader is referred to the web version of this article.)

coordinated HiRISE-CRISM observations enable the characterization of the dynamic behavior of active geological features (e.g., Reiss et al., 2014). The imaging technique employed by CRISM results in net-positive and negative time offsets from the center of the image, which causes a slight offset in the acquisition time between CRISM and HiRISE/CTX. The approximately ± 1 min acquisition time differences can be utilized to track the motion of active geological features such as dust devils (Fig. 6; Reiss et al., 2014). These coordinated observations are an excellent complement to the faster changes due to dust devil rotation that can be investigated between HiRISE color channels (Choi and Dundas, 2011).

Despite their scientific utility, coordinated observations are only planned for a subset of all observations. The HiRISE team requests coordinated observations from CTX for all stereo images and when coordination is mentioned in the image suggestion. Additionally, CTX images are acquired for all targeted observations by both HiRISE and CRISM. By contrast, coordinated CRISM observations are requested by the science theme lead or if an image suggestion mentions composition as one of the targeted science outputs.

The HiRISE team strives to satisfy coordination requests from CTX or CRISM, but this is sometimes impossible due to thermal, data volume, time, or other constraints. Of particular importance, the CTX team alerts the HiRISE team of candidate new impact events for HiRISE follow-up to confirm and measure the craters, if present. >1200 new impact sites are now documented by before-and-after images, most from MRO (Daubar

et al., 2022). Targeting old CRISM data locations with interesting mineral identifications continues beyond the end of CRISM routine operations in 2022 (Seelos et al., 2023).

HiRISE also coordinates observations with CaSSIS on ExoMars TGO to view a location at two different times of day in the same season. Typically observations can be acquired within about two weeks, so seasonal changes are minimized. TGO plans observations weeks in advance of MRO for the same period, so the HiRISE team can target observations that correspond to already-planned CaSSIS observations.

4.10. Lunar observations during extended missions

HiRISE observations of Earth's moon acquired during cruise and PSP were not useful for absolute radiometric calibration due to poor observational geometry. Therefore, new HiRISE images of Earth and the Moon were acquired in 2011 and 2016 that are more suitable for absolute radiometric calibration. The martian moons were also observed in the PSP (McEwen et al., 2010).

4.11. Comet observations

In 2013 and 2014, two comets (ISON and Siding Spring) made close approaches to Mars and were observed by HiRISE (Table 10). For ISON (named after the International Scientific Optical Network), ten useful observations were made near the closest approach. Assuming an albedo

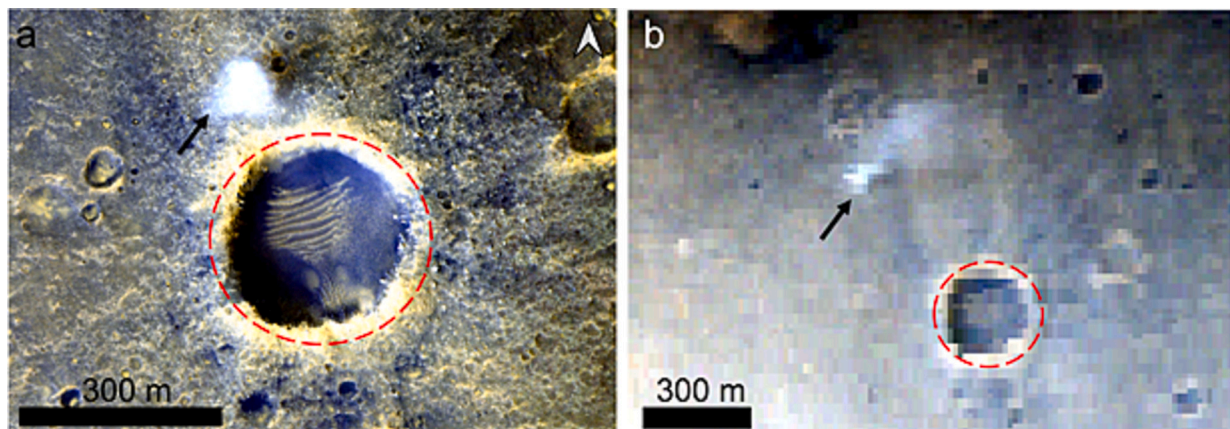


Fig. 6. Coordinated HiRISE observation ESP_021925_1650 (a) and CRISM observation FRT0001D8DC (b). The black arrow points to a ~ 50 -m-diameter dust devil that moved ~ 400 m between the acquisition of the two sub-images (~ 34 s). The red outline shows the same crater in the HiRISE and CRISM view. (For interpretation of the references to color in this figure legend, the reader is referred to the web version of this article.)

Table 10

HiRISE observation campaigns for comets ISON and Siding Spring.

	ISON C/2012 S1	Siding Spring C/2013 A1
Perihelion	28 Nov 2013	25 Oct 2015
CA to Mars	13,000,000 km	138,000 km
Observation time	29 Sep to 02 Oct 2013	17 Oct to 20 Oct 2014
Phase angle (deg.)	47 to 89	88 to 107
IFOV		1 micro-radian
# observations	10	54
Colors	RED, BG	RED, BG, IR
Exposure time		2.5 s max

of 0.03 and using a nucleus phase law, [Delamere et al. \(2013\)](#) estimated an upper limit to the nucleus diameter near 1 km. Early news reports had estimated a 5-km diameter nucleus of ISON. HiRISE obtained 54 observations as close as 138,000 km, for comet Siding Spring, showing the comet and associated jets. The nucleus was largely behind the comet, but [Farnham et al. \(2017\)](#) state that the nucleus is a ~ 1 km non-spherical body. Early news reports estimated a 50-km diameter nucleus for Siding Spring. HiRISE data proved critical to accurately constrain the cometary nuclei size and for deriving high-precision trajectories for the comets (e.g., [Farnocchia et al., 2016](#)).

4.12. How to access the HiRISE data

HiRISE data are archived in the PDS Cartography and Imaging Sciences Node (see [Table 11](#) for links to all the resources in this section). HiRISE releases standard data products to the PDS on a monthly cadence. Data are typically released within two months of receipt of the raw data on the ground. The PDS is designed to be an archive from which various tools query the data for viewing, analysis, or visualization. Here we provide a partial list of current tools and websites that can be used to search, process, or download HiRISE images and DTMs.

The HiRISE website (<https://hirise.lpl.arizona.edu/>) serves as one way to browse and search the catalog. The “Map” page provides a Mars graphical interface showing HiRISE image footprints plus those of CaSSIS, CTX, MOC, and CRISM, as well as suggested targets for HiRISE and CaSSIS. It is searchable by keywords or observation IDs in the main search field or by region, season, theme, or other parameters available in the “Advanced Search” option. DTMs are searchable via the Advanced Search page or a global map linked to the DTM page. The HiRISE website provides a link to download the free HiView (Section 5.2) application (see “software” link at the bottom of the web page), which allows users to easily view the full-scale JPEG2000 image files (JP2 files) without needing to download them. The website also provides CTX images (<https://hirise.lpl.arizona.edu/ctx>) that have been map-projected using the same mapping definition and global shape model as HiRISE, ensuring accurate co-registration with simultaneously-acquired HiRISE products.

The PDS Geosciences node provides a website called Mars Orbiter Data Explorer (Mars ODE) that interfaces with multiple Mars missions, including MRO. Users can query by instrument and data type, by geographic coordinates, time ranges, or within a map. The Mars ODE

Table 11

URLs and descriptions of various tools to query, visualize, and analyze HiRISE data.

Name	URL	Description
PDS	https://pds-imaging.jpl.nasa.gov/volumes/mro.html	MRO volumes on the PDS Cartography and Imaging Sciences Node
HiRISE	http://uahirise.org	HiRISE public website
HiView	https://www.uahirise.org/hiview/	JPEG2000 Viewer provided by HiRISE
HiRISE DTMs	https://www.uahirise.org/dtm/	DTM catalog on the HiRISE website
Mars ODE	https://ode.rsl.wustl.edu/mars/	Search and download Mars data including HiRISE images and DTMs
ASU HiRISE image map	http://global-data.mars.asu.edu/bin/hirise.pl	Global map of HiRISE image footprints that link to downloadable files
PILOT	https://pilot.wr.usgs.gov	Map query and send for processing via POW
POW	https://astrocloud.wr.usgs.gov	Map projection on the web of images selected in PILOT
JMARS	https://jmars.asu.edu	GIS for analysis of HiRISE images and DTMs with the Mars datasets.
HiMap	https://marsweb.nas.nasa.gov/HiRISE/hiweb/marsbrowser/index.html	See section 5.3
MarsSI	https://marssi.univ-lyon1.fr/MarsSI/map/mars/	Web application for processing Mars image data, including HiRISE.

also includes a tool to search for coordinated observations between MRO instruments (e.g., HiRISE and CRISM). Selected files can be downloaded in raw or processed formats. The site provides instrument footprint files in shapefile and Keyhole Markup Language (KML) vector format, enabling users to perform their own spatial queries.

Other free, map-based viewers that serve the HiRISE images (but not DTMs) include the Google Earth app (when set to Mars), Arizona State University’s (ASU) HiRISE image map, and the USGS PDS Planetary Image Locator Tool (PILOT; [Bailey et al., 2013](#)). One caution to users of these sites is to be aware that they may not display all of the most current data available in the PDS. PILOT allows for the selection of images to be sent for further processing (i.e., map projection) via the USGS Map Projection on the Web (POW) service ([Hare et al., 2013](#)) and provides tools for identifying unplanned stereo acquisitions. Perspective views from projected orthoimages and DTMs can also be explored at Areo-Browser (<https://areobrowser.com/>). The online GIS application, MarsSI, is a searchable global map of Mars data that includes services to process HiRISE image data and DTMs ([Quantin-Nataf et al., 2018](#)).

HiRISE data (including DTMs) are available within the Java Mission-planning and Analysis for Remote Sensing (JMARS) application ([Dickenshied et al., 2019](#)). The program is installed locally, but data are served from ASU via the internet. The interface functions as a geospatial information system (GIS) in that it is map-based and can display various datasets in the same geographic coordinate system. JMARS is particularly useful for analysis of HiRISE data directly with other Mars datasets.

4.13. PDS 4 support

We are developing procedures to convert the PDS-3 archive into PDS-4 format ([Rough and Hughes, 2021](#)). The updated PDS-4 standard requires standard science products to be archived without any special encoding (such as JPEG2000) to help ensure very long-term accessibility of the data (Planetary Data System Standards Reference v1.18.0). This restriction poses the greatest challenge to the conversion process, as the JPEG2000 compression can achieve reductions in the product data volume by as much as a factor of 5. Creating these uncompressed products thus presents a significant expansion in the amount of storage required to house the data archive. However, this restriction only applies to the standard science products. JPEG2000 is acceptable for the derived extra products, and it is anticipated that these products will not

be redelivered in an uncompressed format. Table 7 lists all the different types of products in the HiRISE data archive, and how they will be changed for PDS-4 compatibility.

The initial delivery of PDS 4 compatible products is anticipated to occur in 2024. This initial delivery will only contain products derived from data acquired no earlier than October 2022, the start of EM6. All earlier HiRISE data are planned to be reprocessed into PDS-4 format over the next five years. These products will be delivered to a cloud service maintained by the PDS Imaging Node to allow easier management of the increased data volume required by the decompressed science products. All subsequent deliveries will continue to be delivered in the PDS 4 format. We intend to continue delivery in the PDS-3 format as well as PDS-4, because the JPEG2000 format greatly aids accessibility to the large (Giga-pixel) images using tools such as HiView.

4.14. Incomplete observations

When only part of an observation has been returned, it is incomplete. This data loss typically occurs when image packets are overwritten in the SSR by newer data, mostly when the DSN downlink is reduced, such as problems with DSN ground equipment or altered DSN pointing to address a spacecraft problem. Incomplete observations are concentrated in periods of high data rate because there is little time to replay the data before it is overwritten. The partial HiRISE observation is processed and released to PDS but contains gaps with no data. The gaps range from nearly all of the observation to just a single 20-line gap in one channel. Most gaps are at least 20 lines of a channel because that is the image size used for lossless compression in the SSR. Uncompressed images may have gaps of any size. 14.7% of HiRISE observations are incomplete.

5. Special data products and analysis tools

Basic PDS Data Products are summarized in Section 4.1 above. This section provides more details on how PDS products are produced, special data products, and publicly available analysis tools, updating the information in McEwen et al. (2010).

5.1. ISIS updates

HiRISE image processing pipelines utilize individual programs from the Integrated Software for Imagers and Spectrometers (ISIS; Becker et al., 2007). ISIS is frequently updated with new capabilities (Backer et al., 2018). Few such updates have been made specifically for HiRISE in recent years, but some of the updates do change the HiRISE data products in subtle ways, so products are made in different ways over time. In addition, the HiRISE team has made some changes to how images are processed, i.e., using different ISIS input parameters. As part of the PDS-4 conversion effort, we plan to reprocess all images to ensure consistency.

5.2. HiView

HiView is the best way to explore HiRISE images of the martian surface at full resolution, taking full advantage of the JPEG2000 format for rapid response in navigating large images. Once the application has been downloaded to your computer (<https://www.uahirise.org/hiview/>), all that is needed is a quick drag and drop of any of the links for JP2 files on the HiRISE website to the HiView application window. No downloading of multi-gigabyte files is required. HiView also provides dynamically generated statistics about the current area of an image being viewed, whether it is the entire original source at a low resolution, or a small area that has been expanded to full resolution. Multiband histograms can be used to enhance the color stretch and contrast of the currently viewed area and can be reapplied to other areas of an image or to different images. HiView can save the area of an image currently displayed as a TIFF, JPEG, PNG or other format for use in

different image editing applications for further enhancement of any particular region of interest at full resolution.

5.3. HiWeb and HiMap

Prior to the development of HiWish (Section 7.2) in 2013, the HiRISE science team exclusively used HiWeb in selecting imaging targets. The HiRISE team continues to use HiWeb for targeting and for prioritizing image suggestions. HiWeb is a web-launched Java application, and geospatial information system, that enables users to peruse the various Mars orbital data and image sets and enter their desired imaging targets in an image suggestion registry, as described previously (McEwen et al., 2007, 2010). HiWeb is not publicly available, but HiMap (Fig. 7) is a dynamic, multi-faceted web tool that is an updated front-end to the entry maps interface of HiWeb. HiMap was born out of the desire to make HiRISE, CRISM, and CTX footprints and images available on an interactive map interface within HiWeb without having to first access the image suggestion facility. In addition, HiMap allows HiRISE JPEG2000 images to be viewed at full resolution in a web browser environment and adds updated analysis tools such as the automated elevation profiler, distance tool, and interactive contrast image enhancer.

5.4. Color merge products

The official PDS-archived images include a full RED CCD and narrow 3-color products. In 2009 we added a new PDS “extras” product in which the color images (both RGB and IRB in 2 separate products, Table 7) are merged onto the RED image (Fig. 8). We produce this at a scale of 0.5 m/pixel even for bin-1 image modes to keep the data volume reasonable, so users need to be aware that this product may not preserve the full RED-image resolution. We also increase the color saturation to better show the color variations. The COLOR products preserve the correct radiometric balance between colors for photometry.

5.5. Stereo anaglyphs

Stereo anaglyphs have been produced since 2008 for latitudes 80°S–80°N (McEwen et al., 2010) as PDS extras, but initially omitted polar locations where the parallax is complicated because the spacecraft off-nadir pointing is more toward the pole than to the east or west. An update to the procedure was completed in 2014 to enable processing of anaglyphs for polar images. A projection rotation that optimizes parallax must be calculated using geometric and photometric information of the stereo pair.

5.6. HiPrecision

After radiometric calibration, precision geometric calibration is performed to remove distortion across the focal plane due to the optical curvature of the beam, remove the CCD offsets, and optionally correct for spacecraft jitter. All three of these corrections are accomplished by the HiPrecision subsystem, which has two branches. The HiRISE Jitter-analyzed CK (HiJACK) branch applies the jitter modeling described in Sutton et al. (2019) to correct geometric distortions. The NoProj branch performs geometric correction only, without modeling and correcting for jitter, as not all HiRISE images require jitter correction. While we apply HiPrecision to only small numbers of images, as requested by members of the science community, it has been applied to all of the images used to produce DTMs over landing sites (Section 6).

5.7. DTM production

Since the PSP, the number of HiRISE DTMs that have been produced has risen from ~60 to >1000 and counting (Fig. 9). The percentage of planned and acquired HiRISE stereo pairs made into PDS DTMs

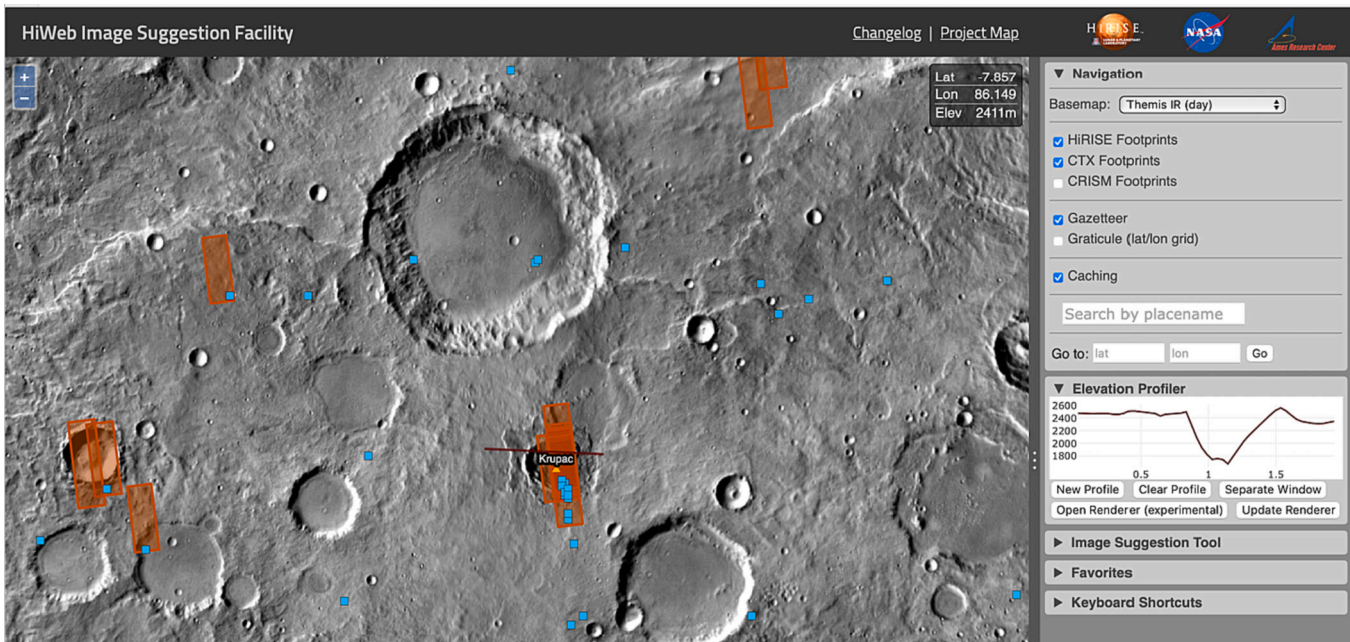


Fig. 7. Example of HiMap's interface. HiRISE, CTX, and CRISM footprints can be displayed and accessed directly by clicking on the footprints. An elevation profiler can give a quick insight to a 3D perspective. Interactive latitude, longitude, and elevation is given by cursor location.

represents $\sim 12\%$ of the >7660 planned stereo pairs acquired as of August 2023. (There are also unplanned stereo pairs due to overlap of image coverage on a target.) DTMs are now released to the PDS monthly as they are completed.

HiRISE DTMs in the PDS are produced using a combination of the ISIS software and the commercial photogrammetry software SOCET Set (BAE Systems, Inc.). Although details of the process have evolved, the basic procedure is consistent with what is described by Kirk et al. (2008) and described in more detail by Sutton et al. (2022b). HiRISE DTMs are typically produced at either 1 m/post for 25 cm/pixel (bin-1) stereo pairs or at 2 m/post for 50 cm/pixel (bin-2) stereo pairs. The accompanying orthoimages are produced at full resolution and the same scale as the DTM, with some exceptions. Files exported from SOCET Set are post-processed in ISIS to generate PDS (v. 3) standard files. DTMs produced using the ISIS/SOCET Set workflow conform to the formats and outputs that can be converted to standard PDS and PDS Extras products. Eight different institutions have contributed to the HiRISE DTM PDS archive.

Modifications to the ISIS/SOCET Set workflow have been developed to incorporate multiple monitoring images taken over a target where a DTM exists to build a time series of orthoimages (Sutton et al., 2022b). Such sequences have been critical for studying active surface processes. The refinement of techniques and analysis have made HiRISE DTMs essential to the characterization of candidate landing sites for robotic and human exploration (Kirk et al., 2008; Ferguson et al., 2017, 2020).

HiRISE DTMs have also been produced (typically at a reduced spatial scale) with the Ames Stereo Pipeline (Beyer et al., 2018). Because this is an automated pipeline that can be re-run relatively easily, we do not attempt to archive these with the PDS.

5.8. DTM extras and visualization products

The HiRISE DTM PDS extras products include “browse” images of the DTM and accompanying orthoimages (Fig. 10). Browse images (JPEG format) of the DTM include a shaded relief map, colorized altimetry combined with shaded relief, and a grayscale image. Browse images are available with and without annotations, including a scale bar and elevation range. The browse images provide a rapid and accessible way to visualize the terrain type, roughness, elevation variability, and

elevation range. A Figure of Merit (FOM) map, provided in the JPEG2000 format, displays a classified map of the quality of each DTM post draped over the shaded relief and is provided at full scale.

A new (to be released by 2024) DTM extras product is a slope map (Sutton et al., 2023). Prior to calculating slope, the DTM is smoothed with three sequential 5×5 lowpass filters followed by a $3 \times$ reduction in scale. This results in a slope calculation over ~ 9 m baseline for a DTM produced at 1 m post spacing. The lowpass filters (smoothing) minimize the systematic texture and small-scale slope errors at the post-spacing scale that is characteristic of the SOCET Set NGATE product (Kirk et al., 2021; Sutton et al., 2022b). Slope is calculated on the lowpass-filtered, reduced DTM using the Horn algorithm (Horn, 1981), as implemented in the ISIS application *slpmap*, which calculates the gradient at each pixel from a weighted difference of the surrounding 8 pixels (Horn, 1981). The grayscale slope map is archived and classified into discrete slope bins for additional color products. The range is 0° – 90° , with breaks at 5° , 15° , 25° , and 35° .

The color slope product is produced in two versions: one displays classified slope map without shaded relief; the other is the same classified slope map combined with a shaded relief image (Fig. 11). The version without the shaded relief serves two purposes. It can be used as a layer in a geographical information system (GIS) and allows for the visualization of the slope classes without shading affecting the color ramp. The version with the shaded relief aids in interpreting landforms and surface textures. A plain text world file is provided that allows any version of the slope map to be displayed in a GIS, along with the DTM and orthoimages, which already have geospatial encoding.

5.9. DTM flyovers

The ability to view terrain and images from non-nadir perspectives aids in the geologic interpretation of landforms (e.g., Banks et al., 2009; Okubo, 2010; Weitz et al., 2011, 2022; Chojnacki et al., 2016), and is effective way to present a more human-relatable landscape. Diverse visualization techniques are available to facilitate the interpretation of topography. HiRISE DTMs have been utilized by an enthusiastic public in a variety of applications from video games to 3D prints. Rendering tools have been developed to ingest and manipulate HiRISE DTMs in freely available software such as Blender (<https://www.blender.org>),

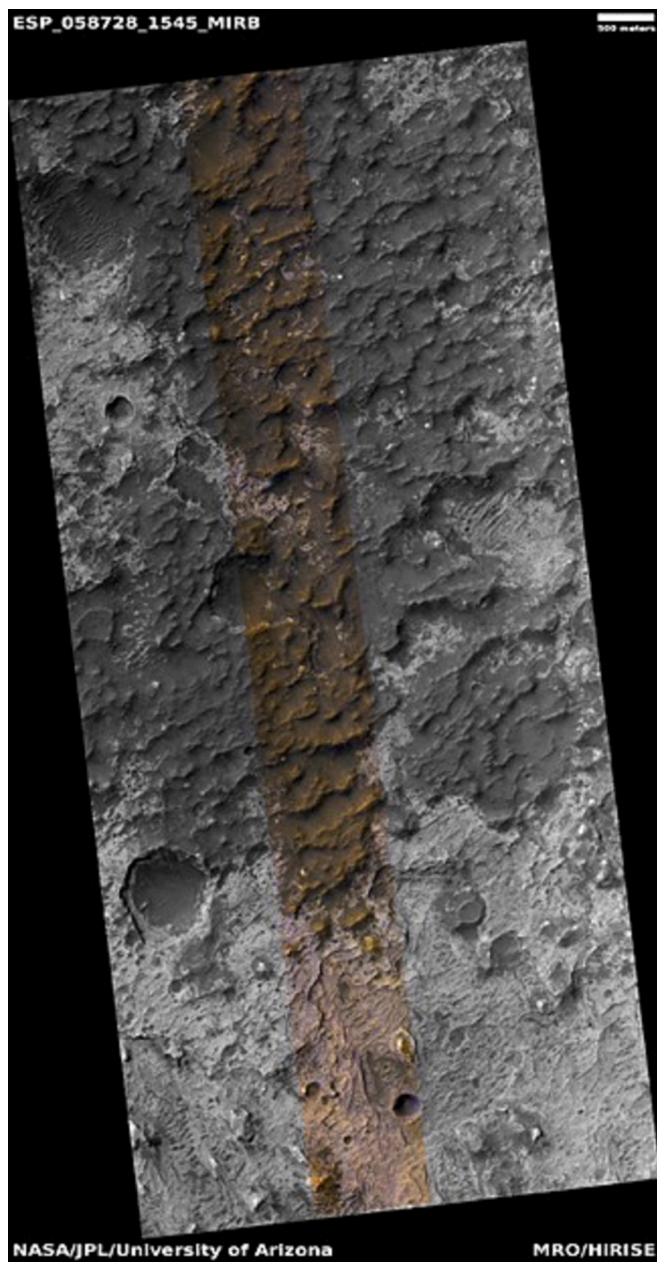


Fig. 8. Example of IRB color-merge image product that was targeted to enable interpretation of stratigraphy exposed in Terra Sirenum.

which includes a community-maintained plugin for HiRISE DTMs, and Areobrowser (<https://areobrowser.org>), which generates 3D perspective views on the fly in an internet browser. Flythrough animations created by both professionals and enthusiasts have been used to great effect engaging the public in Mars exploration and discovery.

5.10. Merged HiRISE-CaSSIS data product

Pan-sharpened images are valuable for detailed investigations of the geology of the martian surface and for landing site characterization (Tornabene et al., 2018). Pan-sharpening is a transformation technique that provides a sharpened color image by merging a higher spatial resolution monochromatic or panchromatic image with a lower resolution color image. Such transformations are desirable because the HiRISE color swath only covers ~20% of the full image.

There are several techniques for pan-sharpening a color image with a

higher-resolution greyscale image. The Gram-Schmidt spectral sharpening transform (Laben and Brower, 2000) was used by Tornabene et al. (2018) as it retains I/F information. I/F is image intensity divided by intensity of solar illumination, and is the radiometrically calibrated output value for each pixel. One of the major challenges with the technique is that most martian datasets are not orthorectified, or are orthorectified to low-resolution topographic data such as MOLA that does not remove small-scale (<1 km) geometric effects on viewing geometry. As such, to pan-sharpen HiRISE with other datasets, a widespread and dense network of 10s to 100 s of Ground Control Points (GCPs) must be defined between the two to warp (i.e., “rubber-sheet”) the lower resolution color dataset to overlay precisely with HiRISE prior to pan-sharpening, with more GCPs being needed in rugged terrain.

Fig. 12 shows 25 cm/pixel pan-sharpened example based on a 4 m/pixel CaSSIS 4-filter color infrared observation, which provides the equivalent to HiRISE IRB colors, of Moni crater situated in the larger Kaiser crater. The HiRISE-CaSSIS pan-sharpened image compares well with the colors provided by the 50 cm/pixel HiRISE IRB color strip despite differences in observation geometries and lighting conditions between the two images.

5.11. Image processing pipelines

The HiRISE image processing pipelines are programs that are responsible for a specific segment of image product processing from raw data to various kinds of finished products. The programs represent logic that mostly script together individual ISIS programs. For example, the HiCal pipeline runs the ISIS program called hical (Becker et al., 2021) and other ISIS programs (whose names are all lowercase). The processing pipelines create various browse and PDS products. Table 12 describes the image processing activities for each of the HiRISE pipeline programs that begin with PDS EDR data (there are earlier pipelines that primarily deal with fetching data and assembling the raw PDS EDRs).

5.12. Reprocessing status

The HiRISE team has begun but not completed reprocessing of older images several times, to incorporate a variety of small improvements. Before completing one reprocessing, there has always been another change, so the effort has not been completed. As part of the full PDS4 conversion effort over the next five years (Section 4.13) we plan to reprocess the entire dataset.

5.13. Replacing erroneous data from bit-flips

During the analog-to-digital conversion of charge from the CCD channels to a 16-bit data number (DN), if one (or more) of those sixteen bits gets incorrectly recorded as a zero instead of a one, or vice-versa, we call this a “bit-flip,” and this results in an incorrectly recorded DN value. During cruise and at Mars, an ever increasing number of images with bit-flip errors were observed, and also an increasing percentage of bit-flipped pixels in an image, at a given FPE temperature (Section 8.9). If the bit that gets “flipped” was a low-significance bit, then the difference between the “real” DN value, and the “recorded” DN value is small (2, 4, 8 DN difference in images whose DN range can typically span a few hundred DN), and this has a low impact on the resulting image. If the bit that was flipped is of higher significance, it could change the DN value by hundreds or thousands of DN, and this results in a pixel that is clearly recording an incorrect value and is anomalously bright or dark compared to its surrounding pixels. The largest bit-flips produce null DN values.

Since many images in the archive contain this bit-flip noise pattern, an improved algorithm for cosmetically improving the images was devised. >10% of the sub-images from three of the 28 image channels (channel 1 of IR10, RED1 and RED3) contain bit-flip noise. The bit-flipped pixels appear as outlying “islands” in a DN histogram plot,

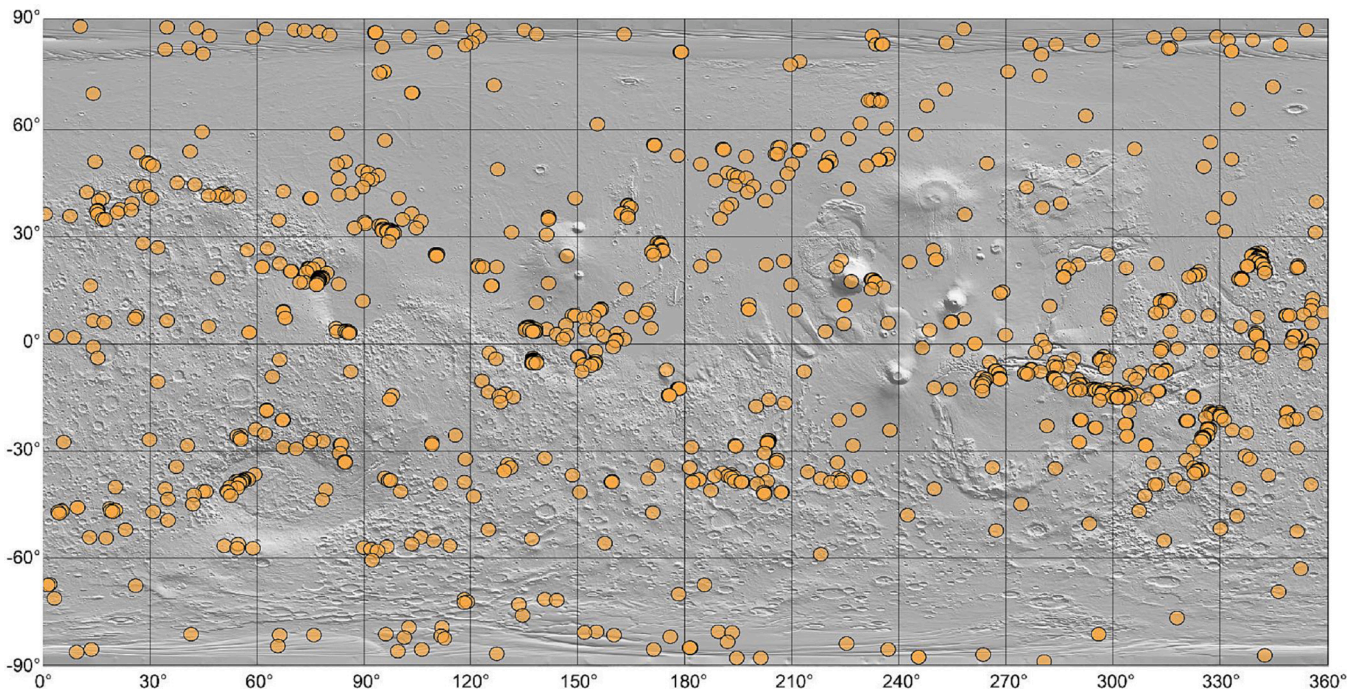


Fig. 9. Global map showing the distribution of >1000 HiRISE DTMs (orange circles) available in the PDS as of August 2023, shown on a basemap of the MOLA shaded relief topography, equirectangular projection. Symbol is much larger than the actual DTM footprint. Axes are latitude and east longitude.

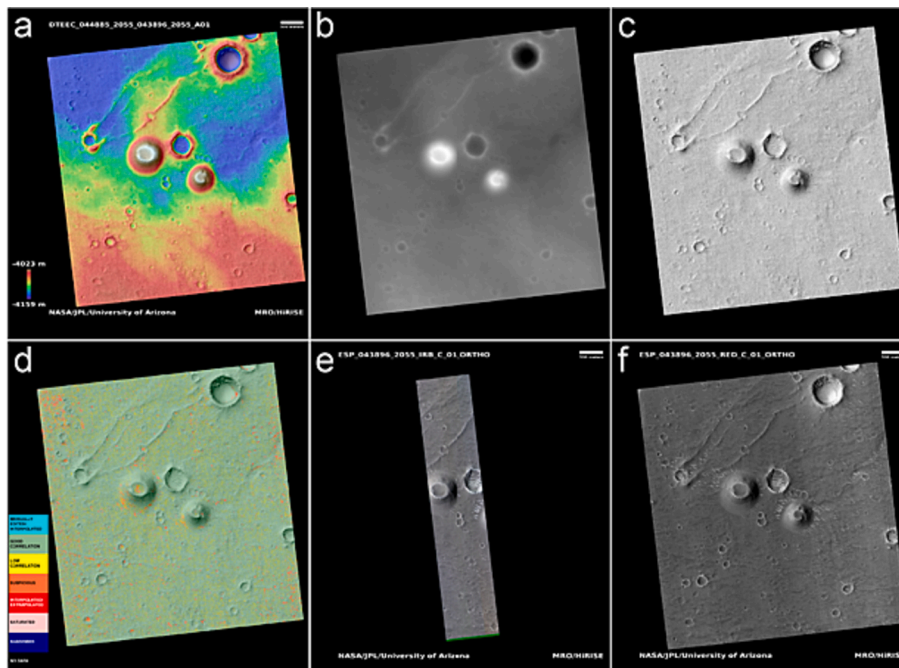


Fig. 10. Examples of PDS browse products of DTM “extras.” (a) Colorized shaded relief, annotated with DTM ID, scale bar (500 m as shown), color ramp legend, and institution image credit. (b) Grayscale image of the DTM, without annotation. (c) Shaded relief image of the DTM, without annotation. (d) Figure of Merit (FOM) map, produced as a full scale JP2 with separate legend. (e) Color orthoimage annotated browse product from one of the source stereo images. (f) Annotated browse product from one of the source stereo orthoimages. An annotated browse, unannotated browse, and unannotated thumbnail image is produced for each product type, except for the FOM map.

away from the main bulk of pixels in an image. The bit-flip correction algorithm attempts to find the best pair of minima on either side of the “good” data so that the erroneous DN values can be masked away, resulting in a well-behaved image histogram, and an image with some null pixels. Isolated null pixels or single-column nulls are replaced by the average of surrounding valid DNs in later stages of the HiCal pipeline.

Data users interpreting small image areas should examine EDRs to be certain that interpolation of erroneous data (or the erroneous data itself) has not changed the result, for example hiding boulders that might be missed in boulder counts.

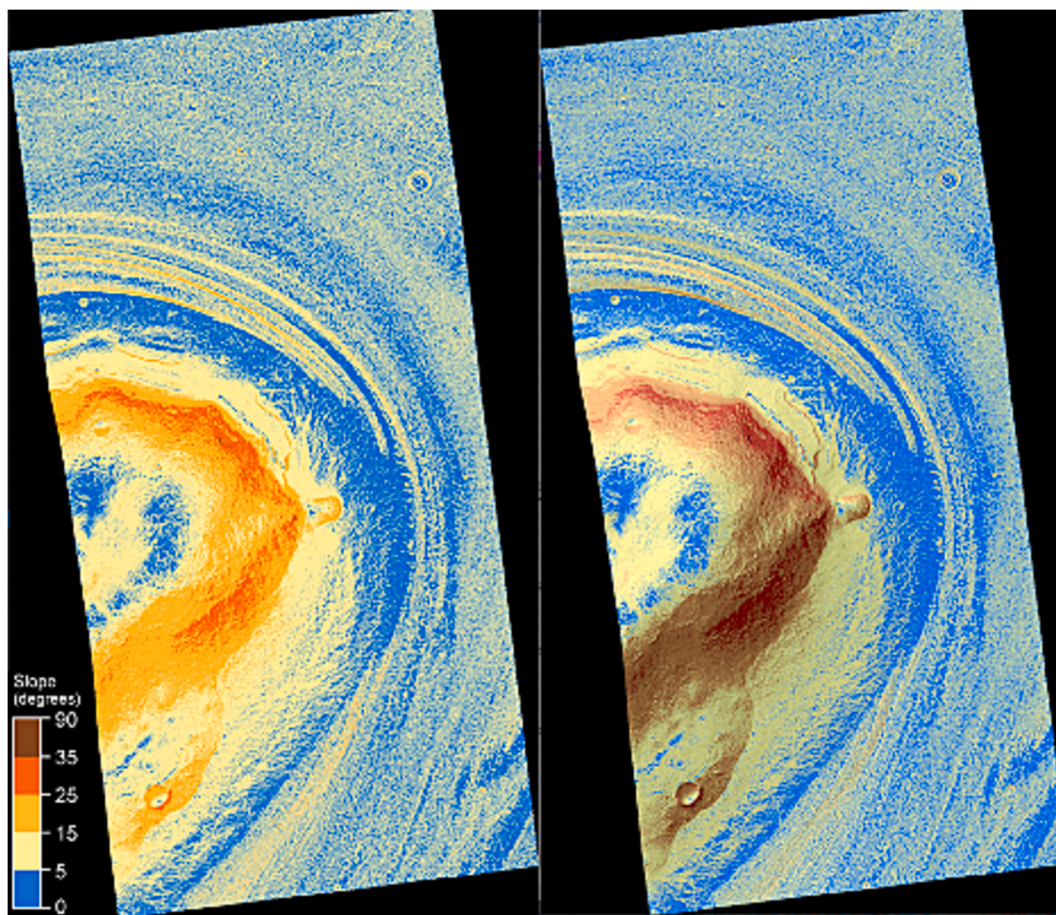


Fig. 11. Example of the new DTM extras slope map browse images. The slope map is produced in two versions: (Left) Slope classified into five bins color-coded as shown in the legend, and (Right) Classified slope map using the same color ramp, combined with the shaded relief image.

5.14. HiRISE image sharpening

There are several techniques used to sharpen digital images, including deconvolution of the point-spread function (PSF) or use of multiple images to derive a sharper image. PSF deconvolution was used on landing site images (Kirk et al., 2008; Golombek et al., 2012a) and on the MSL parachute image (<https://www.uahirise.org/releases/msl/>). The MSL parachute image was acquired via a special sequence for a longer exposure time and higher SNR than is possible for almost all other HiRISE images of Mars.

Tao and Muller (2016) describe stacking and matching HiRISE images of the same area taken from different angles on different orbits for what they call super-resolution restoration. However, the HiRISE dataset is far from ideal for this image restoration, which ideally requires:

1. High SNR (>100:1)
2. A well-sampled point-spread function
3. A set of images that match in resolution and illumination angles
4. Regularly spaced sub-pixel pointing offsets between images in a set of images over a scene.
5. An unchanging scene for the set of images

HiRISE often satisfies #1 above, but the typical SNR with respect to the surface (not the top-of-atmosphere signal after scattering) is typically $\sim 50:1$. As for #2, most planetary mission images are aliased (few pixels across the point-spread function) because data rate is limiting. In other words, it is too expensive in data volume to “oversample” the point-spread function as is done by Earth-based telescopic imaging. The HiRISE image point-spread function is about 2 pixels wide at half max

including both optical effects and smear from spacecraft motion, which is useful but not ideal for restoration. For #3, MRO’s orbit enables crudely identical resolution and illumination conditions via its sun-synchronous orbit, although sun angles vary considerably with season. The viewing angles vary from about -30° to $+30^\circ$ cross-track, which is the only way to image a surface location multiple times per Mars year, and the pixel scale varies by up to 15% with viewing angle. To co-register the images, the geometry difference with viewing angle can be overcome with sufficient processing. Given the changing viewing angles plus pointing jitter, the sub-pixel offsets from image area to image area (#4) are random and variable within the overlap footprint. This means that the resolution improvement varies from place to place in the final image. For #5, Mars’ surface does change over time, especially in places we favor for multiple imaging to monitor the changes.

HiRISE has captured enough (>4) repeat images most useful for image resolution improvement of only about a dozen areas on Mars. Areas with larger numbers of images are targeted repeatedly because of surface changes over time, so a combined product would defeat the purpose of understanding these changes. For large landing sites such as for the ExoMars rover or InSight lander, it takes years to acquire even single HiRISE coverage over the whole “3-sigma” landing error ellipses, and twice as long to acquire full stereo coverage. It would not be wise to sacrifice full coverage of landing ellipses for the sake of image restoration processing on a just a small part of the ellipse. However, a future Mars orbiter may have a much larger data rate and landing site ellipses are shrinking due to advances in EDL technology, which makes resolution improvement more attractive, either onboard the spacecraft or on the ground. For the highest-priority sites, resolution improvement may provide an economical alternative to flying a more capable camera and

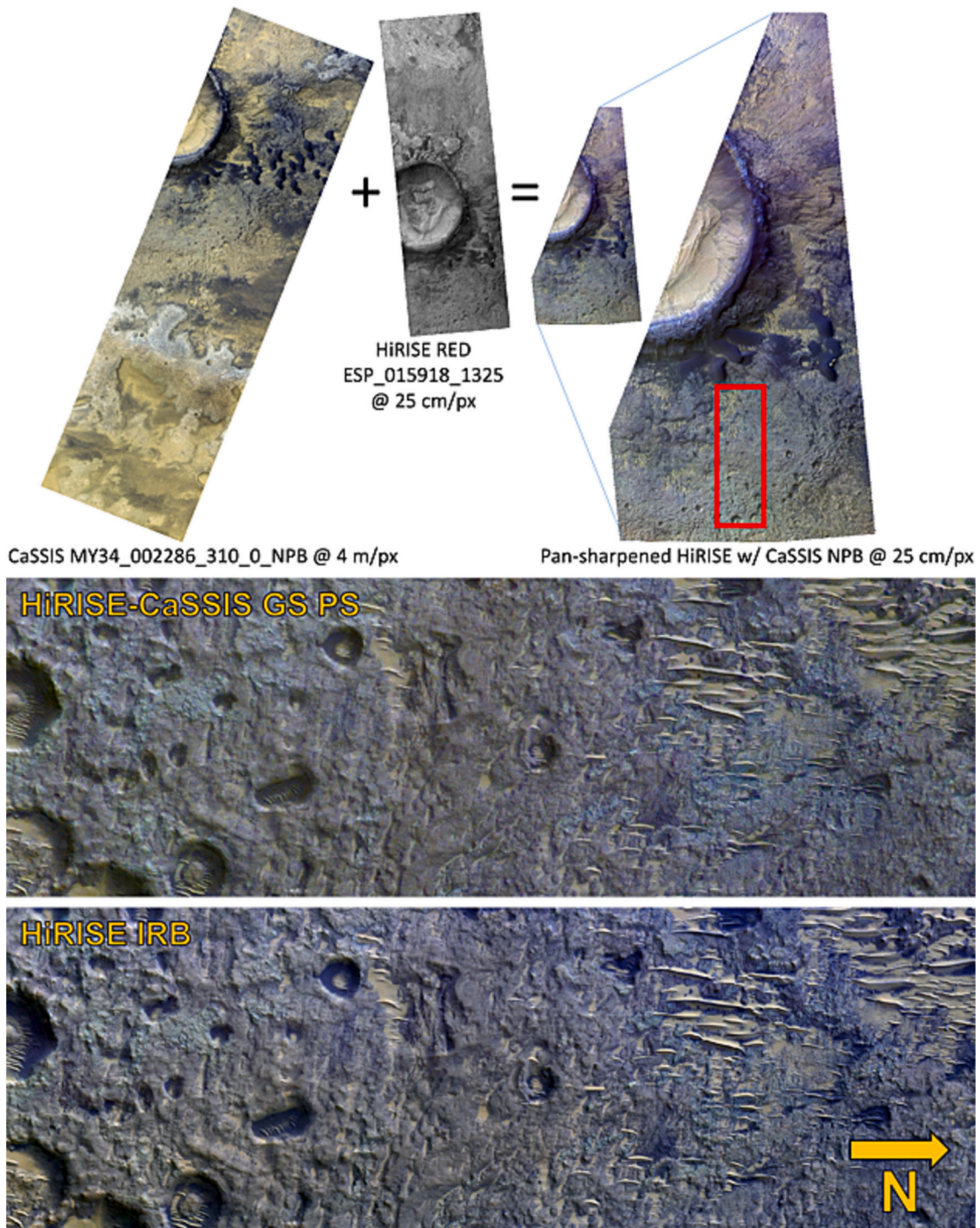


Fig. 12. Context for the inputs and results for pan-sharpening processing of 25 cm/pixel HiRISE RED (ESP_015918_1325) with a CaSSIS NIR-PAN-BLU (NPB) color infrared image (MY34_002286_310_0). Image area is 0.95×2.93 km. (For interpretation of the references to color in this figure legend, the reader is referred to the web version of this article.)

spacecraft, to achieve a modest improvement in resolution (probably no better than a factor of two).

6. Imaging for lander and rover missions

6.1. Pre-MRO landers and rovers

HiRISE has imaged surface hardware from all successful pre-MRO surface missions (Vikings 1 and 2, Pathfinder, Mars Exploration Rover (MER) Spirit and Opportunity; see [McEwen et al., 2010](#)). We have also

carried out campaigns to search for sites of the failed Mars Polar Lander (MPL) and ESA's Beagle-2. MPL was not located and would be very difficult to recognize because it landed within the region of seasonal frost + dust cover, which "repaints" the surface yearly, removing unusual color/albedo patterns. The Phoenix lander ([Smith et al., 2008](#)), at a similar latitude in the northern hemisphere, became very difficult to recognize after a polar winter. Beagle-2 was eventually located ([Bridges et al., 2017](#)). The USSR's Mars 3 lander, which did land successfully and transmitted some data or noise, may also have been located. A written description of this effort appeared in an on-line article for the Planetary

Table 12
HiRISE image processing pipelines.

Pipeline name	Description
EDR_Stats	Runs ISIS hi2isis and histat to gather statistics and information.
HiCal	Runs ISIS hical and performs a variety of noise filtering specific to the HiRISE CCDs (Section 5.13).
HiStitch	Joins two channel products to form a whole CCD product (ISIS histitch), sometimes bin-2 and bin-4 images need extra filtering after that stage. Channel 1 normalized to match brightness of channel 0.
HiccdStitch	Stitches together all of the same-filter CCD images to a single RED, IR, and/or BG nomap image. This step can optionally perform additional correction of vertical striping artifacts via cubenorm. It performs a “balance” operation so that each CCD is radiometrically matched to either RED5, IR11, or BG13 before running ISIS hiccdstitch.
HiColorInit	Prepares images for coregistration. Scales BG and IR products to match the central RED CCD pixel scale.
HiJitReg	Uses ISIS hijitreg to gather registration information for the BG and IR CCDs to the RED CCDs.
HiSlither	Uses ISIS slither to correct for the jitter of the IR and BG CCDs relative to the RED CCDs and creates a three-band “color” mosaic with ISIS hicubeit.
HiColorNorm	Normalizes the BG and IR color across the two-CCD width of the color mosaic.
HiBeautify	Creates a synthetic RGB product and an enhanced IRB product (Delamere et al., 2010).
RedGeom	Perform geometric processing for each CCD, then trigger RedMosaic pipeline
REDMosaic	Create geometrically projected RED and COLOR mosaics.
RDRgen	Create official PDS RED and COLOR RDR products and labels.
HiMosMerge	Merge the geometrically projected RED and COLOR IRB and RGB RDR products into MIRB and MRGB products.
HiPrecisionInit	Prepares images for HiNoProj or HiJACK processing.
HiNoProj	RED images are assembled into a noproj cube with ideal camera geometry (Kirk et al., 2008).
HiJACK	If sufficient jitter was identified, an algorithm (Sutton et al., 2019) uses the two central CCDs of each color to solve for the jitter, and then uses similar approaches to HiNoProj to create “noproj” jitter-corrected versions of the RED, IR, and BG channels.

Society (<https://www.planetary.org/articles/0412-how-we-searched-for-mars-3>).

6.2. New landing sites for MSL, InSight, and Mars2020

HiRISE fundamentally changed how candidates and selected landing sites on Mars are assessed and certified for both science and engineering merits and characteristics. The sub-meter resolution of the images (typically reprojected to 0.25 m/pixel scale) and DTMs processed using stereo image pairs enable a detailed evaluation of the geologic setting and engineering risks associated with landing. For science, HiRISE images enable unprecedented evaluation of geomorphic signatures diagnostic of processes (e.g., details of crater degradation styles, aeolian cross-stratification, fluvial channels, lava levees, etc.) and stratal relationships that are key to assessing geologic settings and scientific merits of a site (Golombek et al., 2018, 2020a; Grant et al., 2010, 2018, 2020; Sweeney et al., 2018; Weitz et al., 2020). For engineering, assessment of hazards to landing and operations using HiRISE data enables direct interrogation of the rock size-frequency distribution on the surface (Golombek et al., 2008, 2012a, 2020b, 2021a; Grant et al., 2022), surface slopes and relief at length scales of a meter or less (Kirk et al., 2008; Beyer, 2017), and surface characteristics that can help evaluate mantling or other undesirable surface materials and properties for rovers (Arvidson et al., 2011; Golombek et al., 2012b, 2017, 2020b, 2021a).

Here we present a summary of how HiRISE data assisted in the assessment and selection of the candidate landing sites for the Mars Science Laboratory Curiosity (MSL) and the Mars 2020 Perseverance (M2020) rover missions, plus the InSight lander. (The Phoenix landing site process was summarized in McEwen et al., 2010.) The interiors of expected landing ellipses were targeted the most by HiRISE, but science targets outside of the ellipses were also imaged. HiRISE acquired >650 images to support landing site selection activities related to these three missions. Additional images were acquired during mission entry, descent, and landing (EDL), and ongoing imaging of landed assets continues. An important note is that HiRISE images acquired to assess the scientific merits of landing sites were quickly released. This rapid release enabled the community to propose and participate in landing site selection activities. The papers cited above present more detailed information regarding the science and engineering processes for selecting landing sites.

6.3. ExoMars

An EDL demonstration module called Schiaparelli was launched to Mars in 2016, along with the ExoMars Trace Gas Orbiter (TGO). During the descent phase, the Schiaparelli module separated from the backshell earlier than expected, so it crashed (see ESP_048120_1780), but valuable engineering data was returned (Bonetti et al., 2018). HiRISE has also extensively imaged the intended landing regions for the ExoMars Rosalind Franklin rover, with over 300 images returned (Fig. 13). The selected region in Oxia Planum (Quantin-Nataf et al., 2021) is one of the largest areas on Mars with complete HiRISE coverage. In addition to the high spatial resolution and stereo from HiRISE, its color products have, together with CaSSIS, enabled detailed mapping and subdivision of the Oxia Planum clay unit (Parkes-Bowen et al., 2022) – the target terrain for the rover and its drill.

6.4. Tianwen-1 lander and Zhurong rover imaging

On 15 May 2021, the lander/rover portion of the Tianwen-1 mission from the Chinese National Space Administration (CNSA) successfully touched down on Mars, and on 22 May, the Zhurong rover drove onto the martian surface (Sun and Rao, 2022). CNSA requested a list of NASA remote sensing datasets covering a region in southern Utopia Planitia a few months before landing, indicating that this would be their preferred landing. HiRISE was able to plan and acquire sample images throughout this region, covering a few percent of the total area; all surfaces were similarly free of small-scale hazards. After the Tianwen-1 landing, with known coordinates, HiRISE acquired a stereo pair over the landing site (ESP_069665_2055 and ESP_069731_2055) and created a DTM. We acquired images to monitor the rover location and wheel tracks about nine months later (ESP_073225_2055) and again after another seven months (ESP_075559_2055). The most recent image (ESP_077511_2055) revealed that the rover had not changed its position between 8 September 2022 and 7 February 2023. Expanded image coverage was acquired because this region exhibits landforms proposed to be the result of mud volcanism, perhaps related to an ancient ocean (e.g., Mills et al., 2021; Huang et al., 2022; Chao et al., 2022).

6.5. Imaging in support of future human exploration

NASA and SpaceX have requested HiRISE images for planning future human exploration. NASA held a single human landing site/exploration zone workshop in 2015, which led to the acquisition of 43 HiRISE images scattered across Mars. There has not been an effort to prioritize

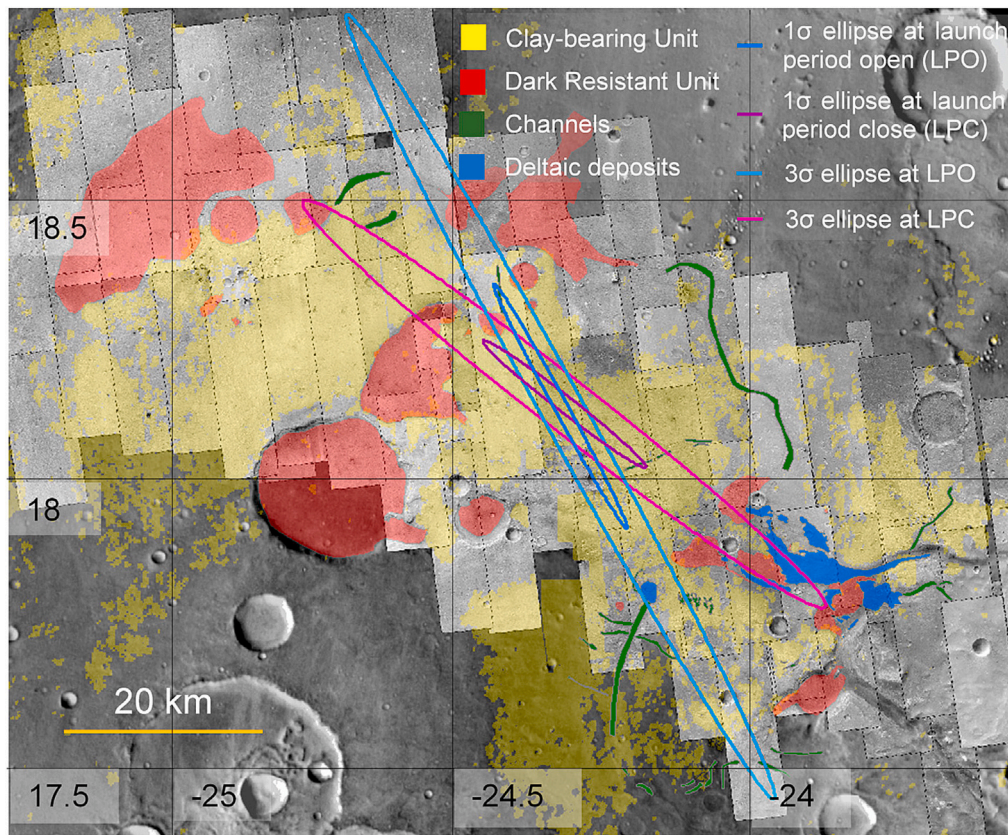


Fig. 13. Footprints of HiRISE images over the Oxia Planum landing region as of August 2022 for the ExoMars Rosalind Franklin rover, near 18.2°N, 24.3°E (map adapted from Parkes-Bowen et al. (2022)).

these regions. SpaceX has sponsored several workshops about future human landings on Mars, focused on the northern middle latitudes where ice is known to exist near the surface down to ~35°N latitude (Morgan et al., 2021; Dundas et al., 2023). A workshop was held at the University of Arizona in January 2019, attended by members of the science community and SpaceX personnel to discuss regions that meet the latitude and elevation constraints and had evidence for substantial ice deposits. Areas of interest in Arcadia Planitia, Erebus and Phlegra Montes, Utopia Planitia and Deuteronilus Mensae were evaluated using HiRISE images to see if suitably smooth and boulder-free areas existed. Golombek et al. (2021b) described potentially safe sites in Arcadia Planitia, and Erebus and Phlegra Montes, but Utopia Planitia and Deuteronilus Mensae appeared too bouldery. At a virtual workshop in August 2020, with more HiRISE and other data acquired and more DTMs produced, the prospective landing sites were evaluated and four leading

candidate sites (one in Phlegra Montes, two in Arcadia Planitia, and one in Erebus Montes) were identified (Golombek et al., 2021b).

6.6. Active mission support

HiRISE images of mission hardware during and after EDL provide a unique opportunity to assess the spacecraft on arrival at Mars and an inventory of where hardware components became distributed near the landing point (Table 13). Over time, these data are supplemented by ongoing imaging of landed assets to monitor traverse progress and spacecraft appearance (Table 13). For example, for the solar-powered MER and InSight missions, monitoring the spacecraft enabled a calibration of dust accumulation over time. In the case of InSight, monitoring also helped to characterize the size and frequency of passing dust devils (Perrin et al., 2020). The InSight team hoped that one of these

Table 13
HiRISE imaging of spacecraft during EDL and soon after landing on Mars.

	Phoenix	MSL	InSight	Perseverance
Date (SCET)	2008-May-25	2012-Aug-06	2018-Nov-26	2021-Feb-18
Range to MRO (km)	793	342	920	696
Image parameters	RED CCDs bin-1 TDI 8 BG and IR CCDs bin-1 TDI 32 uncompressed 126,670 lines	All CCDs bin-1 TDI 32 compressed 85,000 lines	RED CCDs bin-1 TDI 8 BG and IR CCDs bin-2 TDI 8 uncompressed 30,000 lines	All CCDs bin-1 TDI 32 compressed 62,300 lines
EDL observation ID	PSP_008579_9020	ESP_028256_9022	ESP_057820_9023*	ESP_068281_9024
Initial post-EDL landing site observations with hardware	+11 h: PSP_008585_2915 + 22 h: PSP_008591_2485 + 6d: PSP_008644_2485	+1d: ESP_028269_1755 + 6d: ESP_028335_1755 + 12d: ESP_028401_1755	+3d: ESP_057860_1845 + 10d: ESP_057939_1845 + 15d: ESP_058005_1845 *EDL imaging attempt unsuccessful	+1d: ESP_068294_1985 + 7d: ESP_068360_1985 + 12d: ESP_068426_198

vortices might pass over the spacecraft, thereby lofting dust and cleaning the solar panels. Additionally, the MER and MSL teams used HiRISE images to identify and avoid loose aeolian bedforms, such as where the Opportunity rover became stuck for weeks (Arvidson et al., 2011), and to plan MSL rover paths to minimize damage to the wheels (Arvidson et al., 2017).

HiRISE for the first time allowed rover drivers and science teams to know where the rover was after each drive and to accurately navigate to key locations to visit. Prior to HiRISE, knowledge of where the MER rovers were after each drive was approximate, because Mars Orbital Camera (MOC) images (Malin et al., 2010) were not high enough in resolution to localize the rover. After HiRISE arrived, the rover team was able to determine to within 1 HiRISE pixel (~30 cm) where the rover was by taking rover stereo images, creating orthophotos of them and directly correlating and georeferencing them onto a HiRISE image. This process is now standard procedure for rover missions (Golombek, 2019).

7. Science planning and uplink tools and techniques

7.1. Introduction

Here we summarize the internal science planning processes and tools for those who may benefit from the lessons received by the HiRISE team over the years. Additionally, this information may be useful to those who submit image suggestions, enhancing the odds of acquiring the best images.

7.2. HiWish

HiWish public suggestion portal is the primary Web tool for entering suggestions for future HiRISE images (Beyer et al., 2010; Chojnacki et al., 2020). Some of our best image suggestions come from our colleagues in the scientific community actively pursuing research that would benefit from additional, specific HiRISE coverage. The general public also utilizes the HiWish portal, along with the HiRISE team, and other MRO instrument team members. HiWish was announced in early 2010, and through April 2022, a total of 10,140 people have registered and suggested 27,681 images (Fig. 14); of these suggestions, 13,407 have been satisfied. Our most prolific public contributor, James Secosky, has contributed >14,000 suggestions, resulting, so far, in >5000 image

acquisitions.

To suggest a new target, one first creates an account using the HiWish page of the HiRISE website (<https://www.uahirise.org/>). A HiWish user can create a stand-alone, repeat, or stereo suggestion. Suggestions require a Title, Science Rationale, and an appropriate Science Theme. The Title will typically include a location and feature or landform to be imaged (e.g., Crater in Meridiani Planum). The Science Rationale requires a short description of the intended objective, which informs the HiRISE team why this image should be taken. Along with a user-designated priority (1–5; 5 being the highest priority for that user), this rationale communicates to the team the significance of the target. All suggestions in a given Science Theme will be given a team-designated priority (6–10) by the appropriate Science Theme Lead (STL; see Table 2). For more details, including advanced targeting tips for stereo or seasonal suggestions, see Chojnacki et al. (2020) and their E-Poster.

(<https://www.hou.usra.edu/meetings/lpsc2020/eposter/2095.pdf>).

7.3. “Must-have” procedures

The MRO project science planning process is complex. Aspects of this include the round-robin selection process: taking the highest priority target than can be acquired from CTX, CRISM, HiRISE, and SHARAD, then the second-highest priority from each experiment, etc. Other complexities include the MCS rules (Section 7.5), the stereo completion process, and the time-limited nature of certain science objectives. To ensure that the very highest-priority targets are acquired, there is a short list of five highest-priority requests from each science team, dubbed “must-have” (MH) targets, that are integrated by hand before the round-robin selection. MHs are allowed to violate MCS rules and are targeted before the stereo completion process (which happens before the round-robin target selection). For HiRISE, the CIPP will typically select MHs from among the special requests from the team (Section 7.13). Sometimes there are also MEP must-have targets (such as certification of landing sites), and these get the very top priority, above the science MHs.

7.4. 7.4 The planning process; targeted vs. non-interactive observations

The planning process for each two-week cycle is like that described

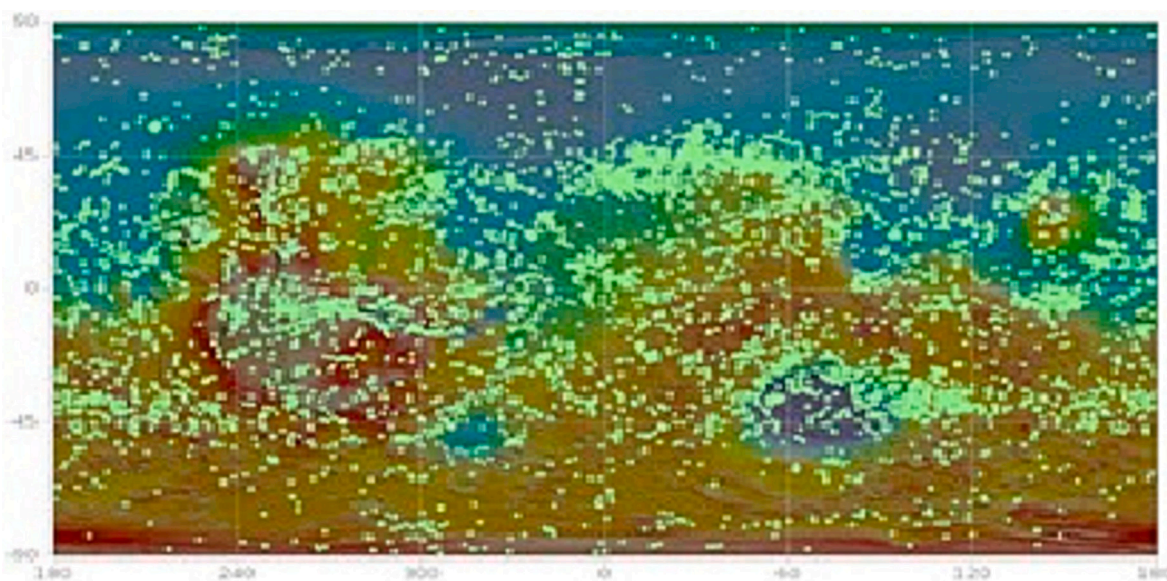


Fig. 14. Global distribution of public HiRISE suggestions in light green, on a colorized MOLA (Smith et al., 2001) basemap, with red as high elevation and blue as low elevation. Simple Cylindrical projection, latitude -90° to 90° , longitude -180° to 180° . (For interpretation of the references to color in this figure legend, the reader is referred to the web version of this article.)

in McEwen et al. (2010) but has been compressed in the extended science phases. The entire planning period lasts four and a half weeks, instead of the five and a half weeks needed in the primary science phase. This period includes 1.5 weeks to plan Interactive Observations (IOs), two weeks to plan Non-Interactive Observations (NIOs), two weeks of sequence execution, and up to two weeks of image validation, with overlaps, so the total is four and a half weeks. IOs may point the spacecraft or require high-stability mode, whereas NIOs do not require any action outside the HiRISE team. The long planning period has logistical complications; cycles begin planning when the prior cycle has yet to start executing, and images from two cycles before have yet to be acquired.

7.5. Large roll restrictions

MRO must point the high-gain antenna at Earth and the solar arrays at the Sun for most of each orbit (except when Mars is relatively close to the Sun and the solar arrays may be parked). Although both the high-gain antenna and solar arrays are on gimbals, there are some periods in which the off-nadir roll angles must be restricted to maintain both requirements. The orbiter seasonally encounters periods during which it cannot take advantage of its full $\pm 30^\circ$ off-nadir swath. In roll-restricted cycles, HiRISE targeting focuses on non-stereo images that can be acquired as small rolls or nadirs; we do not start new stereo pairs unless the first image can be acquired on rolls greater than $\pm 4^\circ$, allowing the second image to be acquired on small rolls ($< 9^\circ$) yet at acceptable convergence angles. Additionally, ongoing stereo completion during this time is limited to second halves for which low convergence angles are acceptable.

Rolling the spacecraft for off-nadir pointing is problematic for MCS observations, particularly large rolls (defined as those $> 9^\circ$) clustered spatially or temporally which produce gaps in MCS monitoring. MRO science teams have agreed to several rules limiting off-nadir observations in order to minimize the impact on MCS data. These rules are automatically enforced for all observations during IO scheduling; observations that do not conform to the MCS rules are removed from the plan. A small number of exceptions are possible but require special efforts. The current MCS rules concerning spacecraft rolls (in place since the PSP but not described in McEwen et al. (2010)) are:

- Maximum of 2 large rolls per orbit, where the second roll must start at least 28 min after the end of the first.
- Large rolls may be in adjacent orbits if, and only if, the end of the earlier roll (in its orbit) is at least 9 min 20 s before the start of the later roll (in its orbit).
- Maximum of 4 large rolls per 24 h period.

Additionally, HiRISE is allowed up to 22 large rolls per cycle, to be used for the team's highest priority science observations, first-look stereo, second-look stereo, and time-critical non-stereo observations.

7.6. CIPP-lite and CIPP-less cycles

A main strength of HiRISE's image acquisition is its diversity in science goals, accomplished by a rotating science lead for each 2-week cycle, called the Co-I of the Pay Period (CIPP; McEwen et al., 2010). Although originally envisioned as a role for a Co-Investigator, this role has also been fulfilled by team affiliates, postdoctoral researchers, and graduate students, providing early career opportunities for mission involvement directly related to scientific research activities.

As science funding declined in the extended missions, reducing the workload on the science and operations teams was necessary. HiRISE developed the option for a science team member to only participate in the first two weeks of the planning process, a role referred to as "CIPP-Lite." This compromise maintains the valuable science input and diversity of interests the science team brings to the IO stage while reducing

their working time. The tradeoff is that the CIPP-Lite cannot select "ride-along" targets, add lower-priority NIOs, or help plan the detailed camera settings for every observation. The use of CIPP-Lite cycles has expanded over time. As instrument temperature management became more demanding (Section 7.14), it became increasingly necessary for the HiTS to override the CIPP-chosen ride-alongs and NIOs, so CIPP-lite became the most efficient work mode.

As HiRISE funding declines, eliminating science team participation from tactical planning may become necessary for some cycles. Cycles could be entirely planned by an uplink engineer, with automated scripts replacing work done by the CIPP. This personnel descope may provide the opportunity to compress the IO planning down to 1 week from 1.5, but it comes at the cost of less scientific input into each image. Cycles without a CIPP would pull suggestions according to specific set rules, guided by STL priorities, but without an opportunity for thoughtful prioritization among science themes and images.

7.7. HiRISE stereo effect analysis software (HiSEAS)

As a single-aperture, fixed-pointing instrument, HiRISE can acquire stereo pairs only on separate orbits, one for each image of the pair. Ideally, these stereo images would be acquired at similar illumination conditions and with minimal variation in surface features, seasonal or otherwise. The MRO near-polar orbit is such that, at the equator, HiRISE can theoretically view the same target every 66 orbits (~ 5.5 days) with a spacecraft cross-track roll angle of 20° . Closer to the poles, the repeat coverage frequency improves, resulting in a dozen or more possible stereo pairs for a single target over the course of a week. If the next observable orbit is unavailable for some reason, then the time between stereo halves grows. This increased time, in turn, results in increasingly complicated lighting and seasonal differences. In practice, it may be months or years before HiRISE has another chance to schedule a stereo completion.

HiSEAS evaluates whether a candidate stereo pair is reasonable and which resulting pair is the best when more than one candidate exists for a target (Becker et al., 2015; Sutton, 2022b; 2022a). It computes the viewing geometry of both halves of each candidate pair and applies user-configurable rules to evaluate the stereo separation angle, the lighting differences, the seasonal differences (in terms of sun position), and the amount of time that has passed since the first half was acquired. The rules can be configured by latitude range, so different criteria are used for polar and equatorial stereo images.

HiSEAS can work with any pair of HiRISE images, whether one or both are still in the planning stage or both are already acquired. We have adapted it to search through the entire HiRISE image catalog to identify candidate stereo pairs that may not have been planned as stereo pairs. In this form, called Parendipity, HiSEAS identifies groups of mutually overlapping HiRISE images and applies the same rules used during operations planning. We have generated and released anaglyphs from these candidate pairs. We have also adapted it to work with the Context (CTX) camera's PDS-released images in the same manner, called Parendipity CTX. Parendipity results are posted at <https://www.uahirise.org/stereo/>, and updated periodically.

7.8. Stereo pair orbits restricted to a cycle (SPORCs)

HiRISE stereo pairs must be acquired with off-nadir spacecraft rolls on two separate orbits (Section 7.7). Initially, evaluating a second orbit for acceptable convergence depended on the geometry of an already-planned first image from a prior cycle. This limitation frequently introduced significant delays between the first and second halves of a stereo pair. Due to the potentially confounding effects of changing illumination angles, surface morphology, and surface albedo on the quality of DTMs, HiRISE developed a procedure to minimize the time between the two halves of a stereo pair. Called SPORCs, (Stereo Pair Orbits Restricted to a Cycle), locations viewable on two or more orbits in

a single planning cycle are considered with the same criteria HiSEAS applies to evaluating second-half stereo opportunities for existing images. This consideration of potential image pairs allows acquisition of stereo pairs within a single two-week cycle, limiting illumination angle difference and minimizing changes to dust or frost cover and potential for changes in surface morphology. However, the MRO planning process often results in the acquisition of just a single image (of a stereo pair) in a cycle, so there are many attempted but not completed SPORCs that are treated like the first of two stereo images.

Once a compatible pair of orbits is found for a given stereo target, those potential observations can be prioritized in that cycle's target list, maximizing the chance for timely acquisition. There is a total of 983 stereo pairs acquired within 14 days as of 8/5/2022. Some of these image pairs were acquired in adjacent planning cycles, so they are not actual SPORCs but are equivalent. A list of known SPORC images (or equivalent) is periodically posted at <https://www.uahirise.org/stereo/>.

7.9. HiRISE Check for exact repeats (HiKERS)

Monitoring the martian surface for changes has led to many new scientific results during the MRO mission (e.g., [Diniega et al., 2021](#); [Dundas et al., 2021a](#)). Change detection is most straightforward using orthoimages (Section 4.1) and is also aided by acquiring images with similar incidence angles, subsolar azimuths, viewing directions, and pixel scales. Subtle changes may only be recognizable from closely matched pairs of images. A pilot effort to identify "exact" match opportunities to previous images was initiated in December 2016, focusing on some Mass Wasting targets and was expanded to be more comprehensive in January 2018. Such opportunities are informally dubbed "HiKERS" as the software tool used to identify them is named the HiRISE Check for Exact Repeats. This tool, similar to HiSEAS, identifies opportunities in each planning cycle that match previous-image incidence and viewing angles to within 5° and subsolar azimuth to within 7°. While there is no sharp threshold for match quality, matches within this range are generally high-quality and make change detection more robust. A list of known HiKER pairs is periodically posted on the HiRISE website.

7.10. HiPhoP

From 2006 to 2019, the HiRISE Photometry Program (HiPhoP) used a Hapke photometric function ([Hapke, 1981](#)), requiring manually-input values for surface and atmospheric parameters for each observation ([McEwen et al., 2007](#)). This procedure was one of the most time-consuming steps in uplink planning. A more automated approach was needed to predict scene brightness (radiance) and set image parameters for CaSSIS ([Almeida et al., 2023](#)), based initially on HiRISE data (before sufficient CaSSIS data was acquired). Subsequently, we modified this automated method for HiRISE. With a database of >60,000 HiRISE images, we determined that scene brightness could be predicted with 10% accuracy (sufficient for setting image parameters) for >95% of the images, by using a simple model:

$$P1 [DN/ms] = (m_1 \times \cos i + b_1) \times (m_2 \times TES + b_2) \times 1.5^2 / AU^2, \quad (1)$$

where P1 is how many DN (Data Numbers) of signal accumulate in a ms of integration, $\cos i$ is cosine of the incidence angle, TES is the Thermal Emission Spectrometer albedo ([Christensen et al., 2001](#)), AU is the Sun-Mars distance in astronomical units, and m_1 , b_1 , m_2 , and b_2 are linear coefficients that fit the average signal levels of acquired HiRISE images. This function ignores atmospheric scattering because the top of the atmosphere brightness (radiance) is insensitive to low to moderate atmospheric opacity. In other words, the signal portions coming directly from the surface, the atmosphere, and more complicated scattering paths result in about the same integrated top-of-atmosphere brightness. The prediction may be too low when the atmosphere is extra hazy or

dusty, especially over low-albedo surfaces, but these conditions do not produce useful images of the surface, so overexposing the image is not a concern. A phase angle correction is needed if the phase angle is $<20^\circ$, but MRO can never image at such low phase angles unless there is a special spacecraft pointing maneuver (done once for testing/validation on ESP_022243_9050 with a phase angle of 2.6° to observe recurring slope lineae in Horowitz crater).

Different empirical coefficients (m_1 , b_1 , m_2 , and b_2) are needed for frosted versus unfrosted ground and for the frost-free north- and south-polar residual ice caps. In addition, frosted ground needs a seasonal correction because the frost albedo is variable ([Pommerol et al., 2011](#)):

$$L_s C = ax^5 + bx^4 + cx^3 + dx^2 + ex + f, \quad (2)$$

where $L_s C$ is the correction factor as a function of L_s , $x = L_s/100$, and a , b , c , d , e , and f are polynomial coefficients that fit the HiRISE image brightness (signal levels) of frosted ground. $L_s C$ values range from about 0.7 to 1.5. To predict when and where frost is present, we created a coarse map based on past HiRISE images for frost presence as a function of L_s and latitude. However, there are local surface anomalies (related to thermal inertia and topography) and season-to-season variability, so predicting scene brightness for these marginal cases when frost may or may not be present is difficult. The conservative approach in such cases is to use Bin 1/TDI 128 or Bin 2/TDI 32 for the RED CCDs, along with Bin 2/TDI 64 for the IR images and Bin 2/TDI 128 for the BG images; these settings almost never saturate.

The largest errors for unfrosted terrain brightness predictions are due to large image areas of steep sunlit or shadowed slopes or to changes in albedo since the TES data was acquired. The largest predict errors for the residual ice terrains occurs in the polar gaps in TES coverage, which we filled with estimated values. Once the mean scene brightness has been predicted, the next steps are to choose TDI and binning and look-up table (Section 4.2). We usually strive to achieve at least 100:1 SNR at the top of the atmosphere, but exceptions are made for special cases.

Updates to the HiPlan suite of tools (Section 7.11) were implemented to extract the TES albedo value at given image center coordinates and to determine the appropriate coefficients for those coordinates at a given L_s . For TES albedo, we use the most complete (MY26) map available at the PDS Geosciences Node ([Christensen et al., 2001](#); [Putzig and Mellon, 2007](#)). Predicted DN values for each combination of binning and TDI may then be calculated and compared against the user-set minimum and maximum threshold values, and appropriate HiRISE LUTs determined for those predicted DN values.

7.11. HiPlan

HiPlan, the HiRISE planning software suite, has received numerous updates during the extended science phases. The core tool is built on top of the MRO project's customized version of JMARS ([Dickenshied et al., 2019](#)). Many HiPlan updates were in response to anomalies and instrument degradation mitigation efforts. Other updates have been for improved efficiency in operations and to accommodate remote operations, such as improvements to the suite's thermal modeling software, HiTemp, and the addition of several bulk or batch operation tools.

To mitigate the degradation of HiRISE's performance over time, we have conducted extensive experiments in which we have adjusted the instrument's analog-to-digital converter (ADC) settings (Section 8.9). The HiPlan tool suite has been updated to visualize and modify those settings as part of the general planning process. Another large-scale update was in the HiRISE photometry predictor tool, HiPhoP (Section 7.10). The HiPlan suite also gained tools (like Data Slacker) to perform a first-order estimate of HiRISE's spacecraft data volume usage (Section 7.15) and to examine short- or long-term trends in spacecraft targeting. Our stereo planning software, HiSEAS, was updated to plan both halves of a stereo pair in a single cycle (Section 7.8). The MRO project's tool reports orbital geometry events such as eclipse entry and exit, which

HiPlan uses for automated bulk planning to limit activity (e.g., to avoid eclipses) or focus activity (e.g., to conduct automated calibration observations on the night side).

7.12. HiTList

The HiTList (HiRISE Target List) is a list of potential observations that can be imaged during a particular 2-week planning cycle. The suggested observations are drawn from a database of Region(s) of Interest (ROIs). The database hosts over 22,000 ROIs made by the science team and the public. These suggestions are filtered to retain only the ROIs suitable for imaging during that planning cycle. This process includes consideration of: 1) whether the spacecraft passes over the ROI, or close enough to view the ROI with a $< 30^\circ$ roll of the spacecraft, 2) whether or not, and on which orbits, there are suitable imaging conditions to complete a viable stereo pair, and 3) any specific requests from the suggester, e.g., a specific orbit for a HiKER target.

The HiRISE Targeting Specialist (HiTS) assigned to the planning cycle constructs the HiTList. They do so using a variety of planning tools and the most recent information on predicted spacecraft groundtracks. Once a file of suitable targets has been constructed, it is limited in length by priority while still providing multiple targets on as many orbits as possible. That list is then prioritized by a science team member (the CIPP), then sent to JPL for the process that resolves conflicts.

7.13. STaR

STaR (Special Target Requests) is an application backed by a web service that allows science team users to enter prioritized requests for acquisition in an upcoming cycle. These requests are validated and stored in the database. In addition, it allows the targeting specialists to manage the process using request categories and user limits. The requests are automatically entered into the HiTList for each planning cycle. Before the implementation of STaR in late 2022, users entered special target requests on the wiki, and incorporation into the HiTList was a manual process.

7.14. Temperature management

HiTemp is a tool used to model temperatures at the HiRISE FPE (focal plane electronics) box and FPA (focal plane assembly) baseplate for a sequence of observations. It allows the HiTS to plan observation

sequences within a range of temperatures that optimize image data quality while keeping within the instrument's allowable flight temperatures (AFTs). Given input HiRISE environment temperatures and initial conditions, HiTemp has been found to accurately predict peak temperatures within $\sim \pm 2^\circ\text{C}$ of actual onboard temperatures. However, unpredictable thermal changes onboard the spacecraft that alter the HiRISE environment temperature can negatively impact the accuracy of predictions. For example, one common event that changes the HiRISE thermal environment is when the MRO spacecraft unexpectedly transitions from All-Stellar (star tracking cameras) to full attitude determination mode. Full attitude determination mode uses inertial measurement units (IMUs) and star tracking cameras to determine spacecraft orientation. Due to spacecraft heaters being activated for IMU operations, the HiRISE environment temperature can increase by $\sim 2^\circ$ when in full attitude determination mode. Since these transitions are frequently unplanned, and there is generally not enough time to generate and uplink new observation commands to account for the increase in environment temperature, peak temperatures must be padded during planning to ensure instrument safety. Exceeding an AFT causes "safing" (powering off) the instrument and losing several days of data collection and downlink. By contrast, if temperatures are too low during imaging, there is a risk of producing major bit-flips, negatively impacting the quality of the image data (Section 8.9).

Achieving warm enough temperatures to mitigate bit-flips and remaining cool enough for instrument safety is challenging. To do so, we limit image size because heating continues while transferring data from the CCD Processing Memory Modules (CPMMs) to the spacecraft solid state recorder (SSR). The frequent changes to temperature limits and resulting approximate maximum image lengths (in Bin 1A mode) are described in Table 14. Bin-2 max image lengths are more than two times longer in the number of lines, which is usually sufficient to meet science objectives.

7.15. Data tracker and slacker

HiRISE uses a third-party tool (Data Tracker) and a less precise, faster, in-house tool (Data Slacker) to model SSR use. This modeling is important because a misunderstanding about how HiRISE operates in the spacecraft flight software results in HiRISE "safing" when the HiRISE raw partition of the SSR is full (this happened twice; see Section 8.2 and Table 15). HiRISE operations are complicated by the need to monitor the SSR partition. The outputs of these tools are used while creating,

Table 14

FPE minimum temperature goals for imaging Mars. The image labels tend to record FPE box temperatures about 1–3 $^\circ\text{C}$ higher than those values listed here, for comparison to Table 16.

Date implemented (month/day/year)	First MRO orbit	FPE minimum T ($^\circ\text{C}$)	FPE/FPA Flight Software Limit ($^\circ\text{C}$)	Upper Planning limit ($^\circ\text{C}$)	Maximum Bin 1A image lines
03/10/2006	1	18	35	31	120 K
02/05/2008	7166	22.5	41	37	100 K
12/16/2009	15,893	22.5	43	37	100 K
10/09/2010	19,706	25	43	37	80 K
01/28/2012	25,815	25	45	39	110 K
02/22/2014	35,517	28	45	39	70 K
10/17/2015	43,243	32	47	39	40K
10/24/2015	43,333	32	47	41	60 K
10/01/2016	47,735	33	47	41	50 K
08/05/2017	51,687	34	47	42	50 K
04/07/2018	54,831	34	47	44	80 K
04/14/2018	54,912	36	65*	44	50 K
06/23/2018	55,820	36	65*	46	80 K
02/23/2019	58,964	38	65*	46	50 K
07/31/2020	65,702	36	65*	46	80 K
12/19/2020	67,499	37	65*	46	70 K
05/08/2021	69,297	39	65*	46	40K
07/02/2022	74,688	36	65*	46	80 K
02/25/2023	77,742	38	65*	46	55 K

* Although Flight Software Limit raised to 65°C , a hard upper limit, the planning limit was kept much lower, at 46°C , potentially preserving instrument lifetime.

updating, and safety-checking imaging sequences before commanding.

Lockheed Martin Corporation developed *Data Tracker*, and it models the SSR input and output of one or all instruments using cycle-specific planning files as input. Before sequence generation, the HiTS use *Data Tracker* to determine whether to increase or reduce data volume use (lengthen or shorten, add or remove observations, or change binning). Because an SSR overflow will trigger HiRISE safe mode and result in lost data, we allow for headroom in the model-predicted raw space, erring on the side of caution. Daily SSR prediction models are generated for monitoring purposes. These model ‘auto-runs’ determine whether on-board files should be re-generated and replaced after commanding to adjust data volume usage.

The HiRISE team developed *Data Slacker*; it models only the HiRISE SSR partition and executes much faster than *Data Tracker* but is not sufficiently accurate for the final command loads. It is integrated within HiPlan, allowing for concurrent decision-making while planning observations.

7.16. Relay shadow zones

MRO relay support for landed assets results in so-called “shadow zones” where the science instruments encounter difficulty scheduling observations. During the interactive portion of the MRO planning process, relay passes are treated as observation records to direct spacecraft pointing and avoid flight rule violations. As such, a relay pass prevents the other MRO science instruments from acquiring science targets near the landed asset on relay orbits. First encountered after the successful landing of the Phoenix surface platform, the Phoenix shadow zone was mitigated by a detailed plan for coordinated science observations between the lander and the MRO science instruments (Tamppari et al., 2010) and by the small spacing between orbit tracks at those higher latitudes, ensuring multiple opportunities to image the same area.

Table 15

Beginning dates and orbit ranges when HiRISE could not image due to safing events.

Date (m/d/yr)	Begin Orbit	End Orbit	Source	Cause of Safing if HiRISE
03/14/2007	2950	3061	Spacecraft	
07/20/2007	4594	4642	Spacecraft	
09/27/2007	5479	5503	HiRISE	SSR full
11/07/2007	6009	6124	Spacecraft	
11/29/2007	6295	6462	Spacecraft	
02/14/2008	7273	7337	Spacecraft	
02/22/2009	12,083	12,194	Spacecraft	
06/03/2009	13,373	13,451	Spacecraft	
08/06/2009	14,191	14,254	Spacecraft	
08/26/2009	14,448	15,892	Spacecraft	
07/21/2010	18,669	18,700	HiRISE	SSR full
09/15/2010	19,396	19,436	Spacecraft	
08/27/2011	23,830	23,904	HiRISE	CPMM 13 (RED9) failed
09/06/2011	23,964	23,992	HiRISE	Test to confirm CPMM 13 failed
09/20/2011	24,141	24,197	Spacecraft	
11/06/2011	24,741	24,803	Spacecraft	
10/14/2012	29,155	29,212	Spacecraft	
08/12/2013	33,022	33,036	Spacecraft	
03/09/2014	35,706	35,755	Spacecraft	
08/26/2014	37,890	37,945	Spacecraft	
03/31/2015	40,679	40,768	Spacecraft	
01/18/2016	44,436	44,473	HiRISE	Detected power supply over-voltage
11/21/2016	48,385	48,408	HiRISE	Over-temperature due to redundant spacecraft solar array controllers being unintentionally commanded on
09/13/2017	52,182	52,203	All Instruments	Under-voltage on instrument switches during eclipse following orbit trim maneuver
02/15/2018	54,172	54,381	Spacecraft	
12/28/2018	58,231	58,360	HiRISE	Detected power supply over-voltage
12/09/2019	62,667	62,701	HiRISE	Detected power supply over-voltage
01/27/2020	63,295	64,443	Spacecraft	
02/15/2020	63,541	63,725	Spacecraft	
06/12/2020	65,053	65,162	Spacecraft	
10/13/2020	66,638	66,743	Spacecraft	
03/24/2021	68,713	68,797	Spacecraft	
04/13/2021	68,577	68,667	Spacecraft	
08/12/2021	70,531	70,734	Spacecraft	
7/14/2023	79,525	79,629	HiRISE	CPMM 5 (RED4) failed

After the successful landing and deployment of the more equatorial MSL the shadow zone soon became a particular impediment for HiRISE science in the area. Relay support for MSL took top priority in each planning cycle; as MRO provided relay support on almost all overflights in the vicinity of the landing site, a shadow zone from roughly 60°S–40°N and 125°E–160°E was rendered largely unavailable for targeted science observation. MRO later determined acceptable roll angle ranges for relay overflights allowing limited science pointing during a relay. In addition, the two projects negotiated a limited number of relay overflights that could be relinquished in favor of high-priority science targets. These two compromises resulted in a more porous shadow zone, particularly at latitudes above 20°S.

Complicating things further, the InSight lander site is aligned with the Curiosity landing site along an MRO ground track, and there is a newer shadow zone near the Perseverance rover. Yet another shadow zone may exist if the ExoMars lander and rover are launched to Mars at an upcoming launch window.

7.17. Use of data volume in extended missions

The volume of data that can be downlinked from MRO fluctuates depending on the distance from the Earth to Mars, the availability of the Deep Space Network (DSN) receivers on different parts of the Earth, and the competition for their use by other spacecraft. The downlink available to the mission is divided between the various instruments on board and telecommunications required by the spacecraft. HiRISE was allotted 35% of the available data volume (ranging from ~150 to 1146 Gb per two-week cycle) prior to retirement of CRISM in May of 2022, and is now allotted 48%. However, thermal management in recent years (Section 7.14) has prevented acquisition of more than ~1000 Gb per cycle of compressed HiRISE data. Most HiRISE images are compressed prior to transmission to Earth, with ~5:1 compression via both DN

conversion from 14 to 8 bits/pixel plus lossless compression in the spacecraft SSR.

7.18. Retiring and unretiring suggestions

Target suggestions submitted through HiWish or HiWeb are ingested into a target database for consideration during each planning cycle (McEwen et al., 2010). Once an image has been planned that satisfies the suggestion, it is “retired”. The initial implementation of the retirement process consisted only of a simple geometric test: If the center point of an acquired observation lay inside the region of interest of a submitted target, or if the center of the region of interest of a submitted target lay inside the footprint of an acquired observation, then the submitted target would be flagged as retired in the target database. In the Extended Science Phase (ESP), the retirement procedure was updated. The current retirement procedure also tests that the acquired observation has met the photometric and seasonal/solar longitude constraints submitted with the target. In addition, stereo and seasonal repeat checks are also applied so that requests for repeat series are not automatically retired.

There are circumstances where a target suggestion may be marked as retired but needs to be reset to active status (unretiring). These cases include observations that were partly or entirely lost due to Deep Space Network ground station issues, instrument problems such as bit-flips, or weather conditions on Mars resulting in a poor image being acquired. Targets retired by lost observations will usually be automatically reset, while others may require an evaluation by a science team member before requesting that the suggestion be unretired by operations staff.

8. Instrument issues and anomalies

8.1. Hi5

Hi5 is a graphical interface developed in Java that easily allows team members to monitor the health and safety of the HiRISE instrument; it displays various HiRISE engineering data such as temperatures, voltages, and currents. These data can be used to create plots within the interface and those plots can be saved as PNG images, or the data can be exported as tab-separated or comma-separated text files. Also included in Hi5 are various status metrics and counters, along with information on errors and commands issued. The input engineering data can be streamed from real-time telemetry, or archived data can be loaded into the application. Hi5 has been an indispensable tool for monitoring HiRISE health and anomaly investigations.

8.2. “Safing” events

When the spacecraft or an instrument experiences an anomaly, it may go into a “safe” mode. For HiRISE, this means powering it off. The HiRISE flight software is very conservative, so if any “red” (uppermost) limit is exceeded from a temperature, current, or another sensor, the “keep-alive” counter is stopped, which then leads to the spacecraft powering off the instrument. When the spacecraft goes into safe mode, it powers off the instruments. No new imaging data can be acquired until HiRISE is powered on, the optics are sufficiently warm, and the LUTS have been re-loaded, resulting in at least several days with no new images. Table 15 lists all such events affecting HiRISE.

HiRISE has safed itself for several reasons during operations. Ideally, a full SSR should never cause an instrument to safe, but a flight software misunderstanding about how HiRISE works produced a problematic scenario. When the HiRISE raw data partition is full, the HiRISE FPS has already been turned on, but the spacecraft never commands an image, so the FPS heats up until it reaches the red limit, then safes the instrument. The HiRISE team developed a method to shut down the CPMMs and prevent overheating, but HiRISE safed a second time because of power supply limits associated with this off-nominal sequence. The team has thus had to carefully monitor SSR data usage (Section 7.15) to prevent

filling of the HiRISE partition of the SSR.

The next two HiRISE safing events were due to the failure in 2011 of CPMM 13, which controls the RED9 CCD (Section 8.5). Three safing events were due to power supply over-voltages, likely either spurious or actual. One safing resulted from exceeding a temperature limit on the IEA due to redundant spacecraft solar array controllers being unintentionally commanded on; that limit was also raised to avoid future safing from overly conservative limits.

An event on orbit 52,182 was due to an unexpected drop of spacecraft battery voltage, triggering safing of all instruments. This was followed by a successful campaign over several years to recondition the spacecraft batteries. Responses to this event led to several other issues (Sections 8.7, 8.8, 12.2).

8.3. Spacecraft jitter

TDI imaging with a 1-microradian instantaneous field of view (IFOV) makes HiRISE very sensitive to image smear from spacecraft pointing jitter. Low-frequency jitter can be measured with HiRISE image data, and the geometric distortions of the images can be corrected (Sutton et al., 2019), but high-frequency jitter (shorter than the typical TDI integration time of 10–13 ms) smears the image, so we strive to minimize this high-frequency jitter. In-flight jitter mitigation has been focused on minimizing instrument and mechanism motions during high-stability imaging modes. The MRO project considered jitter requirements for choosing spacecraft components and subsystems, such as the reaction wheels (Graf et al., 2005). MCS is a known source of jitter that smears and distorts HiRISE images from movement or acceleration of the scanning mechanism. For all high-stability imaging modes, MCS motion is paused.

Additionally, early in the mission, the solar array gimbal motions were paused for off-nadir high-stability images. Between January 2008 and June 2009, pausing the solar array motions for high-stability off-nadir observations was eliminated. The HiRISE team demonstrated an increase in jitter during this period, and pausing the solar array motions for high-stability off-nadir images was reinstated.

We almost always prefer to image in high-stability mode, but this is impossible when conflicts with other instruments or the spacecraft prevent us from using this mode. These non-high-stability (or “normal” stability) images are usually planned in bin-2 or bin-4 modes that are not as sensitive to smear as bin-1 mode. Due to operational constraints, images planned to coincide with relay activities (for data uplink from rovers and landers) must be in normal stability mode, so there is a chance that MCS could be in motion during these images. Approximately 20% of images taken during relay activities overlap with MCS motion. A little over half of these images are negatively impacted by jitter (Fig. 15). We sometimes use bin-1 in normal-stability mode, accepting the risk of jitter-induced smear in parts of the image. The PDS image labels contain information about the image stability mode.

8.4. BG13 blooming

Most images acquired before launch by CCD BG13 with 128 or 64 TDI lines included partial or complete blooming over the image, with saturated data. This blooming was thought to be due to a broken wire trace affecting TDI 128 and 64. HiRISE began the PSP using BG13 with 32 TDI lines and typically bin-4 to achieve a high SNR. However, we experimented with TDI 128 and 64 and did not see any blooming in flight except very rarely for bright scenes, and even then, only near the end of the ramp, bleeding into just the initial few Mars image lines. (The image ramp is produced when the instrument switches from reverse- to forward-clocking of TDI, resulting in double exposure; see Fig. 11 of McEwen et al., 2007). As a result, except for the first two months of the PSP, we have used the full capability of BG13.

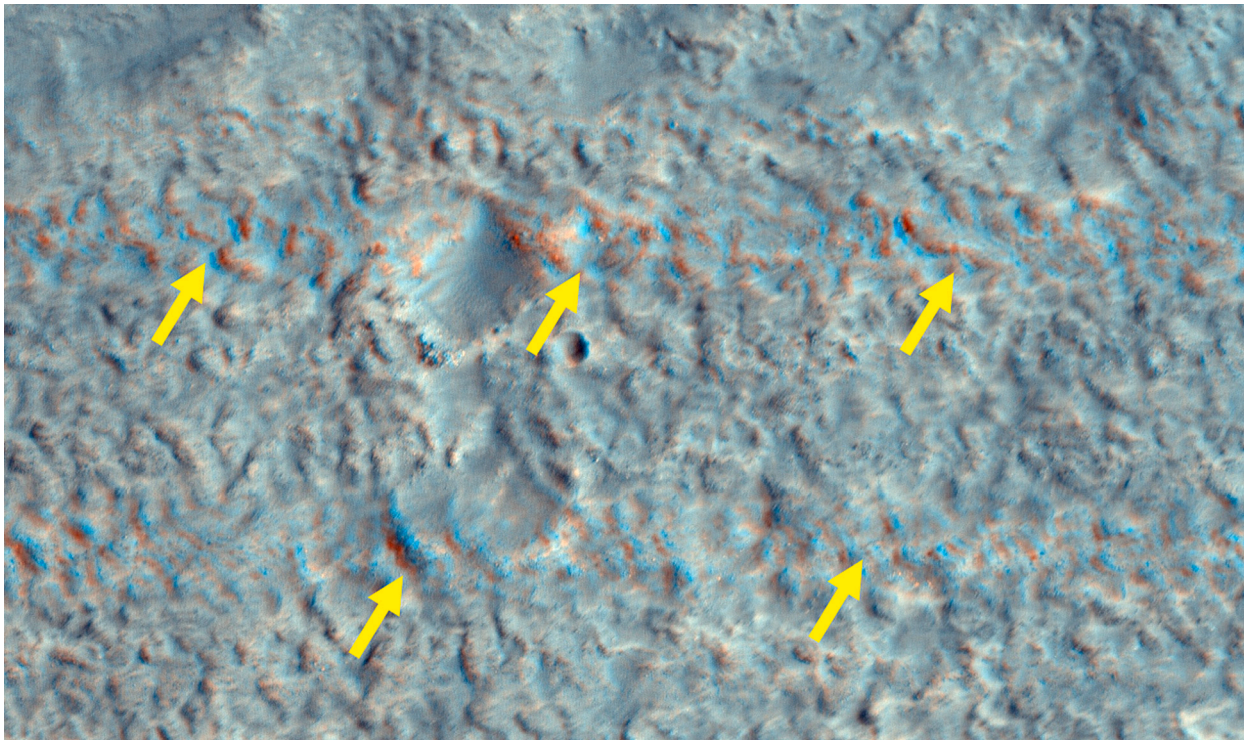


Fig. 15. Example of image smear caused by motions of the MCS. The smear is most obvious in color products from sets of lines with color fringing (see arrows) ESP_055135_2190, RGB color, Bin 1A (NOMAP extras product). North is down. Scene width 0.5 km.

8.5. Failures of RED9 and RED4 CPMMs

In 2011 HiRISE safed (see Table 15) because the instrument flight software received no response from the CPMM for CCD RED9 during the power-up sequence for a commanded image. Analysis of earlier data revealed a temperature dependence that worsened over time and eventually led to complete failure, suggesting an intermittent connection. A later failure of a CPMM in the engineering model at Ball Aerospace suggested a failure of a particular electronic part, the electrically erasable programmable read-only memory (EEPROM) that held the field programmable gate array (FPGA) programming code. A major worry in 2011 was that all the CPMMs could be susceptible to failure in this manner, but the absence of any other failures in more than ten years suggests that there was something unique about the RED9 CPMM, not inherent in the board design. Our planning and commanding software now ensures we never image with this CPMM. Fortunately, RED9 is at the outer edge of the ten RED CCDs, so our swath width was reduced by 10 % rather than creating a gap in the processed images.

In 2023 HiRISE safed (Table 15) because the instrument flight software received no response from the CPMM for CCD RED4 during the power-up sequence for a commanded image. Analysis of earlier data revealed a temperature dependence that worsened over time, similar to the history of RED9, but worsening at a slower rate. Perhaps the same part failed as for RED9, or a different part failed. Either way, the temperature cycling of the HiRISE FPE is suspected to contribute to such failures.

8.6. Preparation for swapping sides of block-redundant electronics

The remote electronics consists of two boxes: the instrument controller and the power supply (see Fig. 1 of McEwen et al., 2007); both are entirely redundant, and together, they are called side A and side B of the electronics. Since MRO launch, HiRISE has always operated on side A. These boxes are cross-strapped to the spacecraft so that either side can be operated from either side A or side B of the spacecraft, which is very

fortunate because the spacecraft often “decides on its own” to swap sides, which has caused many of the spacecraft safing events (Table 15). However, there is no cross-strapping to the solid-state recorder (SSR), nor is the Electra ultra-high frequency (UHF) relay cross-strapped to the SSR. This lack of cross strapping means that if side A of either HiRISE, the SSR, or Electra needs to swap to side B, the other two systems must also swap to side B to store data. We have developed plans to safely switch HiRISE for this possibility.

The HiRISE FPE contains 14 sets of relays on its backplane, five each per CPMM. Swapping redundant sides is accomplished by switching each set of relays on the backplane to the active side. The remote electronics are first booted to the new side by the spacecraft, then each set of relays is moved to the new side via an instrument command, one per CPMM. The most conservative procedure would be to switch the relays for a single CPMM and examine the received power supply telemetry to confirm proper relay operation. Optionally, we may command a confirmation image to verify that the operation was a success if the telemetry is inconclusive. Each such operation requires an uplink window followed by some amount of ground data system time to study the results; the optional confirmation image requires yet another uplink window and more ground time. Swapping sides could take several weeks or months if each CPMM was switched and verified individually. To minimize the total time required while still maintaining some localized knowledge of relay operation, we plan to bundle individual CPMM commands into groups, starting with a single CPMM, followed by two CPMMs, followed by four, followed by five, and concluding with two single CPMMs at the end. The final CPMMs are those for CCDs RED9 and RED4, which no longer work. We do not expect that a side swap would restore RED9 or RED4 functionality, but we would likely try anyway.

8.7. Blurred or out-of-focus images

From early 2017 until 4 Sept 2018, some bin-1 images appeared blurred. Blurring can be challenging to recognize because aeolian processes often smooth the surface, and other factors can reduce image

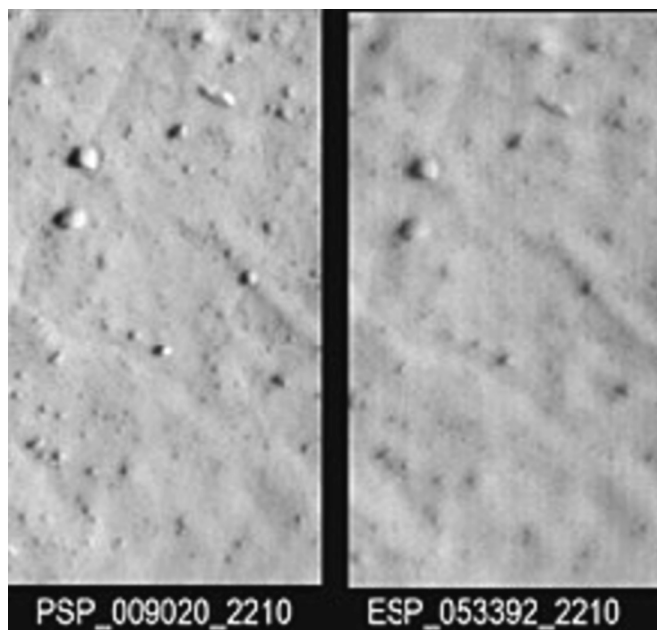


Fig. 16. Comparison of bin-1 images covering the same patch of ground under similar photometric angles but showing reduced resolution in the more recent image (ESP_053392_2210, acquired 16 Dec 2017). Image width is 150 m wide on Mars, and north is down.

quality. However, a comparison to earlier images over the same location makes it clear when an image is blurred (Fig. 16). Through 2017 the percentage of blurred images increased, rising to about 40% of full-resolution images at the end of the year. We initially suspected that

the cause of this blurring was high-frequency pointing jitter introduced by a change to the spacecraft attitude control system. The limited lifetimes of the spacecraft inertial measurement units (IMUs) led to the development of an “All-Stellar” navigation technique that did not utilize the IMUs, saving them for special events when needed. We initially noticed the blurred images during the first in-flight test of All-Stellar mode with HiRISE imaging (20 Oct 2017), so we suspected high-frequency jitter resulting from the test. However, further analysis revealed a temperature dependence to the blurring, and the All-Stellar test happened near martian apoapsis when the spacecraft is coldest. The temperatures of the HiRISE optical components, especially the secondary mirror (Fig. 17) and the “spider” structure holding that mirror were unusually cool in the blurred (or out-of-focus) images. Although such temperature changes, if uniform, were not believed capable of causing such blur, transient temperature gradients became the top suspect, perhaps by changing the primary to secondary mirror spacing.

The secondary mirror and spider were more frequently cold during imaging in 2017 than previously due to various spacecraft changes leading to a colder environment around HiRISE, our use of longer reverse-clock warmup times, and after a HiRISE change made on 11 June 2017 to help mitigate the spacecraft battery undervoltage. Rather than acquire throwaway warmup images during eclipse (simplest for HiRISE operations) to mitigate the ADC bit-flips (Section 8.9), we started acquiring such images immediately before starting the dayside images of Mars. The goal was to reduce power demand during eclipses. However, the Thermal Control System (TCS) was disabled during HiRISE imaging in case it caused minor image noise. This made little difference to the temperatures of optical elements early in the mission because the TCS was only disabled for less than one minute. However, with 300 s of warming up in reverse-clock mode (where the TDI is run in the opposite direction such that charge is removed from the CCD) and throwaway warmup images acquired for up to tens of minutes to further warm up the FPE, the temperatures of small optical elements dropped

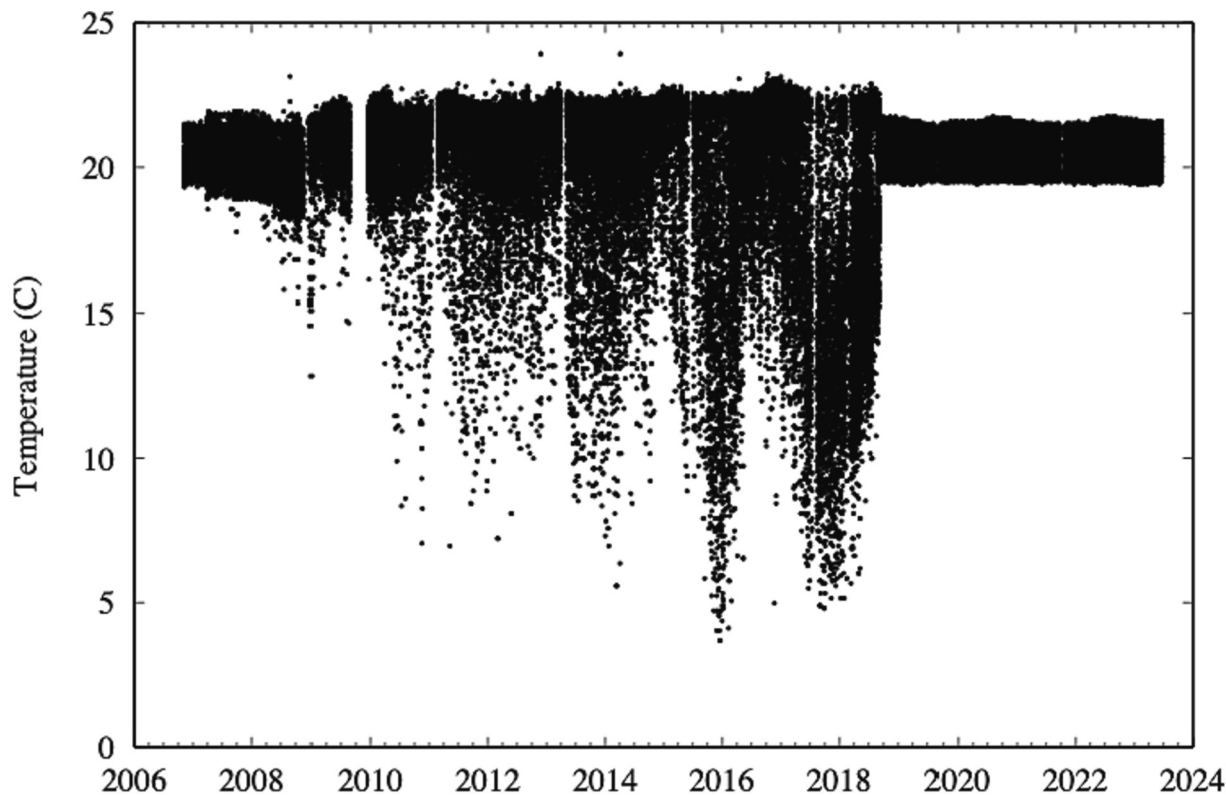


Fig. 17. Secondary mirror temperatures near the start of HiRISE forward-clock imaging. The low temperatures in late 2017 and early 2018 are often associated with reduced-resolution images. The low temperatures in the prior Mars year, such as near the beginning of 2016, may also be associated with other such images, but this has not been investigated.

significantly (Fig. 17). To test this theory, we changed the HiRISE instrument operations on 09/04/2018 so that the TCS remained on during imaging, eliminating the blurring and also not leading to a detectable increase of image noise.

<10 % of HiRISE bin-1 images acquired in 2017 and early 2018 are blurred. The PDS image labels contain information about optical part temperatures, such as SEC_MIRROR_TEMPERATURE, which should be near 20 °C. If this temperature is <17 °C, and part of the image was acquired at full resolution (bin-1), then image blur is possible, but not certain. Blurring was rarely large enough to be noticeable in bin-2 images. Images acquired within $\sim 30^\circ$ of apoapsis (L_s 71°) and with cold optical parts are especially likely to be blurred. No known images were blurred due to low optics temperatures since implementing the operational change on 9/04/2018 that keeps the TCS on during imaging sequences.

8.8. Lowering the setpoint temperature of HiRISE optics?

As part of the spacecraft battery mitigation studies (Section 8.2), the MRO project asked us to consider permanently lowering the optics setpoint temperatures from ~ 20 °C to some lower temperature requiring less battery power during eclipses. Ball Aerospace models indicated that this could be done by lowering the primary mirror temperature to near 0 °C and adjusting other component setpoints, with only a minor loss of resolution if the focus mechanism position was re-set. One challenge with this plan was that the MRO project has been reluctant to turn the spacecraft nadir deck away from Mars to observe stars, so verifying the best focus position may rely on repeat imaging of small-scale features on Mars. With the success of the battery reconditioning, this plan has been on hold, and the major optical components remain at 20 °C nominal temperature.

8.9. ADC bit-flips and mitigation

Soon after launch, when observing the Moon, we saw an unexpected problem in channel 1 of CCD IR10 (McEwen et al., 2010). At the coldest FPE and FPA temperatures, the raw image DN values were mostly zeroes. At somewhat warmer temperatures, there were still significant regions of zeroes or otherwise obviously erroneous data. There was a minor amount of erroneous data at still warmer temperatures, and the images contained all valid DN values at the highest temperatures. Further testing at even colder temperatures during the cruise to Mars revealed this problem in channel 1 of RED0 and RED3. IR10_1 soon had erroneous data even in Mars orbit with the FPE box starting at 18C, and by late 2006 RED9_1 had become very noisy at 18 °C. (The FPE box and the FPA

baseplate temperatures provide the best indicators of the temperatures of electronic components inside the CPMs, which are not measured directly.) We began taking fewer but larger images in case that would slow the degradation; we abandoned that strategy after the PSP because there was no evidence to support that assumption. The erroneous-data problem has worsened over time and affected more and more image channels (each CCD has 2 readout channels).

Analysis of the image data revealed that DN values are in error by 2^n DN values (Fig. 18), so there seem to be bit-flips (explained in Section 5.13). When the most significant bits flip, negative DN values are created that get encoded as zeroes. The very coldest images for the problematic channels tend to be nearly all zeroes or all erroneous data in some manner. Sometimes there are contrast-reversed images—where low signal areas have relatively high DN values and high signal areas have lower DN values, and the DN values are highly quantized.

We suspect that the bit-flipping happens during the analog-to-digital conversion (ADC), although the actual ADC parts are not necessarily to blame—it could also be the input signal to the ADCs. A study at Ball Aerospace concluded that there were two fundamental problems: 1. The Focal Plane Electronics Assembly (FPEA) design produced ringing in the ADC sampling waveforms plus an asymmetric video waveform, and 2. the ADC performance degrades over time. Initial testing showed the problematic ADC sampling waveform could be improved by warming the CPM circuit components, most notably the ADC itself. A life test on the HiRISE engineering model reproduced a loss of ADC sampling margin as a function of time and temperature. Passive bakeout of the ADCs for 48 h at 85 °C resulted in substantial improvement in margin. This behavior is consistent with ionic contamination of the ADCs, which can become aligned and cause faults, and heating can break up the aligned contamination. Later testing at elevated temperatures for 4330 images also improved performance, creating hope that the degradation could be reversed in-flight. However, in-flight attempts to reproduce this result did not show improvement. These experiments included acquiring many small images of Mars near orbit 10,000.

Fortunately, we were able to mitigate this problem for many years by warming the focal plane electronics before imaging. We increased the FPE heater setpoint until the heaters were almost always on, but this only raised the FPE box from our initial 18 °C to about 22 °C (varying with sun-Mars distance). We also increased the reverse-clock imaging time to warm the FPE. A small amount of reverse-clock imaging time was always needed to remove signal to prepare for forward-clock TDI producing the returned images. We increased the reverse-clock time from 30 s incrementally up to the maximum possible of 300 s as the bit-flips worsened. When even the 300 s warmup was insufficient, we began taking nightside warmup images that were effectively thrown away (not

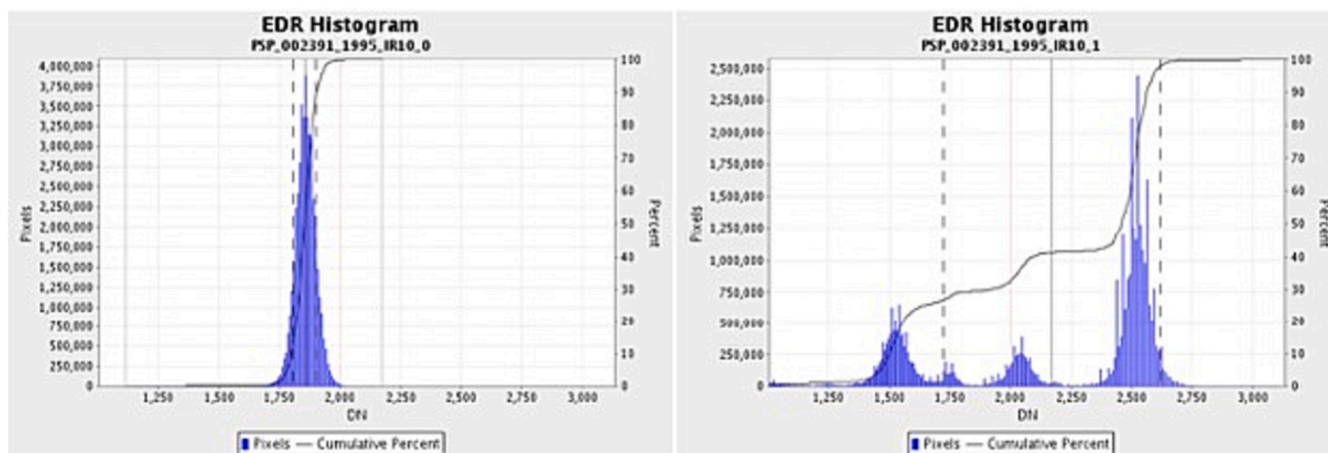


Fig. 18. Rather than having one histogram peak like channel 0 (left), channel 1 (right) has two major peaks that are offset by 1024 (2^{10}) DN, with a peak in the middle offset by 512 (2^9) DN from the largest peaks, consistent with bit-flips creating the spurious data.

returned to Earth). We established a minimum FPE box temperature goal before starting Mars imaging to mitigate major bit-flips. Over time, we raised that limit by taking longer warmup images, up to a maximum of about 39 °C. See Table 14 for when each change was implemented. We had been raising the minimum FPE temperature to start imaging by roughly 2 °C/year until 2019. Concurrently we had to raise the uppermost AFT for the FPE and coupled FPA, or acquire shorter images that ensure we do not exceed the AFT (which triggers “safing” or powering off the instrument). The initial AFTs were set very conservatively, with margin on margin; Ball Aerospace engineers eventually concluded that 65 °C was the safe maximum for the FPE and FPA. Although images acquired in the PSP had up to 120,000 bin-1 lines at full resolution (no pixel binning), limited by the CPMM memory size, the maximum in recent years has been about 60,000 bin-1 lines or 200,000 2 × 2 binned lines. Note that the bit-flips are lessened in bin-2 and bin-4 modes, and high-quality images can be acquired at several degrees cooler temperatures than in full-resolution (bin-1) mode.

Our early strategy was to mitigate bit-flips in the RED channels but allow IR10_1 to have erroneous data when too cold. The image processing pipeline could identify and replace minor erroneous data, but when it became too extreme (>10% zeroes), we did not process IR10_1, so many IRB color products had only ¾ the width of the RGB color. Although IR10_1 was the worst channel for many years, the channels worsened over time at different rates, so by around MRO orbit 50,000 (27 March 2017), RED1_1 and RED3_1 (bin-1 mode) had worse bit-flips than IR10_1 (bin-2 mode); steps taken to mitigate bit-flips in these RED channels also resulted in higher-quality IR10_1 images that were almost always processed.

Despite warming the FPE, bit-flips still occur in some images, especially channel 1 of IR10 and RED 1, 3, and 9 (while in operation); later channel 1 of RED 0, 2, 7, and 8 revealed extra noise. These images will sometimes have columns with all zeroes, and minor bit-flip noise throughout the image (Fig. 19). When especially erroneous (more than some percentage of the data are zeroes), we do not process the data into higher-level products. We recently decided to set the processing limits at 50% zeroes for bin-1 images; 40% zeroes for bin-2 or bin-4 images. CCDs BG12, BG13, IR11, and REDs 4–6 have remained free of bit-flips except at very cold temperatures that we do not normally use for imaging Mars.

By October 2019, we paused raising the FPE and FPA temperatures out of concern that cycling to high temperatures could eventually cause the electronics to fail, and because it became operationally difficult to plan many large warmup images. Fortunately, we had another mitigation strategy. During instrument development, the speed of data processing in the FPS was our major challenge, and the FPGA code was updated right up to the last possible date before launch of MRO. The FPGA code included selectable parameters for where to sample the video

waveform. There are two measurement points (reference and sample), and the difference between those values determines the image DN level. Unfortunately, there is ringing and asymmetries in the video waveforms, so sampling in the wrong locations might create extra noise or erroneous DN values. The FPGA code allows eight measurement points for references and samples. In pre-flight, we determined that the location 5 reference and location 4 sample (which we refer to as setting 54) were the sampling values that resulted in the lowest read noise. However, in case it could help with unexpected future problems, we made those ADC parameters commandable in flight. In 2019 we experimented with different ADC sampling points to see if that affected the bit-flips. To summarize, the use of different ADC sampling values allows us to lower the FPE starting temperature by about 8 °C while maintaining acceptable images. This strategy buys us several extra years in which we can image in bin-1 mode over the full RED swath width with a given starting FPE temperature.

In the FPGA code, both the reference and sampling points move together, always separated from each other by a set period, and some of these combinations are not valid because no signal is measured. There were 33 potentially acceptable ADC settings for a channel. Early in this study, we found ADC setting 74 significantly improved over setting 54 for the worst channels, so we changed our standard setting for REDs 1–3 to 74 on 2 Aug 2020. This change enabled us to lower the minimum FPE temperature by 3 °C. Worsening over time has continued with the new settings, so by 2022 these images were about as noisy as they were in 2020, and we hoped to find better ADC settings. Although there were only 44 possible settings, given how the FPGA code worked, we discovered that the ADC setting for channel 0 significantly affects bit-flips for channel 1, and vice versa. For example, although setting both channels of a CCD to 74 improved channel 1 of several CCDs, it made channel 0 noisier, so we tried 54 for channel 0 combined with 74 for channel 1 (we abbreviate this 54_74), and the resulting images were worse for channel 1 than 74_74. Thus, there were 44² or 1936 possible ADC settings to test. However, we found that five of these settings had large offsets that zeroed out calibration pixel values, 11 others produced very low signal levels in bin-1 mode, and six settings produced consistently erroneous results even at the highest temperatures. Thus, we had 22² or 484 settings to test. Multiple attempts to predict which settings might be best proved incorrect when test images were acquired, so testing all viable settings was the best path forward. We needed an efficient method to test 484 potential settings to be sure we had found the optimal settings for each CCD.

The ADC sampling settings for HiRISE were not intended to be updated frequently; they were implemented as volatile flight software constants that were expected to be updated only via a patch sequence at instrument reboot, if at all. As part of the bit-flip mitigation effort, we

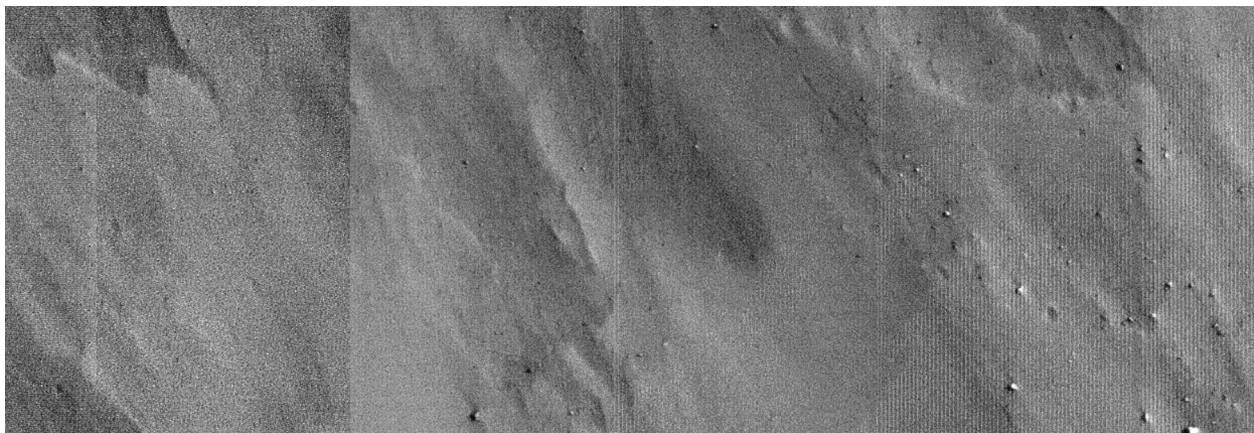


Fig. 19. Bland portion of RED3_1 of ESP_074443_1790 showing minor noise (mostly vertical pattern) due to minor bit-flips. Raw image geometry with north down, image width 0.5 km.

updated our observation command block to include the ADC settings commands. From a ground operations point of view, it was desirable to simplify the experimental procedure and to allow for maximum future flexibility in implementation. We elected to include the ADC commands as part of every observation, even if we were “setting” them to the most recent values. Doing so has led to a larger command block file size, which in turn has led to $\sim 10\%$ longer radiation times, but it greatly simplifies the ground software and reduces the workload; furthermore, since every observation command block includes ADC settings, we can forego updating them in the HiRISE boot patch sequence after safing events. Operations engineers (HiTS) can now modify a particular observation’s ADC settings via the HiRISE planning tool, HiPlan.

In 2022 we executed the ADC study in two basic steps. First, we acquired hundreds of nightside stim-lamp (light-emitting diode or LED) illuminated images with the FPE box in the 35–37 °C range, as a first pass to eliminate many obviously erroneous settings (many bit-flips even at these temperatures). The result was about 8 settings that appeared promising in Bin 1A mode. Next, we acquired sets of images in each of the 8 settings plus the current standard (54_54 except for RED1–3 at 74_74). This test required nadir-only orbits to ensure we could place the images in the exact same sequence for each orbit (and after 3 orbits with no HiRISE imaging). The resulting images have very consistent FPE and FPA temperatures. There are 7 images for each combination of ADC settings, with FPE starting temperatures near 21, 27, 33, 37, 40, 42, and 44 °C. The last image of each sequence is a nightside image illuminated only by stim lamps; these are best for measuring image SNR independent of bit-flips (except minor bit-flips for RED1_1 and RED3_1).

With these results, we could measure the percentage of erroneous pixels due to bit-flips, the signal levels, and the standard deviation of calibration reverse clock pixels (returned with each image) as a measure of image noise. Our primary goal was to eliminate obviously erroneous pixels (DN values outside the valid image range) resulting from bit-flips since this problem worsens over time. However, in many cases, there are effectively “ties” between channel settings, so then we strive to optimize the SNR (high signal and low noise). Seven settings give nearly the same results regarding erroneous pixel values, but two result in low SNRs. The five best settings (at least for the problematic RED CCDs 0–3 and 7–8) are 64_74, 65_74, 66_74, 75_74, and 75_85. After optimizing SNR for each CCD, the best choices are 64_74 for RED2 and RED7, 65_74 for RED0 and RED8, and 75_74 for RED1 and RED3. For the best-behaved

CCDs, there are new settings that result in fewer bit-flips at cold temperatures than setting 54_54, but we will image Mars at warmer temperatures to mitigate bit-flips in other CCDs, so staying with 54_54 is best for the near future. IR10 is close to the edge: currently 54_54 returns acceptable results, but in a few years as bit-flips worsen we may change to an alternate setting. Setting 44_52 looks like the best alternate setting for IR10 in bin-2 mode, but the bin-2 settings will be re-evaluated in future years.

8.10. Predicting future performance

The most significant risk to the future of HiRISE is the complete failure of additional CPMs, as happened to RED9 in 2011 and RED4 in 2023. Continued image degradation due to bit-flips is less catastrophic but sure to happen. There have been no problems with the HiRISE telescope, thermal control system, focus mechanism, or remote electronics (for which there is also a redundant side B).

We have data characterizing how fast some of the worst channels are degrading over time. Plotting the FPE temperature at a certain level of bit-flip noise versus orbit number or time (Fig. 20) reveals how the FPE starting temperature varies over time. These data are mostly collected for setting 54_54, so we must assume the same rate of degradation at new settings. With the reduction in FPE temperature now possible, we can make predictions (Table 16). The 1 °C/yr trends are upper limits for CCDs 4–6 and 11–13, for which there is not enough data for a prediction. RED1_1 may become problematic even in bin-2 mode before 2026; the same is probably true for RED3_1. Since we can image at ~ 3 °C lower temperatures and replace some amounts of erroneous data (Section 5.12), full resolution over the entire swath width will likely be possible until about 2024, but with short image lengths. Sometime after 2024 we will need to either use Bin 1–2 mode instead of Bin 1 (Table 8), or acquire narrow images that exclude RED0–3, or in some cases, use a higher FPE starting temperature and accept the risk from ending temperatures greater than ~ 55 °C. With the AFT at 65 °C (and not likely to be raised), the highest starting FPE temperature in a few years could rise to near 50 °C so that the ending temperature is well below the AFT to avoid safing HiRISE. However, FPE starting temperatures higher than 45 °C might be considered problematic in terms of potential CPM failures. When we can image at full resolution only in RED5–6 (2 contiguous CCDs), we need to acquire ~ 5 images (including overlap) to cover an

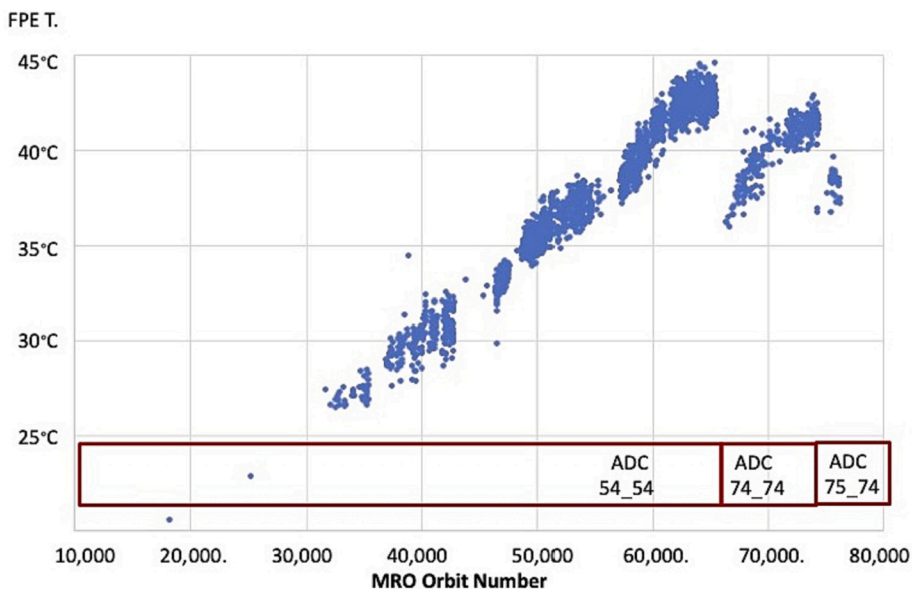


Fig. 20. Plot of FPE starting temperatures (vertical axis) resulting in $>0\%$ and $<1\%$ zero-DN pixels versus orbit number (horizontal axis) for RED1_1. The offset near orbit 65,800 marks the switch from ADC sampling 54_54 to 74_74, and the offset near orbit 74,700 is from the later switch to 75_74. A linear fit to the data with ADC 54_54 yields a slope of 0.00054C increase per orbit, or 2.5C/yr.

Table 16

Minimum FPE temperatures (T) needed to avoid any obvious erroneous pixels with ADC settings in June 2022 and with new ADC settings, and predictions for minimum FPE temperatures needed in 2026 and 2030. Numbers in red may be unacceptably high.

CCD	Bin	Min-T 2021	Min-T with new ADC	Deg C/yr worsening	Min-T needed in 2026	Min-T needed in 2030
RED0	1	43	35.5	1.4	41.1	46.7
RED1	1	43	38.5	2.5	48.5	58.5
RED1	2	40	35.5	2.5	45.5	55.5
RED2	1	38	34	2.5	44	54
RED3	1	43	38.5	2.5	48.5	58.5
RED4	1	25	25	<1	N/A	N/A
RED5	1	25	25	<1	<29	<33
RED6	1	21	21	<1	<25	<29
RED7	1	41	31.5	2.8	42.7	53.9
RED8	1	39	31.5	1.9	39.1	46.7
IR10 (54_54)	2	36	36	1.4	41.6	47.2
IR10 (44_52)	2	36	26	1.4	31.6	37.2
IR11	2	27	27	<1	<31	<35
BG12	2	27	27	<1	<31	<35
BG13	2	21	21	<1	<25	<29

area at full resolution, such as a candidate landing site. The same coverage previously required just one image. However, the rate of degradation might change if we greatly reduce acquisition of bin-1 images. Also, there may be new ADC settings for bin-2 and bin-4 mode that allow lower starting FPE temperatures. These possibilities will be studied to find the best way to optimize the useful lifetime of HiRISE.

9. Calibrations

HiRISE calibrations are of two types: geometric and radiometric. Geometric calibrations such as focal length and optical distortions have been well characterized since early in the mission (McEwen et al., 2007; Kirk et al., 2008). Geometric distortions due to pointing jitter are also correctable, as described by Sutton et al. (2019) (see also Section 8.3). Most science results from HiRISE depend more on geometric corrections than photometric corrections.

Radiometric calibration has been less stable due to FPEA design (to minimize mass and power) and in-flight issues. HiRISE acquires Giga-pixel images in just a few seconds, generating considerable heat in the FPE and FPA. Stable calibration requires precise detector temperature control. However, given mass and power constraints on the imager design, we decided to let the FPE/FPA temperatures rise and fall dramatically. These issues cause relative (pixel-to-pixel) radiometric calibration uncertainty of 1–2% and absolute radiometric calibration uncertainty of ~20% (Milazzo et al., 2015). When the ADC bit-flip issue arose, we mitigated the erroneous data by going to even higher temperatures beyond the range of initial calibrations.

The new ADC settings have complicated radiometric calibration. When we first switched to 74_74 for REDs 1, 2, and 3, the offset changed enough to turn some calibration pixel data into nulls after the Look-Up Table (LUT) compression from 14 to 8 bits per pixel. New LUTs were developed to enable a wide range of potential offset values as a function of ADC setting but were not implemented until 3 Aug 2021. Thus, a year’s worth of HiRISE images (mostly bin-1 images) may contain artifacts introduced by the HiCal pipeline; these may be repaired when we reprocess the entire dataset and convert it to PDS-4 format. New ADC settings also change the image gains, but those should be normalized to channel 0 of RED5 by the image processing pipelines HiStitch and HiccdStitch (Table 12), and RED5 has remained at ADC setting 54_54.

10. Citizen science and machine learning

10.1. Citizen science

HiRISE Clickworkers was a citizen science effort from ~2007 to 2010 (Gulick et al., 2010; McEwen et al., 2010). Our experiences with Clickworkers and our HiRISE Student Image Challenges (Section 11.5)



Fig. 21. Fans in HiRISE image ESP_011960_0925, acquired at 87.3S / 167.8E. RGB color, scene width 0.5 km.

show that given carefully thought-out tasks combined with easy-to-use online tools, students, educators, and the general public are very interested and capable of participating.

A citizen science project known as “**Planet Four**” began in 2013 using the Zooniverse platform built by the Citizen Science Alliance. They provide the web portal and technical expertise for involving large numbers of volunteers in research projects online (described at <http://www.zooniverse.org>). The original Planet Four task asked volunteers to identify and outline fans and blotches in images of Mars’ south polar region that appear every southern spring. The model of Kieffer (2007) describes the seasonal activity: In the winter, under the right conditions, the seasonal CO₂ polar cap becomes a translucent slab of impermeable ice. Penetration of sunlight through the ice, which warms the ground below, results in basal sublimation of the ice. Trapped gas escapes through ruptures in the ice, eroding and entraining material from the surface below. When this dust-laden gas is expelled into the atmosphere the dust settles in fan-shaped deposits on the top of the ice in directions oriented by the ambient wind (Fig. 21). The number, time history, area covered, and changes of the fans provide a wealth of information on the spring sublimation process. The length, width, and direction are snapshots in time of the local wind direction. With the aid of Zooniverse staff, we developed statistical tools to identify the “best fit” outline. The measurements are assembled into a fan and blotch catalog (Aye et al., 2019). Over 150,000 people have generously donated their time to the Planet Four task.

Four peer-reviewed science publications have resulted so far from the Planet Four efforts (Schwamb et al., 2018; Aye et al., 2019; Portyankina et al., 2022; McDonnell et al., 2023). Portyankina et al. (2022)

compared the wind direction indicated by fan orientation to the predicted wind direction of the Mars Regional Atmospheric Modeling System (MRAMS), a mesoscale atmospheric circulation model. Two other citizen science projects were developed under the “Planet Four” brand: Planet Four Terrains and Planet Four Ridges. The Planet Four Terrains task asked volunteers to identify specific features in CTX south polar images: “Spiders” (radially organized channels or araneiform terrain), “Swiss cheese” terrain (quasi-circular erosion), and craters. HiRISE images were targeted to follow up on promising areas. Results showed that araneiform terrain exists in favorable locations, not just on the unit mapped as South Polar Layered Deposits (Schwamb et al., 2018). Planet Four Ridges aims for citizen scientists to map polygonal ridge networks in Nili Fossae and parts of Nilosyrtris/northern Terra Sabaea (Khuller et al., 2022). The catalog is also being used as a means of testing machine learning (McDonnell et al., 2023).

10.2. Machine learning

The volume of HiRISE data greatly exceeds what any individual researcher can analyze in traditional ways. Machine learning methods can more rapidly discover patterns or features of interest in large datasets and automate tedious or time-consuming tasks. There have been machine learning studies with HiRISE data to map linear bedforms (Foroutan and Zimbelman, 2017), detect new block falls in the north polar region (Fanara et al., 2020), detect new impact sites (Wagstaff et al., 2022), to detect recent rockfalls (Bickel et al., 2020), and to classify terrains (Barrett et al., 2022).

11. Education and public outreach (E/PO)

11.1. Mars books

The first full volume of HiRISE images appeared from French publisher Éditions Xavier Barral in 2013, “This is Mars,” featuring black and white images. In 2017, the University of Arizona Press (UA Press) published a large color book, “Mars: The Pristine Beauty of the Red Planet.” The book featured captions written by members of the HiRISE team for hundreds of images that highlighted the enhanced color capabilities of the camera. All captions appeared in English and one of 24 other languages. HiRISE has also produced an ebook about Mojave crater (available for free on the Apple Bookstore and in PDF format) in English and Spanish, with two more planned (see: <https://www.uahirise.org/epo/ebooks/>).

11.2. Captioned releases

Throughout HiRISE operations, we have provided captioned images on a regular schedule to post to our website and social media channels for the benefit of explaining HiRISE science to the public (see <https://www.uahirise.org/catalog/captions/>). As of June 2023, we have over 2249 fully captioned images that include extras such as wallpaper, slides, and flyers. Some products include an audio version of the caption for the visually impaired, and often a video clip. Producing these extras for fully captioned images has become standard procedure, often resulting in media outlets using them when a particular image comes to their attention. Additionally, video and audio clips are posted separately to HiRISE’s YouTube and Soundcloud channels to broaden our reach for those who not utilizing our website. For many years, we have also captioned our video files (HiClips) when posted to our website and other channels.

11.3. Social media presence

HiRISE has maintained several social media channels that promote our captioned images, our HiPOD images (HiRISE Picture of the Day) and Mars and science-related topics. Our verified and flagship Twitter

account has over 91,300 followers; our combined Twitter channels featuring other languages (see below) exceed over 102,000 followers. In total, our social media channels have over 230,000 followers. A full list of our social media accounts is here: <https://www.uahirise.org/epo/map/>

11.4. The beautiful Mars project (formerly HiTranslate)

From the beginning of the mission, HiRISE has adhered to a simple philosophy: we are the People’s Camera. In 2010 we created “The Beautiful Mars Project” to solicit volunteers to help us translate our image titles and captions into various languages (see <https://www.uahirise.org/epo/>). With dozens of volunteers, HiRISE is represented in 24 languages, the most of any active NASA mission. Volunteers from all over the globe have translated over 5220 titles and captions of our complete catalog. Several volunteers have also provided audio files (Spanish, Greek, Catalan, Irish, and Russian) to accompany captioned images that we subsequently posted to various YouTube channels.

11.5. HiRISE image suggestion challenges

Our student image suggestion program, conducted in association with NASA Quest as HiRISE Image Challenges (<https://marsoweb.nasa.gov/HiRISE/quest/all/>), was described in McEwen et al. (2010) and is updated here. Over 600 image suggestions were submitted during the challenges, with over 1164 participants from 45 states and 42 countries. Participants represented over 18,800 students in grades 2 through 14 and consisted primarily of teachers, parents of home-schoolers, student clubs, college students, and life-long learners.

Several participants continued submitting HiRISE image suggestions long after the challenges ended. One of our most active participants was a group of seventh and eighth graders from Evergreen Middle School in Cottonwood, CA, where over half the students were economically disadvantaged. These students, led by their enthusiastic and passionate Math teacher Mr. Dennis Mitchell, formed an after-school NASA Mars club. The Mars club participated in all the HiRISE Challenges and ASU’s Mars Student Imaging program. When the challenges ended, Mitchell and his students continued working with HiRISE Co—I Gulick through Spring 2017, when Mitchell retired. Each Spring, the students would visit NASA Ames to present their research.

11.6. Other outreach

Members of the public utilized HiRISE data in unexpected ways. These efforts were highlighted with the “Made with HiRISE” page on our website: <https://www.uahirise.org/epo/made-with-hirise/>. These uses have ranged from visual artistry through flyovers (made from digital terrain models) to artistic interpretations of the intersection between art and technology (e.g., see <http://hyperspace.beck.com/#content-mars>).

The HiRISE team also engaged in hundreds of public talks as well as tours for classes at the university level focusing on remote sensing and the production of DTMs. We have also answered numerous media requests for our images and coordinated important releases with our counterparts at JPL Media.

12. The future of high-resolution orbital imaging of Mars

12.1. The future of HiRISE

The Mars Exploration Program has relied on HiRISE to characterize landing sites. HiRISE contributes to the analysis of science potential, along with many other remote-sensing experiments, and uniquely contributes to assessing landing site safety (Section 6). DTMs from HiRISE stereo coverage are used for detailed landing simulations, terrain relative navigation (Ferguson et al., 2020) and boulder counts, slopes, and topography to assess small-scale hazards. However, the full resolution of

HiRISE is essential to many of these data products. For example, too many boulders are unresolved in bin-2 images to fit a size-frequency distribution down to the scale relevant to landers (Golombek et al., 2012a). In future years HiRISE will provide less full-resolution coverage, due to ADC bit-flips worsening over time (Section 8.9). These points are especially relevant given that HiRISE is the only Mars orbital imager operating or planned and capable of meeting the data requirements for sufficiently characterizing landing sites.

12.2. Moving to a later LMST?

Although the battery reconditioning has removed the need to move MRO to a near-terminator orbit to keep solar arrays in the Sun for most of each orbit, the Mars2020 project still prefers to receive the relay data later each Mars day, which facilitates rover planning by increasing the amount of time for operations prior to uplink of critical data to the orbiter for downlink to Earth. The Mars2020 project receives a small fraction of its data through MRO relative to the Mars Atmosphere and Volatile Evolution (MAVEN; Jakosky et al., 2015) and TGO spacecraft. MRO teams evaluated a 4:30 PM LMST and found it significantly worse for science. In the case of HiRISE, the main issues are (1) loss of signal from poorly illuminated surfaces, (2) different illumination angles complicate long-term change detection comparisons with previous data taken at other local times, and (3) shortened observing seasons for features of interest, such as frosted gullies. The later local time would also preclude stereo completion of pre-existing images with matching illumination angles. The later LMST is an advantage for imaging the morphology of subdued (low slope) terrains near the equator.

12.3. Simplified operations?

Operations have grown more complicated over the PSP and early mission extensions as the MRO project has balanced various science and engineering issues. Resolving pointing conflicts between experiments is handled with an automated round-robin scheme with multiple iterations, automatically incorporating MCS rules that limit large rolls, spacecraft exclusion zones, and other planning restrictions. As a result, HiRISE planning is indeterminate—we must plan about four times as many observations as are acquired each cycle. This overplanning could be avoided if planning were determinate, i.e., all or most planned observations were actually acquired. The recent termination of observation planning by CRISM has helped: now we only need to over-plan by about a factor of three.

While resources are more limited in each extended mission, the workload involved in observation planning has increased for HiRISE, to manage temperatures to mitigate ADC bit-flips while protecting electronics, and tracking SSR data volume to avoid safing HiRISE. The team has developed new software and procedures to streamline operations, such as the new HiPhoP (Section 7.10), STaR (Section 7.13), CIPP-lite (Section 7.6), and other measures. The latest development efforts were made possible by “standing down” and not acquiring data in some cycles (Table 6). If funding continues to decline and MRO operations remain complicated, we will need to either find further streamlining or use more stand-down cycles. Abandoning the use of CIPPs is one possibility (Section 7.6).

12.4. Lessons received for future high-resolution orbital imaging

MEPAG has posted reports from the Next Orbiter Science Analysis Group (NEX-SAG) and other studies that describe the value of a new orbiter to support future Mars robotic and human exploration. The top priorities were understanding active processes and locating and characterizing candidate landing sites and surface exploration regions with HiRISE-class (30-cm-per-pixel) or better (10- to 15-cm-per-pixel) imaging. NEX-SAG proposed using solar-electric propulsion and advanced telecommunications (Ka-band and high-power RF amplifiers and a laser

communication experiment), enabling a much higher data rate to Earth than past orbiters. Solar-electric propulsion also increases the potential mass of the science instrument payload that can be launched to Mars by a given launch vehicle. The desire to achieve a spatial resolution better than HiRISE is driven by scientific objectives related to determining process-diagnostic morphology and structure (such as understanding recurring slope lineae (RSL)), to support landing site characterization, aid in surface activity planning, and even diagnosis of engineering anomalies (such as clues to the Beagle-2 lander failure). Accordingly, we discuss challenges and lessons learned for the benefit of future high-resolution imaging science at Mars.

A factor of two or three improvement over HiRISE image resolution doesn't sound very difficult, but it is. Increasing a small camera resolution by a factor of two or three is not challenging. However, HiRISE—the largest telescope ever sent to another planet—is already pushing against several limits. Large telescopes are difficult to accommodate on spacecraft, including the mass, volume, and pointing stability. Resolution is inversely proportional to the diameter of the telescope aperture. HiRISE has a half-meter aperture, so doubling the optical resolution requires a primary mirror about a meter in diameter, which, in turn, enlarges the other mirrors and their support structure. This more capable instrument would significantly increase mass and volume. Alternatively, new technologies can reduce the mass of the telescope (as with James Webb Space Telescope), but that increases cost and risk. However, new launch vehicles may make it more economical to send larger payloads to Mars (Heldmann et al., 2021).

The challenges continue beyond simply flying a larger telescope. If the pixel scale is smaller or more TDI lines are required, the pointing stability requirement for the entire spacecraft becomes even more challenging. The stability challenge may be worsened by flying large solar arrays needed for solar-electric propulsion. Finer pixel scale over the same FOV also increases the data processing load, but advances in detectors and other electronics since 2001 are expected to reduce electronics mass and power requirements compared to HiRISE.

High-resolution imaging of Mars from orbit is also challenging because the atmosphere causes two problems. First, the orbit cannot be lower than about 250 km (or even 300 km when the air is especially dusty and warm) because of drag on the spacecraft (unless specially designed). The MRO project had considered a periapsis at 200 km but opted for the present orbit for precisely this reason (Zurek and Smrekar, 2007). We have substantial coverage of the Moon at half a meter per pixel from the Lunar Reconnaissance Orbiter Camera (LROC; Robinson et al., 2010), which is much smaller than the HiRISE camera, but in its prime mission the Lunar Reconnaissance Orbiter traveled at an altitude of just 50 km, compared to about 300 km for HiRISE.

The thin atmosphere of Mars is also surprisingly bright due to suspended dust. As a result, more than half of the radiance of Mars orbital images is typically from atmospheric scattering; less than half of the light reaching the camera is from direct reflection from the surface that reveals small-scale features. This atmospheric haze can be subtracted from the images to increase contrast, but it still contributes photon noise proportional to the square root of the signal. The solution is to acquire images with a very high signal-to-noise ratio (SNR). The top-of-atmosphere SNR needs to be about 150:1 (a typical value for HiRISE) to ensure that the SNR of surface features is at least 50:1 in most images. Sometimes the dust is so thick that the surface SNR is much worse, approaching zero.

Another challenge is that the mass of Mars dictates that low circular orbiters must travel at a velocity of about 3.2 km per second. Imaging at a scale of 0.3 m per pixel requires a line time of 94 microseconds ($(0.3 \text{ m}) / (3200 \text{ m/s}) = 0.000094 \text{ s}$) with a requirement of one pixel of smear in the down-track direction. With an integration time of 94 microseconds, HiRISE optics would result in a typical image with a SNR of only 10 rather than 150. HiRISE overcomes the SNR challenge with a TDI sensor, imaging each surface patch up to 128 times and summing the signal on the CCD detector. What if the imaging scale is reduced to 15 cm

per pixel? Then the integration time is just 47 microseconds, and ~ 256 time-delay integration lines are needed for adequate SNR (assuming a 1-m primary mirror), and the pointing stability must be two times better. The spacecraft pointing stability needs to be very precise to ensure a surface feature is re-imaged in the same TDI column, not jittering or wandering over multiple columns, smearing the image. The Mars Reconnaissance Orbiter was designed to achieve high stability for HiRISE (Lee et al., 2003). Improving image resolution by a factor two is not confined to the cost of the camera; this improvement drives the cost of the entire spacecraft.

HiRISE has provided several lessons that may be useful for future instruments. The baseline characteristics of HiRISE (high resolution and signal-to-noise ratio, and color capability) have all proven highly valuable to science analysis, as described previously. We focus here on lessons learned that may be useful for future high-resolution orbital imaging systems at Mars or elsewhere.

- The “People’s Camera” concept of HiRISE has been valuable. Public target suggestions constitute a significant fraction of our target database and ensure that no aspect of Mars science is overlooked, while prioritization of targets by a group of specialist team members has optimized the use of limited coverage. The rapid release of images has benefited the community, especially early-career scientists who are less likely to be on instrument teams.
- Many of the challenges the HiRISE team faces can be summarized as *complexity*. The instrument has been challenging to calibrate and command, given the 28 separate CCD channels. Requirements developed to accommodate all MRO instruments with different pointing desires also result in complex and labor-intensive operations. Stereo observation planning requiring images on two orbits also adds operational challenges compared with single-pass-stereo used by the High Resolution Stereo Color Camera (HRSC; Jaumann et al., 2007) and CaSSIS. “Keep it simple” is excellent advice.
- The Sun-synchronous 3 PM orbit has generally been a good choice for providing adequate illumination and topographic shading without harsh shadows. The fixed local time of day has been valuable for obtaining repeat images with similar lighting. Future Mars imagers in a similar orbit would benefit from consistency with this existing record. The orbit does impose some limitations, notably the inability to observe phenomena at other times of day (such as morning frost) and limits on the temporal frequency of some repeat observations.
- Although it poses accommodation challenges for some other instruments on MRO, the ability to conduct precision off-nadir targeting has been invaluable for rapid coverage of key events like a new landed asset or ice-exposing impact, stereo coverage, change detection imaging of specific locations, and efficient mosaicking of image coverage.
- Coordinated observations between HiRISE, CRISM, CTX, SHARAD, and CaSSIS have multiplied the value of each. Absence of any one of these instruments would have reduced the science impact.
- HiRISE color has been extremely valuable, but color imaging of only 20% of the image swath is a significant limitation. It forces choices about optimizing placement of the color swath or overall image footprint, and at least $5\times$ as many images (each planned separately) are required if full-color coverage is desired.
- Jitter correction, enabled by the along-track offset of HiRISE CCDs, has been invaluable for DTM production and reduces “wasted” stereo images that require re-acquisition.
- Change detection was originally only a limited part of the planned operations of HiRISE but has grown over time. Planning for such campaigns from the beginning would have influenced early targeting, via an effort to systematically acquire baseline images early in the mission. Change detection would also have influenced tool development, as HiKER observations were a late development and

planning tools such as our target database lack the capability to flag images for annual imaging or for high-quality repeat opportunities.

- Generation of map-projected, radiometrically calibrated RDRs has greatly improved ease-of-use of HiRISE data, and the ability to “stream” images via HiView rather than download complete files has also been beneficial. The JPEG2000 file format, however, is not allowed for standard data products in PDS-4.

Declaration of Competing Interest

The authors declare that they have no known competing financial interests or personal relationships that could have appeared to influence the work reported in this paper.

Data availability

Data will be made available on request.

Acknowledgments

We are grateful to have known the following HiRISE team members who have passed away: Ed Bortolini (Ball Aerospace), Kathi Baker (UArizona), Nathan Bridges (Applied Physics Lab), Wojciech Markiewicz (Max Planck Institute), and Bob King (UArizona). This manuscript benefited from constructive reviews by Mark Robinson (ASU) and Matt Golombek (JPL). The NASA/JPL MRO project supported this research. LLT acknowledges funding and support from the Canadian Space Agency through their Planetary and Astronomy Missions Co-Investigator programme (22EXPCO13) and the Canadian NSERC Discovery Grant programme (RGPIN 2020-06418). Any use of trade, firm, or product names is for descriptive purposes only and does not imply endorsement by the U.S. Government. All original data used for this paper are available via the PDS.

References

- Almeida, M., et al., 2023. Targeting and image acquisition of Martian surface features with TGO/CaSSIS. *Planet. Space Sci.* 231 <https://doi.org/10.1016/j.pss.2023.105697> article #105697.
- Arvidson, R.E., et al., 2011. Opportunity Mars Rover mission: Overview and selected results from Purgatory ripple to traverses to Endeavour crater. *J. Geophys. Res.* 116 <https://doi.org/10.1029/2010JE003746>. E00F15.
- Arvidson, R.E., et al., 2017. Relating geologic units and mobility system kinematics contributing to curiosity wheel damage at Gale crater, Mars. *J. Terramech.* 73, 73–93.
- Aye, K.-M., et al., 2019. Planet four: probing seasonal winds on Mars by mapping the southern polar CO₂ jet deposits. *Icarus* 319, 558–598.
- Backer, J.W., et al., 2018. Updates to integrated software for imagers and spectrometers. In: 49th Lunar and Planetary Science Conference 19–23 March, 2018, held at The Woodlands, Texas LPI Contribution No. 2083, id.3007.
- Bailen, M.S., Sucharski, R.M., Akins, S.W., Hare, T., Gaddis, L., 2013. Using the PDS planetary image locator tool (PILOT) to identify and download spacecraft data for research. In: 44th Lunar and Planetary Science Conference, #2246.
- Banks, M.E., et al., 2009. An analysis of sinuous ridges in the southern Argyre Planitia, Mars, using HiRISE and CTX images and MOLA data. *J. Geophys. Res.* 114, E09003 <https://doi.org/10.1029/2008JE003244>.
- Barrett, A.M., et al., 2022. NOAH-H, a deep-learning, terrain classification system for Mars: results for the ExoMars rover candidate landing sites. *Icarus* 371 article id. 114701.
- Becerra, P., Byrne, S., Sori, M.M., Sutton, S., Herkenhoff, K.E., 2016. Stratigraphy of the north polar layered deposits of Mars from high-resolution topography. *J. Geophys. Res.: Planets* 121 (8), 1445–1471.
- Becerra, P., et al., 2019. Timescales of the climate record in the south polar ice cap of Mars. *Geophys. Res. Lett.* 46 (13), 7268–7277.
- Becker, K.J., Anderson, J.A., Sides, S.C., Miller, E.A., Eliason, E.M., Keszthelyi, L.P., 2007. Processing HiRISE Images Using ISIS3. 38th Lunar and Planetary Science Conference, (Lunar and Planetary Science XXXVIII), held March 12–16, 2007 in League City, Texas. LPI Contribution No. 1338, 1779.
- Becker, K., Archinal, B., Hare, T., Kirk, R., Howington-Kraus, E., Robinson, M., Rosiek, M., 2015. Criteria for automated identification of stereo image pairs. In: Proceedings of the 46th Annual Lunar and Planetary Science Conference, The Woodlands, TX, USA, 16–20 March 2015; Abstract #2703.
- Becker, K.J., Milazzo, M.P., Delamere, W.A., Herkenhoff, K.E., Eliason, E.M., Russell, P. S., Keszthelyi, L.P., McEwen, A.S., 2021. hical—The HiRISE Radiometric Calibration Software Developed within the ISIS3 Planetary Image Processing Suite: U.S.

- Geological Survey Techniques and Methods, book 7, chap. C27, 23 p. <https://doi.org/10.3133/tm7C27>.
- Beyer, R.A., 2017. Meter-scale slopes of candidate InSight landing sites from point photogrammetry. *Space Sci. Rev.* 108 (E12), 97–107. <https://doi.org/10.1007/s11214-016-0287-7>.
- Beyer, R.A., McArthur, G., Heyd, R., Deardorff, D.G., Gulick, V., Team, H., 2010. HiRISE Web-based Public Suggestion Tool, in 41st Lunar and Planetary Science Conference. Lunar and Planetary Institute, Houston. Abstract #2458. <https://www.lpi.usra.edu/meetings/lpsc2010/pdf/2458.pdf>.
- Beyer, R.A., Alexandrov, O., McMichael, S., 2018. The Ames stereo pipeline: NASA's open source software for deriving and processing terrain data. *Earth and space science* 5. Issue 9, 537–548.
- Bickel, V.T., Conway, S.J., Tesson, P.-A., Manconi, A., Loew, S., Mall, U., 2020. Deep learning-driven detection and mapping of rockfalls on Mars. *IEEE J. Sel. Top. Appl. Earth Obs. Remote Sens.* 1–1 <https://doi.org/10.1109/JSTARS.2020.2991588>.
- Bonetti, D., et al., 2018. ExoMars 2016: Schiaparelli coasting, entry and descent post flight mission analysis. *Acta Astronaut.* 149, 93–105.
- Bridges, N.T., et al., 2011. Planet-wide sand motion on Mars. *Geology* 40, 31–34. <https://doi.org/10.1130/G32373.1>.
- Bridges, J.C., et al., 2017. Identification of the beagle 2 lander on Mars. *R. Soc. Open Sci.* 4 (10) id.170785.
- Brož, P., et al., 2022. New evidence for sedimentary volcanism on Chryse Planitia, Mars. *Icarus* 382 article id. 115038.
- Butcher, F.E.G., et al., 2020. Morphometry of a glacier-linked esker in NW Tempe Terra, Mars, and implications for sediment-discharge dynamics of subglacial drainage. *Earth Planet. Sci. Lett.* 542, 116325. <https://doi.org/10.1016/j.epsl.2020.116325>.
- Byrne, S., 2008. The polar deposits of Mars. *Annu. Rev. Earth Planet. Sci.* 37 (1), 535–560. <https://doi.org/10.1146/annurev.earth.031208.100101>.
- Calvin, W.M., James, P.B., Cantor, B.A., Dixon, E.M., 2015. Interannual and seasonal changes in the north polar ice deposits of Mars: observations from MY 29–31 using MARCI. *Icarus* 251, 181–190. <https://doi.org/10.1016/j.icarus.2014.08.026>.
- Chao, L., et al., 2022. Layered subsurface in Utopia Basin of Mars revealed by Zhurong rover radar. *Nature* 610. Issue 7931, 308–312. <https://doi.org/10.1038/s41586-022-05147-5>.
- Choi, D.S., Dundas, C.M., 2011. Measurements of Martian dust devil winds with HiRISE. *Geophys. Res. Lett.* 38, L24206 <https://doi.org/10.1029/2011GL049806>.
- Chojnacki, M., McEwen, A., Dundas, C., Ojha, L., Urso, A., Sutton, S., 2016. Geologic context of recurring slope lineae in Melas and Coprates Chasmata, Mars. *J. Geophys. Res. Planets* 121, 1204–1231. <https://doi.org/10.1002/2015JE004991>.
- Chojnacki, M., et al., 2020. HiWish: The High Resolution Imaging Science Experiment (HiRISE) Suggestion Tool. In: 51st Lunar and Planetary Science Conference. Lunar and Planetary Institute, Houston. Abstract #2095. <http://www.lpi.usra.edu/meetings/lpsc2020/pdf/2095.pdf>.
- Chojnacki, M., Vaz, D.A., Silvestro, S., Silva, D.C.A., 2021. Widespread megaripple activity across the north polar ergs of Mars. *J. Geophys. Res. Planets* 126, 1–19.
- Christensen, P.R., et al., 2001. Mars global surveyor thermal emission spectrometer experiment: investigation description and surface science results. *J. Geophys. Res.* 106, 23,823–23,871.
- Daubar, I.J., et al., 2022. New craters on Mars: An updated catalog. *J. Geophys. Res.: Planets* 127 (7) article id. e07145.
- Delamere, W.A., et al., 2010. Color imaging of Mars by the high resolution imaging science experiment (HiRISE). *Icarus* 205 (1), 38–52.
- Delamere, W.A., et al., 2013. In: Green, D.W.E. (Ed.), Comet C/2012 S1 (Ison). Central Bureau Electronic Telegrams, No. 3720, #1 (2013).
- Dickenshied, S., et al., 2019. JMARS — easy visualization and analysis of planetary remote sensing data. In: 4th Planetary Data Workshop, held 18–20 June, 2019 in Flagstaff, Arizona. LPI Contribution No. 2151, id.7108.
- Diniega, S., Byrne, S., Bridges, N.T., Dundas, C.M., McEwen, A.S., 2010. Seasonality of present-day Martian dune-gully activity. *Geology* 38. <https://doi.org/10.1130/G31287.1>, 1,047–1,050.
- Diniega, S., et al., 2021. Modern Mars' geomorphological activity, driven by wind, frost, and gravity. *Geomorphology* 2021 (380), 107627.
- Dundas, C.M., McEwen, A.S., Diniega, S., Byrne, S., Martinez-Alonso, S., 2010. New and recent gully activity on Mars as seen by HiRISE. *Geophys. Res. Lett.* 37, L07202 <https://doi.org/10.1029/2009GL041351>.
- Dundas, C.M., et al., 2017. Granular flows at recurring slope lineae on Mars indicate a limited role for liquid water. *Nat. Geosci.* 10, 903–907.
- Dundas, C.M., McEwen, A.S., Diniega, S., Hansen, C.J., Byrne, S., McElwaine, J.N., 2019a. The formation of gullies on Mars today. *Geol. Soc. Lond. Spec. Pub.* 467, 67–94. <https://doi.org/10.1144/SP467.5>.
- Dundas, C.M., Cushing, G.E., Keszthelyi, L.P., 2019b. The flood lavas of Kasei Valles, Mars. *Icarus* 321, 346–357.
- Dundas, C.M., et al., 2021a. Active Mars: A dynamic world. *J. Geophys. Res.* 126 <https://doi.org/10.1029/2021JE006876> e2021JE006876.
- Dundas, C.M., et al., 2021b. Widespread exposures of extensive clean shallow ice in the Martian mid-latitudes. *J. Geophys. Res. Planets* 126. <https://doi.org/10.1029/2020JE006617> e2020JE006617.
- Dundas, C.M., et al., 2023. A large new crater exposes the limits of water ice on Mars. *Geophys. Res. Lett.* 50 <https://doi.org/10.1029/2022GL100747> e2022GL100747.
- Ehlmann, B.L., Edwards, C.S., 2014. Mineralogy of the martian surface. *Annu. Rev. Earth Planet. Sci.* 42 (1), 291–315.
- Fanara, L., Gwinner, K., Hauber, E., Oberst, J., 2020. Automated detection of block falls in the north polar region of Mars. *Planet. Space Sci.* 180 article id. 104733.
- Farley, K.A., et al., 2020. Mars 2020 Mission overview. *Space Sci. Rev.* 216 (8) article id.142.
- Farnham, T., Kelley, M.S., Bodewits, D., Bauer, J.M., 2017. The resolved nucleus of comet siding spring (C/2013 A1) in MRO HiRISE images. *American Astronomical Society, DPS meeting #49*, id.403.01.
- Farnocchia, D., et al., 2016. High precision comet trajectory estimates: the Mars flyby of C/2013 A1 (siding spring). *Icarus* 266, 279–287.
- Ferguson, R.L., et al., 2017. Analysis of local slopes at the InSight landing site on Mars. *Space Sci. Rev.* 2017 (211), 109–133.
- Ferguson, R., et al., 2020. Mars 2020 terrain relative navigation flight product generation: digital terrain model and orthorectified image mosaic. In: Proceedings of the 51st Annual Lunar and Planetary Science Conference, The Woodlands, TX, USA, 16–20 March 2020. Abstract #2020.
- Foroutan, M., Zimbelman, J.R., 2017. Semi-automatic mapping of linear-trending bedforms using 'Self-organizing Maps' algorithm. *Geomorphology* 293, 156–166.
- Gallagher, C., Balme, M.R., Conway, S.J., Grindrod, P.M., 2011. Sorted clastic stripes, lobes and associated gullies in high-latitude craters on Mars: landforms indicative of very recent, polycyclic ground-ice thaw and liquid flows. *Icarus* 211, 458–471. <https://doi.org/10.1016/j.icarus.2010.09.010>.
- Golombek, M., 2019. How HiRISE changed Mars exploration: Geological Society of America. In: Annual Meeting, September 22–25, 2019, Phoenix, AZ, Abstracts with Programs. v. 51, No. 5, Paper No. 86–13.
- Golombek, M.P., et al., 2008. Size-frequency distributions of rocks on the northern plains of Mars with special reference to Phoenix landing surfaces. *Journal of Geophysical Research Planets* 113. <https://doi.org/10.1029/2007JE003065>. E00A09.
- Golombek, M.P., et al., 2012a. Detection and characterization of rocks and rock size-frequency distributions at the final four Mars Science Laboratory landing sites. *Mars* 7, 1–22. <https://doi.org/10.1555/mars.2012.0001>.
- Golombek, M.P., et al., 2012b. Selection of the Mars Science Laboratory landing site. *Space Sci. Rev.* 170, 641–737. <https://doi.org/10.1007/s11214-012-9916-y>.
- Golombek, M.P., et al., 2017. Selection of the InSight landing site. *Space Sci. Rev.* 211, 5–95. <https://doi.org/10.1007/s11214-016-0321-9>.
- Golombek, M.P., et al., 2018. Geology and physical properties investigations by the InSight lander. *Space Sci. Rev.* 214, 84. <https://doi.org/10.1007/s11214-018-0512-7>.
- Golombek, M.P., et al., 2020a. Geology of the InSight landing site on Mars. *Nat. Commun.* 11 <https://doi.org/10.1038/s41467-020-14679-1>. Article number: 1014.
- Golombek, M.P., et al., 2020b. Assessment of InSight landing site predictions. *J. Geophys. Res.: Planets* 125. <https://doi.org/10.1029/2020JE006502> e2020JE006502.
- Golombek, M.P., et al., 2021a. Rock size-frequency distribution of the InSight landing site. *Mars. Earth Space Sci.* <https://doi.org/10.1029/2021EA001959>.
- Golombek, M., et al., 2021b. SpaceX Starship Landing Sites on Mars. In: 52nd Lunar and Planetary Science Conference, held virtually, 15–19 March, 2021. LPI Contribution No. 2548, id.2420.
- Graf, J.E., Zurek, R.W., Eisen, H.J., Jai, B., Johnston, M.D., DePaula, R., 2005. The Mars reconnaissance orbiter Mission. *Acta Astronaut.* 57, 566–578.
- Grant, J.A., Wilson, S.A., 2019. Evidence for late alluvial activity in Gale crater, Mars. *Geophys. Res. Lett.* 46, 7287–7294.
- Grant, J.A., et al., 2010. The science process for selecting the landing site for the 2011 Mars science laboratory: planet. *Space Sci.* 59, 1114–1127. <https://doi.org/10.1016/j.pss.2010.06.016>.
- Grant, J.A., Golombek, M.P., Wilson, S.A., Farley, K.A., Williford, K.H., Chen, A., 2018. The science process for selecting the landing site for the Mars 2020 rover: planet. *Space Sci.* 164, 106–126. <https://doi.org/10.1016/j.pss.2018.07.001>.
- Grant, J.A., et al., 2020. Degradation of homestead hollow at the InSight landing site based on the distribution and properties of local deposits. *J. Geophys. Res.* 125 <https://doi.org/10.1029/2019JE006350>.
- Grant, J.A., et al., 2022. Degradation at the InSight landing site, homestead hollow, Mars: constraints from rock heights and shapes. *Earth Space Sci.* 9 <https://doi.org/10.1029/2021EA001953> e2021EA001953.
- Gulick, V.C., Deardorff, G., Kanefsky, B., 2010. Online Citizen Science with Clickworkers & MRO HiRISE E/PO, AGUFM 2010 ED13B-08. <https://ui.adsabs.harvard.edu/abs/2010AGUFMED13B..08G/abstract>.
- Hamilton, C.W., Mougini-Mark, P.J., Sori, M.M., Scheidt, S.P., Bramson, A.M., 2018. Episodes of aqueous flooding and effusive volcanism associated with Hrad Vallis, Mars. *J. Geophys. Res.: Planets* 123 (6), 1484–1510.
- Hansen, C.J., et al., 2011. Seasonal erosion and restoration of Mars' northern polar dunes. *Science* 331, 575–578.
- Hapke, B., 1981. Bidirectional reflectance spectroscopy. 1. Theory. *J. Geophys. Res.* 86, 4571–4586.
- Hare, T.M., Akins, S.W., Sucharski, R.M., Bailen, M.S., Anderson, J.A., 2013. Map projection web services for PDS images. In: 44th Lunar and Planetary Science Conference, #2068.
- Heldmann, J.L., et al., 2021. Mission Architecture Using the SpaceX Starship Vehicle to Enable a Sustained Human Presence on Mars. *New Space, Ahead of Print*, id. 1. <https://doi.org/10.1089/space.2020.0058>.
- Horn, B.K.P., Jan. 1981. Hill shading and the reflectance map. In: Proceedings of the IEEE, vol. 69, pp. 14–47. <https://doi.org/10.1109/PROC.1981.11918> no. 1.
- Howard, P.G., Vitter, J.S., 1993. Fast and efficient lossless image compression. In: Proceedings of the 1993 IEEE Data Compression Conference (DCC '93), Snowbird, UT, April 1993, pp. 351–360.
- Huang, H., et al., 2022. The analysis of cones within the Tianwen-1 landing area. *Remote Sens.* 14 (11), 2590.
- Jakosky, B.M., et al., 2015. The Mars atmosphere and volatile evolution (MAVEN) Mission. *Space Sci. Rev.* 195 (1–4), 3–48. <https://doi.org/10.1007/s11214-015-0139-x>.

- Jaumann, R., et al., 2007. The high-resolution stereo camera (HRSC) experiment on Mars express: instrument aspects and experiment conduct from interplanetary cruise through the nominal mission. *Planet. Space Sci.* 55 (7–8), 928–952.
- Khuller, A., et al., 2022. Irregular polygonal ridge networks in ancient Noachian terrain on Mars. *Icarus* 374, 114833.
- Kieffer, H.H., 2007. Cold jets in the martian polar caps. *JGR* 112, E08005.
- Kirk, R.L., et al., 2008. Ultrahigh resolution topographic mapping of Mars with MRO HiRISE stereo images: meter-scale slopes of candidate Phoenix landing sites. *J. Geophys. Res.: Planets* 113 (E3). <https://doi.org/10.1029/2007JE003000>.
- Kirk, R., et al., 2021. Adventures in Mars DTM quality: smoothing errors, sharpening details. *Remote Sens.* 43, 659–666.
- Kite, E.S., Mayer, D.P., Wilson, S.A., Davis, J.M., Lucas, A.S., Stucky de Quay, G., 2019. Persistence of intense, climate-driven runoff late in Mars history. *Sci. Adv.* 5 <https://doi.org/10.1126/sciadv.aav7710> eaav7710.
- Laben, C. A., Brower, B. V., 2000. Process for enhancing the spatial resolution of multispectral imagery using pan-sharpening. U.S. Patent 6,011,875.
- Lee, S.W., Skulsky, E.D., Chapel, J., Cwynar, D., Gehling, R., Delamere, A., 2003. Mars reconnaissance orbiter design approach for high-resolution surface imaging. In: 26th Annual AAS Guidance and Control Conference, AAS-03-067. <http://hdl.handle.net/2014/37230>.
- Lewis, K.W., Aharonson, O., 2014. Occurrence and origin of rhythmic sedimentary rocks on Mars. *J. Geophys. Res.: Planets* 119 (6), 1432–1457.
- Malin, M.C., et al., 2001. The Mars color imager (MARC) on the Mars climate orbiter. *J. Geophys. Res.* 106, 17651–17672.
- Malin, M.C., et al., 2007. Context Camera Investigation on board the Mars Reconnaissance Orbiter. *J. Geophys. Res.* 112, E05S04.
- Malin, M.C., et al., 2010. An overview of the 1985–2006 Mars orbiter camera science investigation. *Int. J. Mars Sci. Explor.* 4, 1–60. <https://doi.org/10.1555/mars.2010.0001>.
- McCleese, D.J., et al., 2007. Mars Climate Sounder: an investigation of thermal and water vapor structure, dust and condensate distributions in the atmosphere, and energy balance of the polar regions. *J. Geophys. Res.* 112 (E5). [CiteID E05S06](https://doi.org/10.1029/2006JE002745).
- McDonnell, M.D., Jones, E., Schwamb, M.E., Aye, K.-M., Portyankina, G., Hansen, C.J., 2023. Planet four: a neural Network's search for polar spring-time fans on Mars. *Icarus* 391. <https://doi.org/10.1016/j.icarus.2022.115308> article id. 115308.
- McEwen, A.S., et al., 2007. Mars reconnaissance orbiter's high resolution imaging science experiment (HiRISE). *J. Geophys. Res.* 112, E05S02.
- McEwen, A.S., et al., 2010. The high resolution imaging science experiment (HiRISE) during MRO's primary science phase (PSP). *Icarus* 205, 2–37.
- McEwen, A.S., et al., 2011. Seasonal flows on warm Martian slopes. *Science* 333, 740–743. <https://doi.org/10.1126/science.1204816>.
- McEwen, A.S., Schaefer, E.I., Dundas, C.M., Sutton, S.S., Tamppari, L.K., Chojnacki, M., 2018. Abundant recurring slope lineae (RSL) following the planet-encircling dust event (PEDE) of 2018. *J. Geophys. Res.: Planets* 123, e2018JE005675.
- McLennan, S.M., Grotzinger, J.P., Hurowitz, J.A., Tosca, N.J., 2019. The sedimentary cycle on early Mars. *Annu. Rev. Earth Planet. Sci.* 47, 91–118.
- Milazzo, M.P., Herkenhoff, K., Becker, K., Russell, P., Delamere, W.A., McEwen, A.S., 2015. MRO/HiRISE radiometric calibration update. *Lunar Planet. Sci. XLVI abstract* 1498.
- Mills, M.M., McEwen, A.S., Okubo, C.H., 2021. A Preliminary Regional Geomorphologic Map in Utopia Planitia of the Tianwen-1 Zhurong Landing Region. *Geophysical Research Letters* 48 (18), e94629. <https://doi.org/10.1029/2021GL094629>.
- Morgan, G.A., et al., 2021. Availability of subsurface water-ice resources in the northern mid-latitudes of Mars. *Nat. Astron.* 5, 230–236.
- Murchie, S.L., et al., 2007. Compact reconnaissance imaging spectrometer for Mars (CRISM) on Mars reconnaissance orbiter (MRO). *J. Geophys. Res.* 112 <https://doi.org/10.1029/2006JE002682>. E05S03.
- Murchie, S.L., et al., 2009. A synthesis of martian aqueous mineralogy after one Mars year of observations from the Mars Reconnaissance Orbiter. *J. Geophys. Res.: Planets* 114 (E2). [CiteID E00D06](https://doi.org/10.1029/2008JE003000).
- Ojha, L., et al., 2017. Seasonal slumps in Juventae Chasma, Mars. *J. Geophys. Res.: Planets* 122, 2193–2214.
- Okubo, C.H., 2010. Structural geology of Amazonian-aged layered sedimentary deposits in southwest candor Chasma, Mars. *Icarus* 207, 210–225. <https://doi.org/10.1016/j.icarus.2009.11.012>.
- Okubo, C.H., 2016. Morphologic evidence of subsurface sediment mobilization and mud volcanism in candor and Coprates Chasmata, Valles Marineris, Mars. *Icarus* 269, 23–37.
- Parkes-Bowen, A., et al., 2022. A CaSSIS and HiRISE map of the clay-bearing unit at the ExoMars 2022 landing site in Oxia Planum. *Planet. Space Sci.* 214, 105429.
- Perrin, C., et al., 2020. Monitoring of dust devil tracks around the InSight landing site, Mars, and comparison with in situ atmospheric data. *Geophys. Res. Lett.* 47 (10), 1–11. <https://doi.org/10.1029/2020GL087234>.
- Piqueux, S., Byrne, S., Kieffer, H.H., Titus, T.N., Hansen, C.J., 2015a. Enumeration of Mars years and seasons since the beginning of telescopic exploration. *Icarus* 251, 332–338.
- Piqueux, S., Kleinböhl, A., Hayne, P.O., Kass, D.M., Schofield, J.T., McCleese, D.J., 2015b. Variability of the Martian seasonal CO₂ cap extent over eight Mars years. *Icarus* 251, 164–180. <https://doi.org/10.1016/j.icarus.2014.10.045>.
- Pommerol, A., et al., 2011. Evolution of south seasonal cap during Martian spring: Insights from high-resolution observations by HiRISE and CRISM on Mars Reconnaissance Orbiter. *J. Geophys. Res.* 116 (E8). [CiteID E08007](https://doi.org/10.1029/2010JE003607).
- Portyankina, G., Hansen, C.J., Aye, K.M., 2017. Present-day erosion of Martian polar terrain by the seasonal CO₂ jets. *Icarus* 282, 93–103.
- Portyankina, G., Aye, K.-M., Schwamb, M.E., Hansen, C.J., Michaels, T.I., Lintott, C.J., 2022. Planet four: derived south polar martian winds interpreted using mesoscale modeling. *PSJ* 3, 31.
- Posiolova, L.V., et al., 2022. Large hypervelocity impact on Mars co-located by orbital imaging and surface seismic recording. *Science* 378, 412–417. <https://doi.org/10.1126/science.abq7704>.
- Putzig, N.E., Mellon, M.T., 2007. Apparent thermal inertia and the surface heterogeneity of Mars. *Icarus* 191, 68–94. <https://doi.org/10.1016/j.icarus.2007.05.013>.
- Quantin-Nataf, C., et al., 2018. MarsSI: Martian surface data processing information system. *Planet. Space Sci.* 150, 157–170. <https://doi.org/10.1016/j.pss.2017.09.014>.
- Quantin-Nataf, C., et al., 2021. Oxia Planum: the landing site for the ExoMars “Rosalind Franklin” rover Mission: geological context and Prelanding interpretation. *Astrobiology* 21, Issue 3, 345–366.
- Raugh, A., Hughes, J.S., 2021. The road to an archival data format-data structures. *Planet. Sci. J.* 2 (5) id.204, 12 pp.
- Reiss, D., Spiga, A., Erkeling, G., 2014. The horizontal motion of dust devils on Mars derived from CRISM and CTX/HiRISE observations. *Icarus* 227, 8–20.
- Robinson, M.S., et al., 2010. Lunar reconnaissance orbiter camera (LROC) instrument overview. *Space Sci. Rev.* 150 (1–4), 81–124.
- Russell, P., et al., 2008. Seasonally active frost-dust avalanches on a north polar scarp of Mars captured by HiRISE. *Geophys. Res. Lett.* 35 <https://doi.org/10.1029/2008GL035790>.
- Schwamb, M.E., et al., 2018. Planet four: terrains - discovery of araneiforms outside of the south polar layered deposits. *Icarus* 308, 148–187. <https://doi.org/10.1016/j.icarus.2017.06.017>.
- Seelos, F.P., et al., 2023. The CRISM investigation in Mars orbit: overview, history, and delivered data products. *Icarus* (in press).
- Seu, R., et al., 2007. SHARAD sounding radar on the Mars reconnaissance orbiter. *J. Geophys. Res.* 112 <https://doi.org/10.1029/2006JE002745>.
- Silvestro, S., Fenton, L.K., Vaz, D.A., Bridges, N.T., Ori, G.G., 2010. Ripple migration and dune activity on Mars: evidence for dynamic wind processes. *Geophys. Res. Lett.* 37, L20203 <https://doi.org/10.1029/2010GL044743>.
- Silvestro, S., Chojnacki, M., Vaz, D.A., Cardinale, M., Yizhaq, H., Esposito, F., 2020. Megaripple migration on Mars. *J. Geophys. Res.: Planets* 125. <https://doi.org/10.1029/2020JE006446> e2020JE006446.
- Smith, M.D., 2008. Spacecraft observations of the Martian atmosphere. *Annu. Rev. Earth Planet. Sci.* 36, 191–219. <https://doi.org/10.1146/annurev.earth.36.031207.124334>.
- Smith, D.E., et al., 2001. Mars orbiter laser altimeter: experiment summary after the first year of global mapping of Mars. *J. Geophys. Res.: Planets* 106 (E10), 23689–23722.
- Smith, P.H., et al., 2008. Introduction to special section on the Phoenix mission: Landing site characterization experiments, mission overviews, and expected science. *J. Geophys. Res.* 113 (E12). [CiteID E00A18](https://doi.org/10.1029/2008JE003000).
- Soare, R.J., Conway, S.J., Dohm, J.M., 2014. Possible ice-wedge polygons and recent landscape modification by “wet” periglacial processes in and around the Argyre impact basin, Mars. *Icarus* 233, 214–228. <https://doi.org/10.1016/j.icarus.2014.01.034>.
- Sori, M.M., Becerra, P., Bapst, J., Byrne, S., McGlasson, R.A., 2022. Orbital forcing of martian climate revealed in a south polar outlier ice deposit. *Geophys. Res. Lett.* 49 (6) <https://doi.org/10.1029/2021GL097450> article id. e97450.
- Sun, Z., Rao, W., 2022. Entry, descent, and landing of China's Tianwen-1 Mars Mission. *Space Sci. Technol.* 2022 <https://doi.org/10.34133/2022/9809054> article id. 9809054.
- Sun, V.Z., Stack, K.M., 2020. Geologic map of Jezero crater and the Nili Planum region, Mars. In: US Geological Survey Scientific Investigations Map 3464.
- Sutton, S.S., et al., 2019. Correcting spacecraft jitter in HiRISE images. In: Wu, et al. (Eds.), *Planetary Remote Sensing and Mapping*. Taylor & Francis Group, London, pp. 91–106.
- Sutton, S., Hamilton, C.W., Cataldo, V., Williams, D.A., Bleacher, J.E., 2022a. Sinuous channels east of Olympus Mons, Mars: implications for volcanic, hydrological, and tectonic processes. *Icarus* 374 article id. 114798.
- Sutton, S.S., et al., 2022b. Revealing active Mars with HiRISE digital terrain models. *Remote Sens.* 14 (10), 2403.
- Sutton, S.S., et al., 2023. Slope and roughness maps from HiRISE digital terrain models. In: 6th Planetary Data Workshop, LPI Contribution, #7031.
- Sweeney, J., et al., 2018. Degradation of 100-m-scale rocky ejecta craters at the InSight landing site on Mars and implications for surface processes and erosion rates in the Hesperian and Amazonian. *J. Geophys. Res.: Planets* 123, 2732. <https://doi.org/10.1029/2018JE005618>.
- Tamppari, L.K., et al., 2010. Phoenix and MRO coordinated atmospheric measurements. *J. Geophys. Res.: Planets* 115 (5). <https://doi.org/10.1029/2009JE003415>.
- Tao, Y., Muller, J.-P., 2016. A novel method for surface exploration: super-resolution restoration of Mars repeat-pass orbital imagery. *Planet. Space Sci.* 121, 103–114.
- Taubman, D., Marcellin, M., 2012. *JPEG2000 Image Compression Fundamentals, Standards and Practice*. Springer Science & Business Media. ISBN 9781461507994.
- Thomas, N., et al., 2017. The colour and stereo surface imaging system (CaSSIS) for the ExoMars trace gas orbiter. *Space Sci. Rev.* 212 (3–4), 1897–1944.
- Tornabene, L.L., et al., 2018. Image simulation and assessment of the colour and spatial capabilities of the colour and stereo surface imaging system (CaSSIS) on the ExoMars trace gas orbiter. *Space Sci. Rev.* 214 (1), 1–61.
- Wagstaff, K.L., et al., 2022. Using machine learning to reduce observational biases when detecting new impacts on Mars. *Icarus* 386 article id. 115146.
- Weitz, C.M., Bishop, J.L., Thollot, P., Mangold, N., Roach, L.H., 2011. Diverse mineralogies in two troughs of Noctis Labyrinthus, Mars. *Geology* 39 (10), 899–902. <https://doi.org/10.1130/G32045.1>.

- Weitz, C.M., et al., 2020. Comparison of InSight homestead hollow to hollows at the Spirit landing site. *J. Geophys. Res.* 125 <https://doi.org/10.1029/2020JE006435>.
- Weitz, C.M., et al., 2022. Clay sediments derived from fluvial activity in and around Ladon basin, Mars. *Icarus* 384. <https://doi.org/10.1016/j.icarus.2022.115090>.
- Wilcoski, A.X., Hayne, P.O., 2020. Surface roughness evolution and implications for the age of the north polar residual cap of Mars. *J. Geophys. Res.: Planets* 125 (12) article id. e06570.
- Wilson, S.A., Morgan, A.M., Howard, A.D., Grant, J.A., 2021. The global distribution of craters with alluvial fans and deltas on Mars. *Geophys. Res. Lett.* 48 e2020GL091653.
- Wood, S.E., Paige, D.A., 1992. Modeling the Martian seasonal CO₂ cycle 1. Fitting the Viking Lander pressure curves. *Icarus* 99, 1–14. [https://doi.org/10.1016/0019-1035\(92\)90166-5](https://doi.org/10.1016/0019-1035(92)90166-5).
- Wray, J.J., et al., 2011. Columbus crater and other possible groundwater-fed paleolakes of Terra Sirenum, Mars. *J. Geophys. Res.: Planets* 116 (E1).
- Zurek, R.W., Smrekar, S.E., 2007. An overview of the Mars reconnaissance orbiter (MRO) science mission. *J. Geophys. Res. Planets* 112, 1–22.